

MCMASTER UNIVERSITY
McMaster Automotive Resource Centre (MARC)



MASTER THESIS ON
*Component Sizing and Real time Control using
the A-ECMS method in a Parallel HEV*

Author: *Alessandro Simone G. Picchirallo*

Supervisors: *Prof. Dr. Ali Emadi*
Prof. Dr. Giovanni Belingardi

Co-Supervisor: *Ing. Pier Giuseppe Anselma*



DEPARTMENT OF MECHANICAL ENGINEERING

POLITECNICO DI TORINO

October 2019

Greetings

To my family, in particular my brother Marco, my parents and my grandparents, to all my friends, starting from the ones I met when I was in primary school, till the newest met during my experiences abroad in Erasmus or Canada. A heartfelt thanks to all those who have supported me in this long journey....

Table of contents

List of Figures	III
List of Tables	V
1 Introduction	1
1.1 Automotive Industry: New Perspective of HEVs	1
1.2 Electrification Degree	4
1.3 Hybrid Powertrain Architectures	6
1.3.1 Series Power-trains	6
1.3.2 Parallel Power-trains	7
1.3.3 Series-Parallel Powertrains	10
1.3.4 Power-split Powertrains	11
1.3.5 Two-mode Powertrains	13
2 Physical Model	15
2.1 Road Load Model	15
2.2 Powertrain Components Model	17
2.2.1 ICE Model	17
2.2.2 MGU Model	19
2.2.3 Battery Model	21
2.3 Sizing Components Strategy	24
2.3.1 ICE Sizing	24
2.3.2 MGU Sizing	27
2.3.3 Battery Sizing	30
3 Energy Management Strategy	33
3.1 Offline Control Strategies	38
3.1.1 Dynamic Programming	39
3.1.2 Pontryagin's Minimum Principle	40
3.1.3 Slope-weighted Energy-based Rapid Control Analysis (SERCA)	42
3.2 Online Control Strategies	47
3.2.1 Rule-Based	47
3.2.2 Equivalent Consumption Minimization Strategy (ECMS)	49

3.2.3	Adaptive Equivalent Consumption Minimization Strategy (A-ECMS)	53
4	A-ECMS Controller	54
4.1	Gear Selection	56
4.2	ICE Status Determination	60
4.3	Torque Split Determination	62
4.4	Equivalence Factor Control	63
4.4.1	Preliminary Studies on EF	63
4.4.2	EF Controller Overview	67
4.5	FC Comparisons	74
4.5.1	3 Speed Transmission	74
4.5.2	5 Speed Transmission	77
4.5.3	8 Speed Transmission	79
4.6	Graphical User Interface	85
5	Optimization Algorithms	87
5.1	Genetic Algorithm	88
5.2	Machine Learning	90
5.3	Particle Swarm Optimization	92
6	Multi-Objective Particle Swarm Optimization	95
7	Considerations	102
7.1	Future work	103
	References	104

List of Figures

0.1	Workflow of the Simulation	X
1.1	Toyota Prius 1997 [1]	3
1.2	Representation of a Series HEV Power-train Architecture.	6
1.3	Representation of Parallel HEV Architectures	8
1.4	Representation of the Series-Parallel Power-train Architecture.	10
1.5	Representation of the THS Power-Split Power-train Architecture.	11
1.6	Representation of the HSD Power-Split Power-train Architecture.	12
1.7	Representation of the GM's Allison Two-Mode Power-train Archit.	13
2.1	Ice Fuel Losses Map	17
2.2	ICE Maximum Torque	18
2.3	MGU Power Losses Map	19
2.4	MGU Maximum Torque	20
2.5	Battery Model	21
2.6	Open Circuit Voltage Map	21
2.7	Internal Circuit Resistance Map	22
2.8	Setting of the ICE parameters	24
2.9	Maximum Torque ICE Model Comparison	25
2.10	Fuel Consumption ICE Model Comparison	26
2.11	Setting of the GMU Parameters	27
2.12	Maximum Torque GMU Model Comparison	28
2.13	Power Losses GMU Model Comparison	29
2.14	Open Circuit Voltage Trend	30
2.15	Internal Resistance Trend	31
3.1	WLTP Speed Profile	34
3.2	Global Minimum and Local Minimum Representation	35
3.3	Comparison Backward and Forward Looking Models	38
3.4	SERCA FC and SOC graph	43
3.5	Slope Evaluation of Adjacent points	44
3.6	Fuel Consumption Evaluation	46
3.7	Rule-Base look-up table	48
3.8	ECMS Results	52

4.1	A-ECMS workflow	55
4.2	SERCA Gear Distribution	56
4.3	EM Torque for the Different Gear at different Speed	57
4.4	Battery Power for the Different Gear at different Speed	58
4.5	Battery Power and Power Demand graph	60
4.6	Torque Split	62
4.7	EF related to the Vehicle Speed	64
4.8	EF related to the Vehicle Acceleration	65
4.9	3D trend of EF, Vehicle Sp. and Battery Power	65
4.10	3D trend of EF, Vehicle Acc. and Battery Power	66
4.11	ECMS Rules: SOC and EF	69
4.12	ECMS Rules: Speed and SOC	70
4.13	ECMS Rules: Torque Split	71
4.14	ECMS Rules: Trip %	72
4.15	SOC and EF Trends	72
4.16	Comparison A-ECMS & SERCA Gears Selection	81
4.17	Comparison A-ECMS & SERCA Torques Trends	82
4.18	Comparison A-ECMS & SERCA FC, SOC and EF Trends	83
4.19	Controller Interface	85
5.1	Flowchart of Genetic Algorithm	89
5.2	Interactions representation of Reinforcement Learning	90
5.3	Particle Swarm Optimization scheme	92
5.4	Particle Swarm Optimization workflow	93
6.1	Particle Swarm Optimization Parameters	95
6.2	Optimization of FC and PI: Powertrain 5 Speed Transmission	96
6.3	Optimization of FC and PI: Powertrain 3 Speed Transmission	96
6.4	Optimization of FC: Powertrain 5 Speed Transmission	99
6.5	Optimization of FC: Powertrain 3 Speed Transmission	99
7.1	Co-Simulation Workflow	103

List of Tables

1	Two-mode Hybrid Transmission Operation Modes	13
2	Vehicles Data	16
3	ICEs Data	18
4	MGUs Data	20
5	Vehicles Data	23
6	Battery Data	30
7	Functions Battery Range	31
8	Equivalence Factors Comparison	50
9	ECMS Table	51
10	Gear Shifts Comparison	59
11	ICE ignitions Comparison	61
12	ECMS Versions FC comparison	67
13	Tuned ECMS FC comparison	68
14	3 Speed Transmission A-ECMS Results	74
15	3 Speed Transmission Comparison	75
16	3 Speed Transmission Ratios	76
17	5 Speed Transmission A-ECMS Results	77
18	5 Speed Transmission Comparison	77
19	5 Speed Transmission Ratios	78
20	8 Speed Transmission A-ECMS Results	79
21	8 Speed Transmission Comparison	79
22	8 Speed Transmission Ratios	80
23	Minimum Acceleration Times	87
24	Optimized Components by FC and PI	97
25	Optimized FC and PI	97
26	Comparison Optimized and Non Optimized FC	98
27	Optimized Components by FC	100
28	Optimized FC	100

Nomenclature

ECMS	Equivalent Consumption Minimization strategy
HEV	Hybrid Electric Vehicle
PHEV	Plug-in Hybrid Electric Vehicle
BEV	Battery Electric Vehicle
CS	Charge Sustain
DOV	Degree of Freedom
DP	Dynamic Programming
EPA	Environmental Protection Agency
EVT	Electrical Variable Transmission
ICE	Internal Combustion Engine
MGU	Motor/Generator Unit
MY	Model Year
PEARS	Power-weighted Efficiency Analysis for Rapid Sizing
PMP	Pontryagin's Minimum Principle
PG	Planetary Gear
SERCA	Slope-weighted Energy-based Rapid Control Analysis
SOC	State of Charge
SOH	State of Health
HWFET	Highway Fuel Economy Test
UDDS	Urban Dynamometer Driving Schedule
WLTP	Worldwide Harmonized Light Vehicle Test Procedure
EF	Equivalent Factor
FC	Fuel Consumption
GA	Genetic Algorithm
ML	Machine Learning
PSO	Particle Swarm Optimization

Abstract

The automotive sector is constantly trying to develop new strategies to decrease the consumption and to improve the performances.

The market and the world need are converging with a paradigm shift to the renewable sources. At the present time the two options of the Electric Vehicle (EV) and the Hybrid Electric Vehicle (HEV) are two of the best perspective in which we can put our efforts.

The first one, the EVs, is still limited by technical and engineering issues due to the knowledge of this time, in particular about the Energy density of the batteries.

From this issues started to develop the possibility to associate an Ice Combustion Engine (ICE) to the Motor-Generator Unit (EM) with the HEVs technology.

This field is huge and in continuous growth, the market in particular is leading the attention on the Parallel technology for which the motion units cooperate to develop the power for the user, it's one of the easiest way to design an HEV but it's still possible to reach values of Fuel Consumption that are really lower than the Traditional Vehicle, keeping also the performances able to afford every kind of situation of the real driving life and also maintaining an high driving pleasure for the journey.

In this work the aim is to develop an online controller, in Real-Time for the real driving life, for and HEV with a parallel configuration P2 (one ICE and one MGU).

The controller use the Adaptive Equivalent Consumption Minimization Strategy (A-ECMS) based on an Equivalent Factor (EF) between the cost of the Power developed by the ICE and the GMU, the controller can see only the request of torque of that precise instant, obtained from the speed and the acceleration of the vehicle, and the state of all the components of the HEV: battery, transmission, GMU and ICE.

The difficulty is to have the possibility to reach the Charge Sustain (CS) when the car will reach the destination, which is to say keeping the same value of the State of Charge (SOC) of the battery at the time in which the vehicle started the track. This condition must be respected, not knowing what the future driving conditions would be.

Once developed a controller that can reach the CS in different simulated driving cycles the second goal is to develop an algorithm that can investigate the design space looking for a combination of ICE, GMU, Battery and gear ratios for the transmission that can decrease the FC keeping the sufficient

performances to deal with every kind of situation of the real driving life. The data to develop the design space are taken from the library of AMESIM by Siemens, that is public and also really reliable.

It has been chosen a Particle Swarm Optimization (PSO) algorithm for this aim, for his good qualities with this kind of problem, the PSO would take into account as said of both the FC and of a performance index in his cost function.

Here we will show the workflow of the procedure presented before:

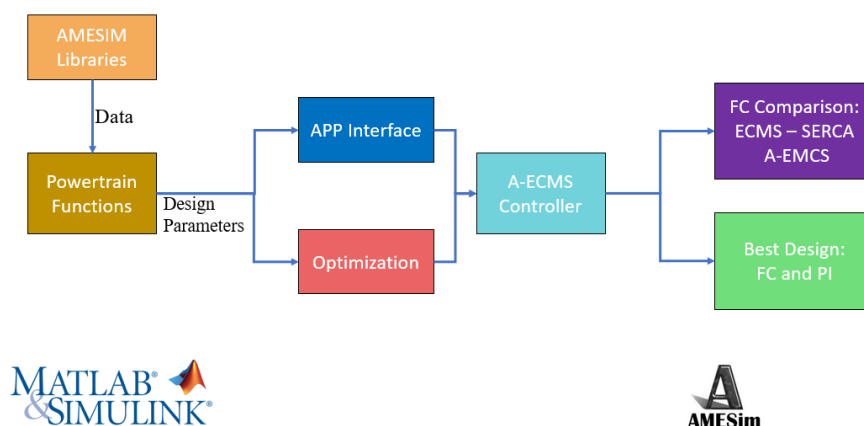


Figure 0.1: Workflow of the Simulation

This study started on MATLAB by MathWorks, in a quasi-static environment, the idea is to extend it for a Co-Simulation between AMESIM and Simulink (by MathWorks), in the first one is possible to use a vehicle model more refined, more dynamic phenomena of the components, such as the transmission for example, in the second one is possible to use the A-ECMS controller.

All the study is taking in consideration as a Benchmark the values provided by the Slope-Weighted Energy-Based Rapid Control Analysis (SERCA) algorithm for the controller, that is an offline controller that could reach the optimal result for the FC with a lower computational effort than the Dynamic Programming (DP).

At the end are shown the result from both the software to compare the results of the FC, will be also proposed the result of the optimization of the PSO with the best candidates to decrease the FC. All the candidates can be tested in the co-simulation to see their performances compared to the other controller SERCA.

1 Introduction

Firstly it's necessary to explain the choice of this kind of vehicle and this particular architecture.

There will be an explanation of the state-of-art of the HEV and a presentation of the different design that are possible with their main characteristics, will also be explained why it's been chosen this parallel architecture and provided also some real examples of vehicles of the different categories and the trend of the market for the immediate future [[2],[3]].

1.1 Automotive Industry: New Perspective of HEVs

The Automotive sector is one of the largest and most expensive sectors of the modern industry, in the 2019 estimate that there are more than 1 billion vehicles all over the world and could reach 2 billions by the 2035. Only in the USA in the 2018 there was a marginal increase of 400 thousands vehicle only in the 2018.

In this scenario is no longer sustainable to produce only tradition vehicle with an ICE that will need only fossil fuels, there is the need for a paradigm shift that has to lead to new opportunities, new kind of fuels and new ways to get the power for our vehicles, on the other side would be necessary to keep decreasing all the consumption and the emissions to decrease the request of energy.

In United States the interest in reducing the dependency from oil started between 1973 and 1974, with the oil embargo imposed by the OPEC (Organization of Petroleum Countries).

As consequence, in 1975, the Congress created the CAFE (Corporate Average Fuel Economy) with the aim of issue standards to regulate the fuel consumption [4].

By the time the interest towards the reduction of pollutant emissions and greenhouse gases (GHG), to which the transportation sector greatly contributes, has been increased all over the world.

The first European regulations for passenger trucks and light duty application dates to 1992, with the introduction of the EURO 1 standard.

The actual regulations decisions are undertaken by the European Parliament and Council, with the knowledge and data provided by the advisory organ, which is the European Environmental Agency (EEA) [5].

In US, instead, the current harmonized National Program is composed by three legal authorities: NHTSA (National Highway Traffic Safety Administration) which administrates the CAFE standard, EPA (Environmental Protection Agency) which set the maximum pollutants tolerated level and the CARB (California Air Resource Board) which historically focus is related to more stringent standards proposed for California [4].

All over the world are present different regulations for the FC and for the emissions of pollutants, the most famous it's for sure the CO_2 .

After a steady decline from 2010 to 2015, by almost 4 grams per year of CO_2 per kilometer, according to provisional data published today by the European Environment Agency (EEA), the average carbon dioxide (CO_2) emissions from new passenger cars registered in the European Union (EU) in 2018 increased for the second consecutive year, reaching 120.4 grams of CO_2 per kilometer [6].

To meet the requirements of 95 grams per kilometer from 2021, imposed by the new European regulation, the most promising solution is represented by the electrification which would allow to switch to a new concept of more sustainable transportation.

This paradigm shift will be, eventually, completed with a market dominated by xEV.

This alternative become a promise with the development of the power electronics technologies that allow to get full advantage of both DC and AC system introduced during the early 1900s by Edison and Tesla [7].

Some limitation due to the knowledge of the batteries, such as power density and cost, lead in a transition phase dominated by the HEV. This vehicles are already characterized by higher values of efficiency that the traditional ones and by interesting performances.

Having a look to the history of the automotive sector we can see that the improvement introduced in the internal combustion engine (ICE) technology by some innovators of the 19th century as Rudolf Diesel, Nikolaus Otto, Karl Benz and James Atkinson creates a large gap between the engine-based propulsion and the electrified one.

We have to wait till the 1997 when Toyota sold in the Japanese market the first modern hybrid car, the Toyota Prius (Figure 1.1).



Figure 1.1: Toyota Prius 1997 [1]

This date can be identified as an initial point of the paradigm shift which we expect will deeply change the concept of transportation in the next decades. In the 2018 the sales of xEV vehicles raised of the 38% and reached the 7 millions units with 25 new EV models and 18 new Plug-in Hybrid EVs (PHEVs) models. [8]

1.2 Electrification Degree

The HEV represents an intermediate solution between the conventional and the pure electric vehicles (BEV). A power-train is defined hybrid if at least two different energy sources are used for the propulsion [9].

The HEVs are classified by the degree of electrification, that defines the ratio between the electric and the total power of the vehicle. Changing the design and the dimension of the components we can obtain totally different degrees of electrification.

In the literature are classified as reported according a crescent degree of electrification:

- **Start-stop Hybrid:** usually are equipped with a small electric motor that works only as a starter for the ICE avoiding the FC during idle operations.
The cost for the electrification is negligible, this improvement can lead to the 2-3% on the fuel economy of the vehicle. Quite all the new models on the market are equipped with this system;
- **Micro Hybrid:** normally the propulsion is not related with the electrification, but part of the accessories, such as pumps, activators, air conditioning and other systems, are all powered by an MGU.
- **Mild Hybrid:** usually equip some important functionalities such as regenerative braking, which allows to recover the kinetic energy during braking operation to charge the battery.
They can also use the electric power for the propulsion, so are equipped by bigger MGU with high or low voltage. This items can lead to a decrease of around 10% on the FC;
- **Full Hybrid:** electric machines directly contribute to the propulsion leading to higher and more important benefits in terms of fuel consumption, typically between 20% and 50%.
The benefits are strongly related with the type of power train architecture and with the kind of circuit, city, highway, suburban or mixed;
- **Plug-in Hybrid EVs (PHEV):** the main difference with a standard HEV is the size of the battery, in this kind of vehicle the energy can be stored

directly in the battery with an advantage in terms of energy cost.

This sector is increasing the number of vehicles because has benefits in particular in short distance travels, for who has infrequent long distance journeys;

- Battery Electric Vehicles (BEV): the vehicle is only propelled by MGU, with the absence of the ICE. This means some limitations due to the actual technologies, the limited range affordable and in particular the characteristics of the batteries on the market right now, as said before.

Increasing the degree of electrification we can reduce the FC. Every kind of design and power-train architecture can lead to local maxima, it's interesting to investigate how can we decrease the consumption tuning some parameters of the components of the vehicle.

It's possible to reach the global minimum of FC with a BEV, but all the limitations that we have cited can affect the performances and the everyday usage of the consumers.

From this point of view the HEV can overcome the efficiency of the ICE, strongly reducing the FC and having good performances, such as the acceleration due to the characteristics of the MG, that today are mainly Permanent Magnet machines (PM) or Induction motors.

The first are characterized by lower losses, higher torque capability and power density, the second are simpler to build and robust but with a lower efficiency and some limitations about the speed range and the cost of the permanent magnets.

For this reason in the next future the motors will follow more the necessity of the HEV to fulfill the paradigm shift, an interesting solution is the Switched Reluctance Machine (SRM).

This motor is characterized by a wide speed range and a lower cost keeping a good robustness, at the moment there are some issues about the torque ripple and acoustic noise [2,7].

1.3 Hybrid Powertrain Architectures

In the following sections are shown the principal kind of hybrid power-train architectures, with their main characteristics and some comparison between the benefits and the drawbacks of each one. There will be for each case also a schematic representation of the main components involved in the architecture [10]. All the architectures are composed by: ICE, MGUs, Battery, Transmission, Final Drive and Differential.

1.3.1 Series Power-trains

The Series Power-train Architecture is characterized by the ICE that is not directly coupled with the differential, there is the Generator that is connected with the ICE, the Motor that instead is linked with the transmission and will provide the power to the wheels, as shown in (figure 1.2).

vspace-6 mm

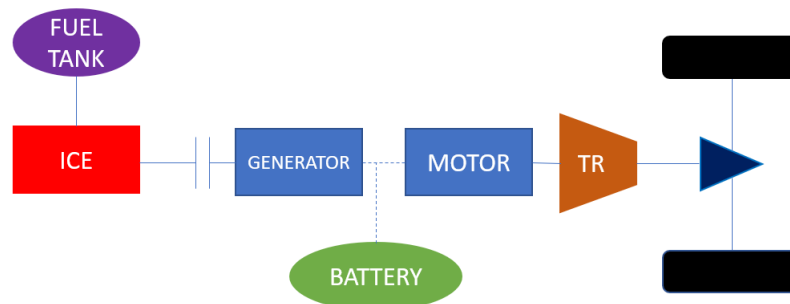


Figure 1.2: Representation of a Series HEV Power-train Architecture.

In this architecture the ICE can be seen as the charger of the battery in an electric architecture, it will work just in case the battery will discharge under a certain threshold of the SOC.

To keep the battery in the best condition is better to use a range of the SOC between 50%-75% and in particular around 60%, this will ensure a longer life for the battery and better performances.

For the fact that the ICE is not directly connected to the wheels, it is possible to keep the working point close to the Optimum Operating Line (OOL) space of best torque-speed combination for the fuel economy [9].

The series architecture represents the simplest solution for HEV design and different researches have been conducted searching for the optimal control strategy [11].

The largest limitation is related to the multiple energy conversions required from mechanical to electrical power with the related losses.

Furthermore, the system sizing represents a restriction because the electrical components needs to be chosen big enough to ensure the achievement of the power demand. Due to these limitations this architecture is applied mainly for truck and urban buses[11].

1.3.2 Parallel Power-trains

The Parallel architecture is characterized by both the contribution of the ICE and MGU for the propulsion. The "parallel" name is due to the fact that the mechanical and the electrical power can be summed up.

Unlike the series architecture is possible to use also only electric machine, for these reasons the efficiency is higher since less energy conversions are required.

About the design of the components, both ICE and MGU can be downsized obtaining the same performances of the series counterpart.

The higher flexibility in operations is associated also with the variety of possible arrangements. Usually the parallel architectures are categorized in 4 groups, from P1 to P4 as reported in (figure 1.3).

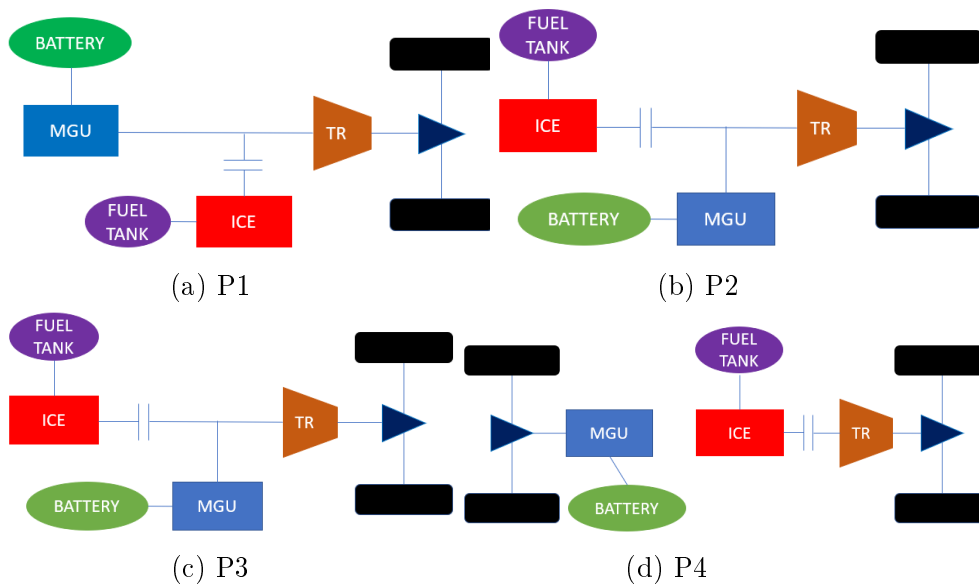


Figure 1.3: Representation of Parallel HEV Architectures

The energy recovered by braking operations is stored in the battery.

This architectures are the most diffused in the market in this moment, cause the simple arrangement and the contained number of mechanical parts and links, on the other side the it's possible to markedly reduce the FC and the other emissions.

In particular the focus of the market is on the P2 architecture, with the MGU after the IC.

In the P3 disposition the ICE is directly couple with the transmission and the MGU is connected after it.

The most complex parallel architecture is the P4 that can provide power to the axes independently.It combines power from the engine and the electric motor to drive the vehicle directly.

Within the P4 configuration, when the electric machine is on a different axle, it is commonly referred to as parallel through-the-road architecture. The most important advantages are the performance benefits of an all-wheel drive (AWD) design [12].

In these architectures in particular, but also in all the other kind of hybrid vehicles, the control strategy is fundamental to make the right choices during the mission to reduce the consumption.

Usually at low speed or under a certain level of longitudinal acceleration will work only the MGU, in other case to balance all the energy spent is necessary to activate the ICE.

Actually in the market we can find several models of this category such as: Audi Q5, BMW Active-hybrid 7L or 5, KIA Optima, Honda CR-Z, Volkswagen Jetta.

1.3.3 Series-Parallel Powertrains

The series-parallel architecture is an alternative to power-split architectures, shown in the following section, that use planetary gear sets to split the power flow of the ICE into different paths.

The ICE has a direct mechanical connection to two electric machines. One of the machines, usually referred to as the generator, is always connected to the ICE.



Figure 1.4: Representation of the Series-Parallel Power-train Architecture.

The two MGUs are separated by a clutch, the MG2 acts as the main traction motor, there are three different modes:

- Electric-only Operation: the clutch is open and only the MG2 provide the power;
- Series Operation: with the clutch open, the engine is disconnected from the road but can drive MG1 to provide electrical energy to MG2. Since the ICE is not coupled with the road can operate in its greatest efficiency range. This mode is typically used at low speed;
- Series-Parallel Operation: the clutch is engaged, the ICE provides power to the road in parallel with MG2. The MG1 can be used only as resistive torque source to force the ICE in the higher efficiency operating range possible.

The most important vehicles that are using this architecture in the market are: Hyundai Sonata, Honda Accord, KIA Optima.

1.3.4 Power-split Powertrains

The Power-split system is an input-split hybrid transmission that utilize planetary gears sets as devices to power split between the ICE and MGU [13],[14],[15] .

The planetary gears divide the energy in the two different forms, the mechanical one and the electric one. In this way is possible to use a Continuous Variable Transmission (CVT) for the ICE, for the fact that is controlled using the electric machines this type of transmission is known as the electronic-continuously variable transmission (e-CVT) [16].

This configuration is capable to reach more favorable working points for the FC and emissions due to his complexity and to the more possibilities offered by the architecture [17].

This kind of architecture was introduced by the Toyota Prius in the 1997 with the Transmission known as Toyota hybrid System (THS), shown in the following figure:

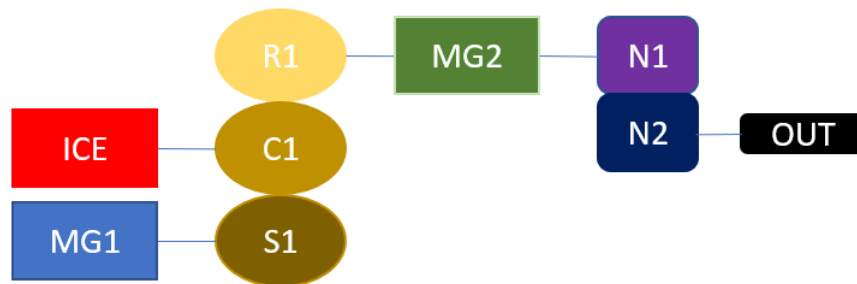


Figure 1.5: Representation of the THS Power-Split Power-train Architecture.

The figure shows that the engine is connected to the planetary Carrier, the first electric machine is attached to the Sun gear, the second one is connected between the Ring gear and and the Reduction gear.

The MGU2 functions are to supplement the engine torque, thus allowing the engine to operate in greater efficiency regions.

With the following generations of Prius, Toyota developed more sophisticated systems, starting from the 2010 they produced the III generation of the Prius using the new version of this system, named Hybrid Synergy Drive (HSD), then this power-train has been widely used in Toyota and Lexus hybrid line-ups and licensed to Ford and Nissan.

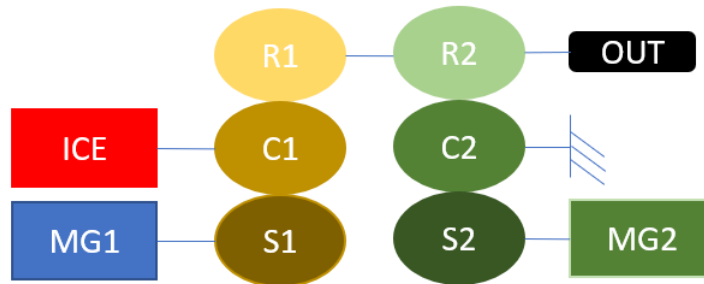


Figure 1.6: Representation of the HSD Power-Split Power-train Architecture.

The main difference introduced is the second power-split device and the removal of the chain connected to the final drive [[12],[18]].

There are other architectures that have been developed, such as one on SUVs Lexus RX450h and Toyota Highlander for all-wheel drive (AWD) using a third electric machine (MGR) on the rear axle.

By coordinating the motor and generator output, the power-split power-trains realize electric-only mode, engine start mode, motor assist mode, battery charging mode, and regenerative braking mode.

The more complex the architecture the more possibilities of different modes to save energy for different driving situations are available but also the design and the construction costs will increase.

As samples of this category we can find in the market the following models: Lexus RX450h, Toyota Camry, Ford Fusion Hybrid FWD, Toyota Prius.

1.3.5 Two-mode Powertrains

The introduction of clutches permits to improve the transmission flexibility and other modes compared to the power-split system, this enables the two-mode hybrid transmission to achieve improved fuel economy and uncompromising performance at both low and high vehicle speed.

One of the first architecture in this category is the one developed by General Motors which patented the Allison hybrid system that you can see in the next figure:

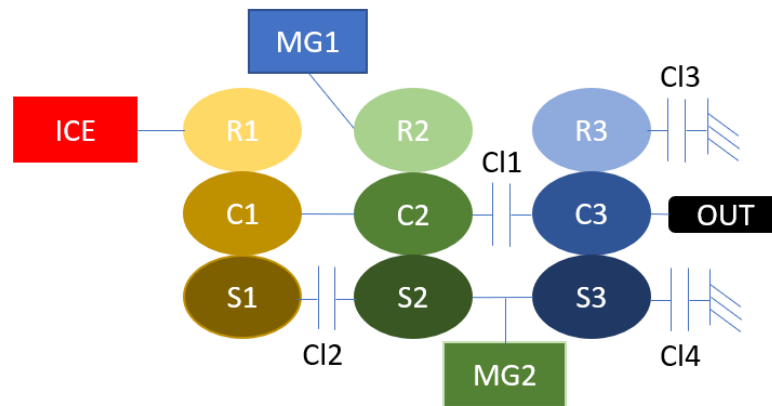


Figure 1.7: Representation of the GM's Allison Two-Mode Power-train Archit.

The transmission of Allison is made of three PG sets and two continuous variable transmission modes and four fixed-gear ratio modes. In the following table there is the scheme to see the configuration of each mode:

		Cl 1	Cl 2	Cl 3	Cl 4
CVT modes	Input-split			x	
	Compound-split	x			
Fixed gear ratio modes	1st Fixed gear		x	x	
	2nd Fixed gear	x		x	
	3rd Fixed gear	x	x		
	4th Fixed gear	x			x

Table 1: Two-mode Hybrid Transmission Operation Modes

The Input-split mode is achieved by engaging Clutch 3 while disengaging all other clutches. In this configuration the first machine serve as the speed coupler to regulate engine speed while the MG2 serve as the torque coupler to regulate engine torque, decoupling the engine from the output shaft, and so increasing the engine efficiency.

This is a low-speed driving mode mostly. Higher speed will increase the losses by the energy conversion [[12], [19]].

The compound-split mode is achieved by engaging Clutch 1 and disengaging all other clutches. All the planetary gear sets function as power split devices to split and adjust the power ratio between the electric power path and the mechanical power path.

The engine speed and torque are regulated by both electric machines.

This mode has higher efficiency at higher vehicle speed due to the lower power ratio on the electric path.

To use a fixed gear ratio mode is necessary to use two clutches at the same time, for example the combination can increase the output torque for the first gear or to make a transient between the input-split and the compound-split modes.

The GM's two-mode transmission can switch from the continuously variable modes to fixed gears ratios.

We can see this architecture in models such as: Mercedes ML450, Chevrolet Tahoe, BMW Active Hybrid X6.

2 Physical Model

This chapter will explain the physical models used in Matlab to define the controller, first will analyze the simplified road load model used, then the focus would be on the different components of the power-train architecture, at the end there will be a presentation of how would be scaled and sized the components for the research in the design space implemented in the optimization algorithm.

All the data are from online sources or from the libraries of AMESIM, so are public and trustworthy.

2.1 Road Load Model

This simplified Road Load Model use the contribution of three forces: the rolling resistance F_{roll} , the air drag resistance F_{air} and the gravity resistance due to the slope of the road F_{grade} .

We obtain the following equations:

$$F_{road} = F_{roll} + F_{air} + F_{grade} \quad (2.1)$$

$$F_{roll} = \mu m_v g \quad (2.2)$$

$$F_{air} = \frac{\rho A_f C_d v^2}{2} \quad (2.3)$$

$$F_{grade} = m_v g \sin(\alpha) \quad (2.4)$$

Are reported the three components (2.2,2.3,2.4), in which m_v is the vehicle mass, μ is the rolling resistance coefficient, g is the acceleration of gravity, ρ is the air density, A_f is the vehicle frontal area, C_d is the drag resistance coefficient, v is the vehicle longitudinal speed given by the driving cycle, α is the road slope angle.

Normally is easier to get three parameters, coast-down coefficients [20], to express the road force related with the velocity and the velocity square, this model can be less precise than the other but require less parameters.

In this case the equation would be:

$$F_{road} = R_{LA} + R_{LB} \cdot v + R_{LC} \cdot v^2 \quad (2.5)$$

From the eq. 2.5 is possible to calculate the torque needed by the wheel:

$$T_{load} = \frac{F_{road} \cdot r_{dyn} + \frac{I_v \cdot a}{r_{dyn}}}{K} \quad (2.6)$$

In this equation are used: r_{dyn} the dynamic radius of the wheel in meter, I_v the vehicle inertia, a the longitudinal acceleration, K the final drive ratio [21]. To compute the acceleration in the eq. 2.6 is possible to use the continuous derivative of the velocity imposed by the driving cycle, we are using the forward difference approximation, using the ΔT as time interval between $(i + 1)$ and (i) :

$$a(i) = \frac{v(i + 1) - v(i)}{\Delta t \cdot K} \quad (2.7)$$

In the model we will use two sets of parameters, the first one is of a general mid-size vehicle from AMESIM, the second one is referred to a general Mini SUV model, all the values are listed here:

Data	Unit	Mid-size	Mini SUV
M_v	kg	1400	2381
r_{dyn}	m	0.301	0.358
R_{LA}	N	100	158
R_{LB}	$N/\frac{m}{s}$	3.00	3.25
R_{LC}	$N/(\frac{m}{s})^2$	0.15	0.36

Table 2: Vehicles Data

2.2 Powertrain Components Model

In this section we will show the model used for the components of the vehicles chosen, in particular we will discuss about the ICE, the MGU and the Battery.

All the data are taken from AMESIM libraries, from there in the next section we will present how we found some relations to size the component in a specific range.

It's important to specify that the controller has been developed starting from a specific set of components from the libraries, once was set up we started changing the components to test it.

2.2.1 ICE Model

The map used for the ICE can be seen in figure:

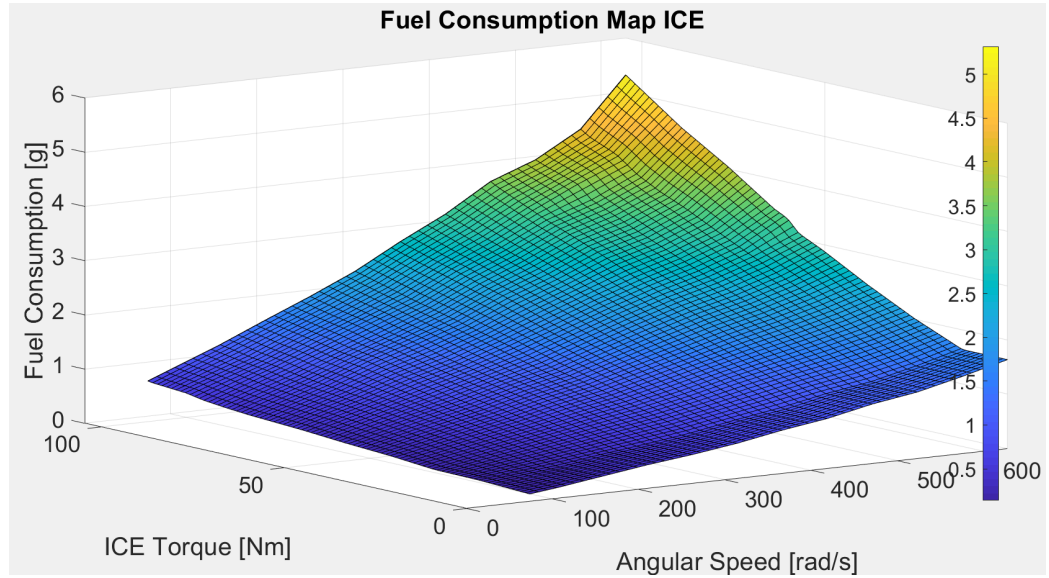


Figure 2.1: Ice Fuel Losses Map

The map shows the Fuel Losses in grams as function of the ICE torque and angular speed, from these data is possible to calculate the efficiency of each point with the following formula:

$$\eta_{ENG_i} = \frac{P_{OUT_i}}{P_{IN_i}} = \frac{P_{IN_i} - P_{Losses_i}}{P_{IN_i}} = \frac{T_i \cdot \omega_i}{\dot{m}_{fuel_i} \cdot LHV_i} \quad (2.8)$$

In the equation T_i is the Torque, ω_i is the angular velocity, \dot{m}_{fuel_i} is the injected fuel flow rate of the ICE and LHV is the fuel lower heating value. The other data needed for the ICE are about the maximum torque achievable with the wide open throttle function of the angular speed, obtaining the following graph:

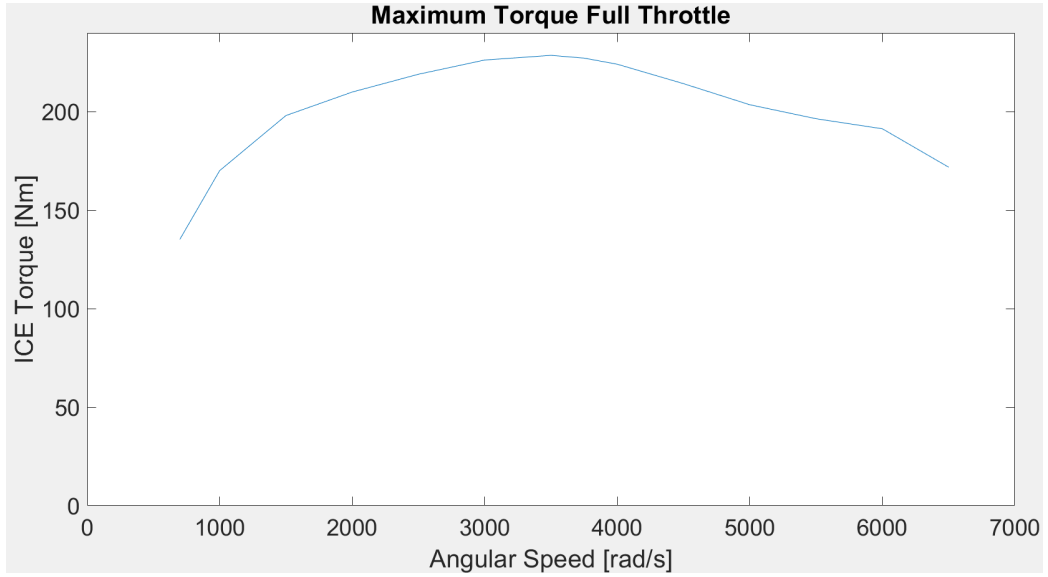


Figure 2.2: ICE Maximum Torque

These data will be used to calculate the opening percentage of the throttle and to control if the gear is the right one for the torque requested. Here we present the starting values of the two ICE of the vehicles from which we developed the A-ECMS controller:

Parameter	Unit	Mid-size	Mini SUV
V_d	m^3	1.6	3.3
P_{ICE}	kW	67	188
LHV	J/g	43700	
ρ_{fuel}	g/l	737	

Table 3: ICEs Data

2.2.2 MGU Model

Our controller will use the Fuel losses and the Maximum torques showed before for his calculations.

For the MGU we need similar data, the first thing is to get the Efficiency Map or the Losses Map, for our controller we will use the losses.

The losses are due to the electro-magnetic phenomena and to the mechanical dissipation and frictions.

The Map is shown in the next figure:

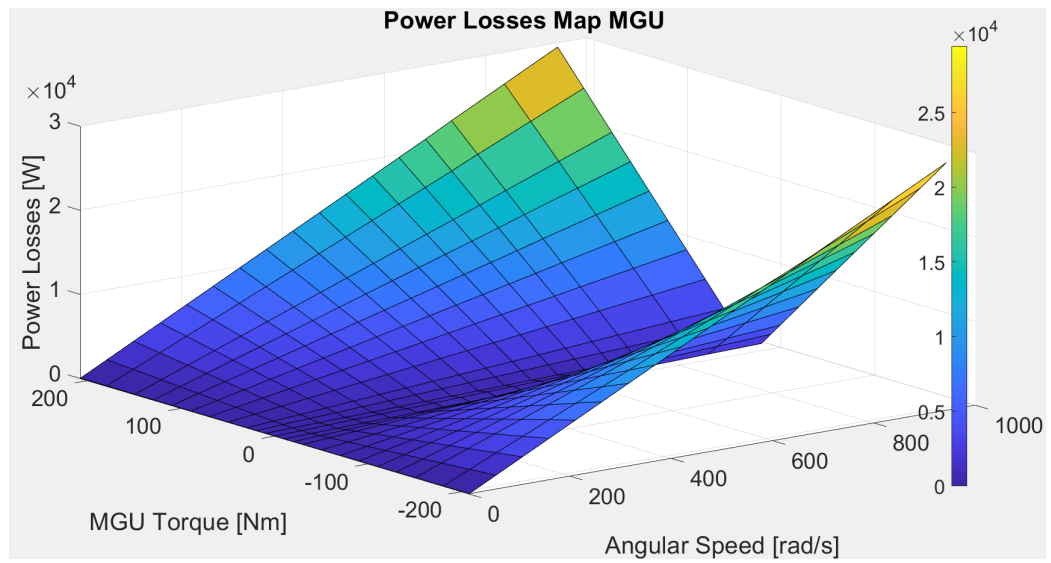


Figure 2.3: MGU Power Losses Map

As shown for the ICE, also in this case is possible to obtain the efficiency for each point with the following equation:

$$\eta_{MGU_i} = \frac{P_{OUT_i}}{P_{IN_i}} = \frac{P_{IN_i} - P_{Losses_i}}{P_{IN_i}} = \frac{T_i \cdot \omega_i}{T_i \cdot \omega_i + P_{Losses_i}} \quad (2.9)$$

We can plot the same curve of the maximum torque function of the angular speed also for the MGU, and here is how it looks like:

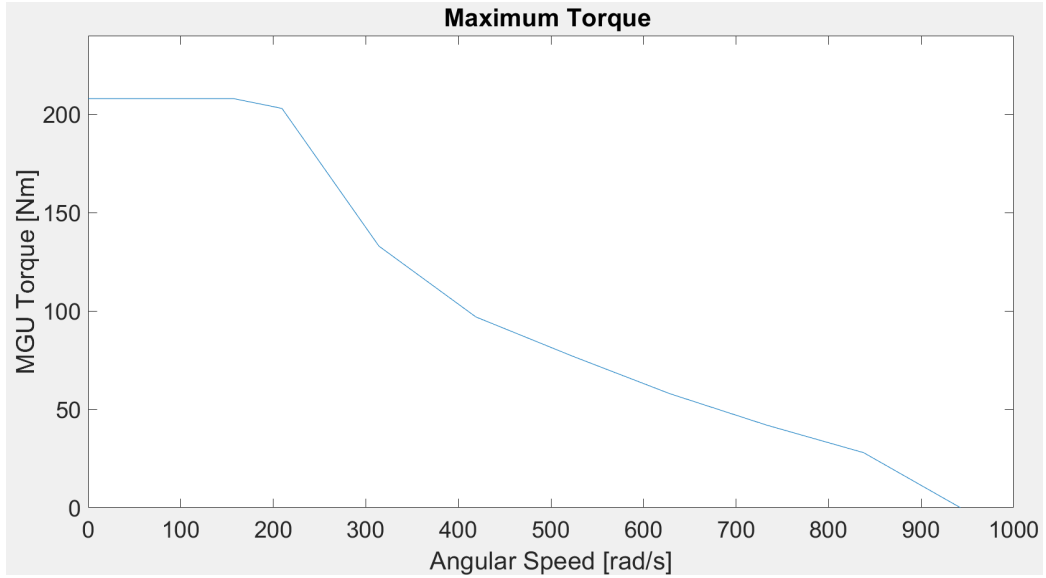


Figure 2.4: MGU Maximum Torque

We would need these data for the same purpose of the ones of the ICE. Here we present the starting values of the MGU used for both the vehicles from which we developed the A-ECMS controller:

Parameter	Unit	Mid-size	Mini SUV
P_{MGU}	kW	40	85
T_{max}	Nm	200	
n_{max}	RPM	9000	

Table 4: MGUs Data

2.2.3 Battery Model

For the Battery model we would use a simple equivalent circuit based on the Open Circuit Voltage (OCV) indicated by the V_{oc} parameter. The circuit will be the following:

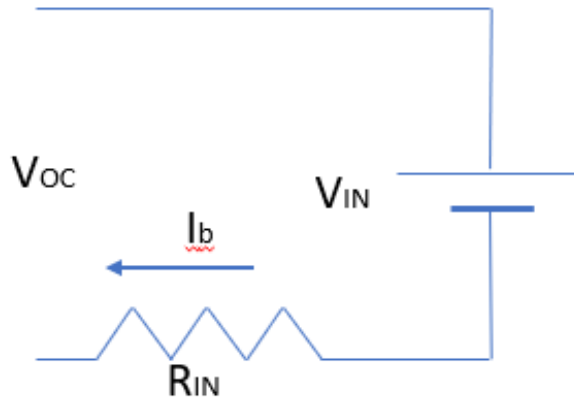


Figure 2.5: Battery Model

The OCV and the Battery Resistance are both functions of the State of Charge (SOC), temperature and State of Health (SOH) of the battery. We got these data from a library of AMESIM and here is their trend:

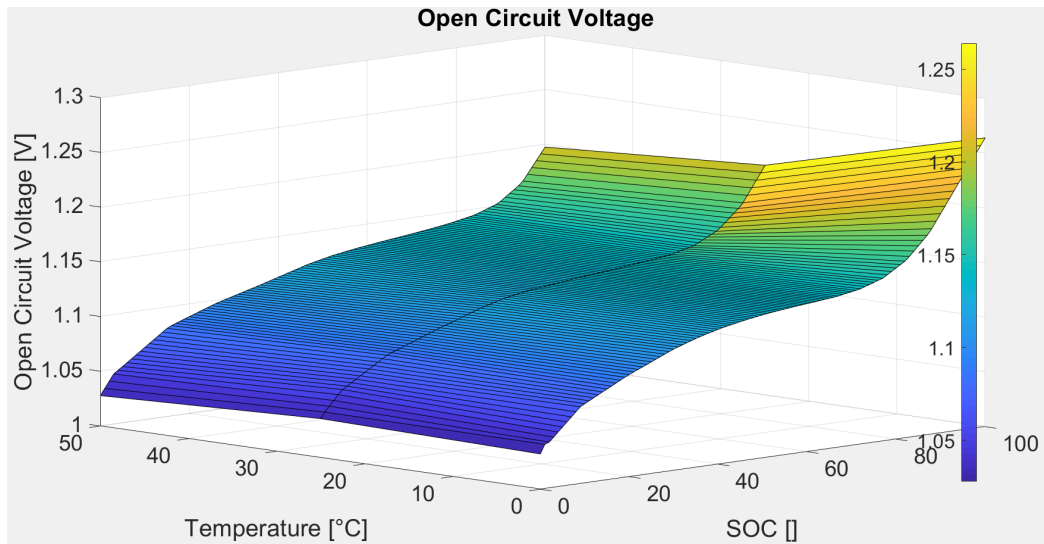


Figure 2.6: Open Circuit Voltage Map

And also the same for the Internal Resistance of the Circuit:

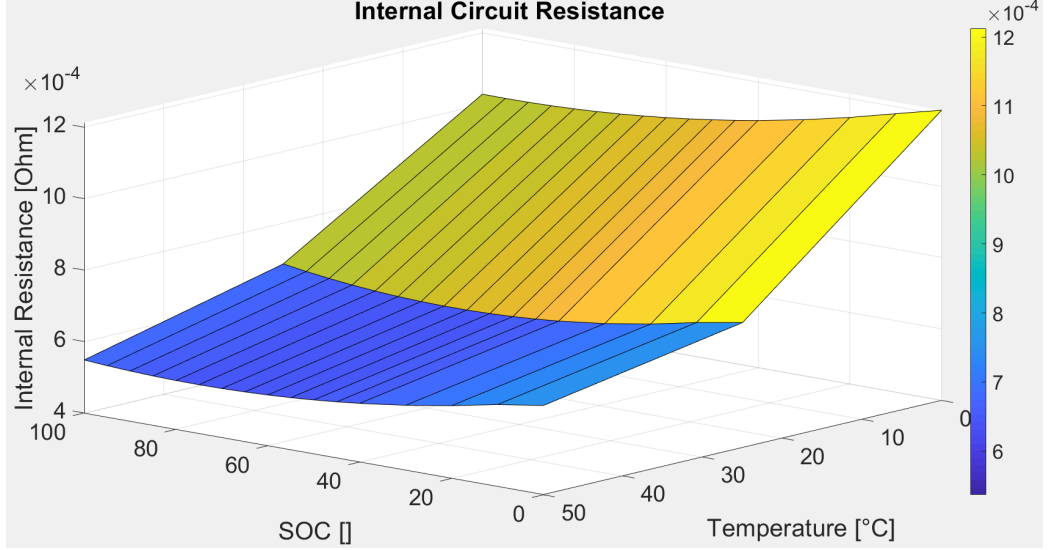


Figure 2.7: Internal Circuit Resistance Map

In our case we are assuming that the parameters during the charging and the discharging are the same, so the OCV and the Internal Resistance would be the same while charging or discharging. With these data we can compute the other parameters:

$$V_{OC} = V_{IN} - R_{IN} \cdot I_b \quad (2.10)$$

$$P_{batt} = \frac{V_{OC}^2 - V_{OC} \cdot \sqrt{(V_{OC}^2 - 4 \cdot P_{inv,DC} \cdot R_{IN})}}{2R_{IN}} \quad (2.11)$$

$$I_b = \frac{V_{OC} - \sqrt{(V_{OC}^2 - 4 \cdot P_{inv,DC} \cdot R_{IN})}}{2R_{IN}} \quad (2.12)$$

$$E_{batt}(t) = E_{batt}(t_0) - \int P_{batt}(t) dt \quad (2.13)$$

$$SOC = \frac{E_{batt}(t)}{E_{batt,nom}} \quad (2.14)$$

With these equations we can compute all the parameters needed during the mission, we can also compute an efficiency of the battery to see the performance in each instant:

$$\eta_{batt_{charg}} = \frac{V_{OC} \cdot I_b}{P_{batt}} = \frac{V_{OC} \cdot I_b}{V_{OC} \cdot I_L - R_{IN} \cdot I_b^2} \quad (2.15)$$

$$\eta_{batt_{discharg}} = \frac{P_{batt}}{V_{OC} \cdot I_b} \quad (2.16)$$

As told before we started developing the controller with some specific values, and then we have tested it with generalized parameters. Here we enlist the starting values for the battery of the two vehicles:

Parameter	Unit	Mid-Size	Mini SUV
V_{OC}	V	310	310
P_{target}	kW	75	150
E_{target}	kWh	20	40

Table 5: Vehicles Data

2.3 Sizing Components Strategy

In this section we will show an overview of the procedure developed to size each of the component showed before.

In all the cases we have started with the real data in our possession, from there we have evaluated how was possible to scale the size of the component only changing one parameter that then we can insert in the optimization algorithm [22].

Is not easy to select the right range in which this scaling procedure is still working properly, because there are linear quantities but most of the parameters are not linear and in particular change second totally different laws.

Fortunately we can check if the parameters of the scaled component are similar to the real one using the libraries of AMESIM, in which are developed some sophisticated tools from which it's possible to get different components changing the interesting parameters.

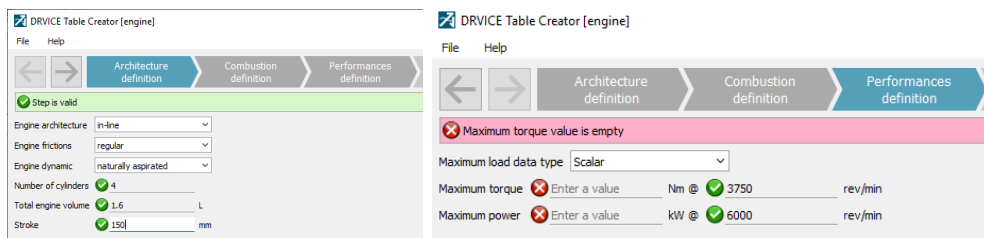
For these reason we will specify in which range we have seen that the components have parameters similar to the real ones and so can be useful for our research in the design space.

As before we will subdivide the work for each component.

2.3.1 ICE Sizing

The evaluation of the parameters of the ICE and their relations to obtain the data that we need are made after reading the consideration about sizing an ICE basing all the calculations on the total displacement at the different angular speeds[23] [24].

Then to obtain all the models we used as a base, the data obtained from the AMESIM tool using these parameters:



(a) Architecture Parameters

(b) Performance Parameters

Figure 2.8: Setting of the ICE parameters

We have used engines with a fixed proportion between the maximum torque developed and the maximum power, fixing the number of RPM in which we can obtain these two values:

$$T_{MAX} = P_{MAX} \cdot 1.85 \quad (2.17)$$

For the ICE we will need the maximum torque developed by the ICE at different angular speeds, in case of full throttle, from the graph would be possible to inter-pole the percentage needed of throttle knowing the torque requested and the angular speed. Here we can see the comparison between the model obtained from the data and the curve exported from the data of AMESIM for an ICE with a maximum torque of 230 Nm:

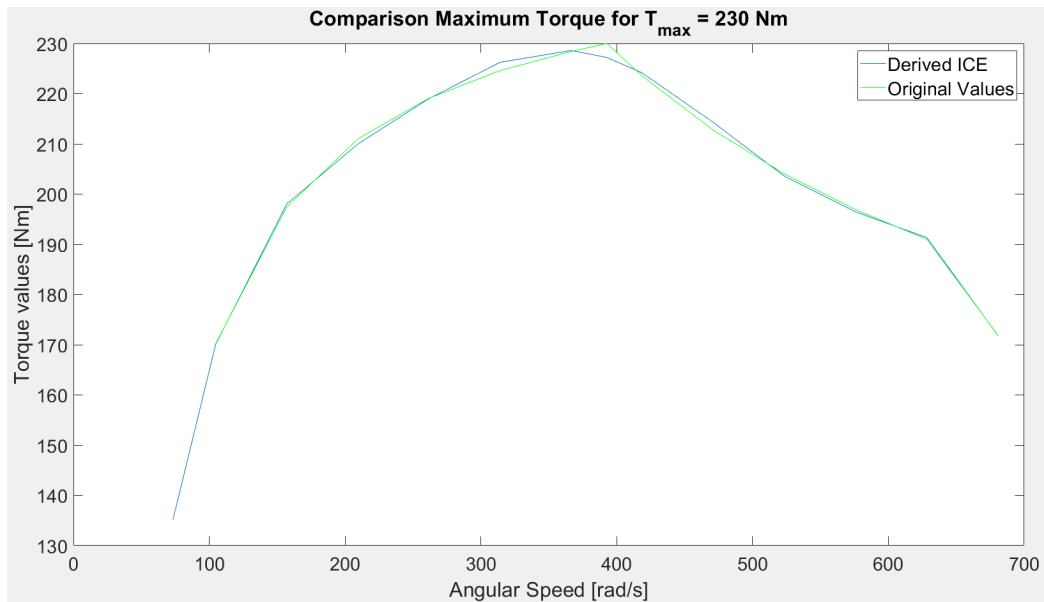


Figure 2.9: Maximum Torque ICE Model Comparison

As we can see from the figure the derived model is pretty similar to the original one, there is a little gap around 400 rad/s between the curves, precisely of 2.8 Nm (1.2% error), so we can say that the model is pretty accurate. We obtained this model fitting the data with a polynomial curve of the 6th order. We can obtain results with this kind of error between the original one and the modeled one in this range of values for the maximum torque and power:

$$\begin{aligned} 120 \text{ Nm} < T_{MAX} < 360 \text{ Nm} \\ 65 \text{ kW} < P_{MAX} < 200 \text{ kW} \end{aligned}$$

The next data needed are for the fuel consumption extracted from the fuel consumption map, to obtain a model sufficiently reliable we need to subdivide the data for each angular speed and obtain the pattern of the curve, we did that for 15 different values of the angular speed and we can show one example of the result at a fixed speed $n = 3500$ *RPM*:

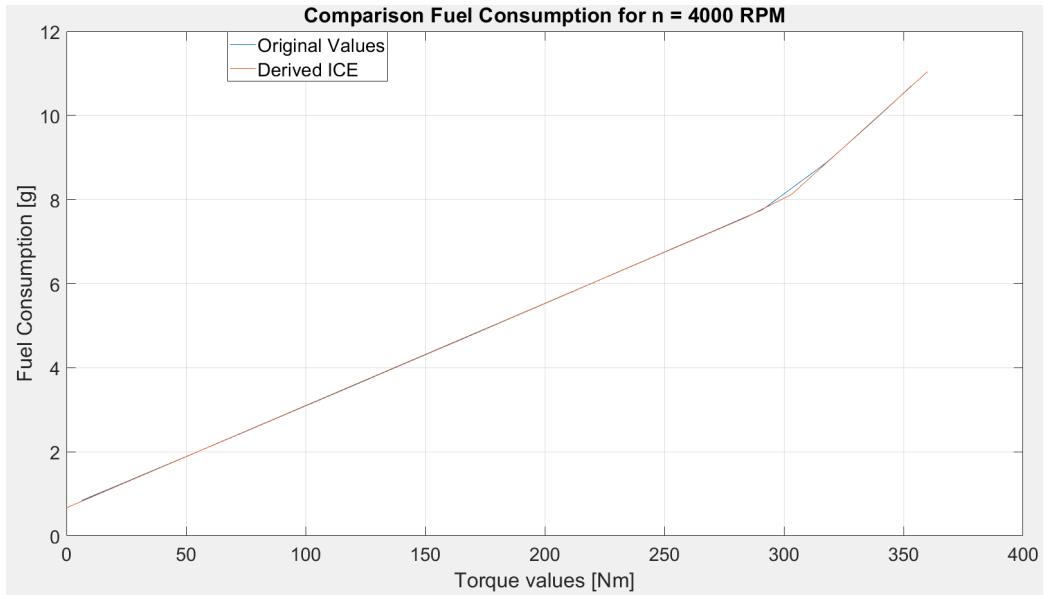


Figure 2.10: Fuel Consumption ICE Model Comparison

We can notice that the curve is composed by two straight lines, the maximum error is around the connection of the two lines, is around 0.12 g at 125 Nm torque (4.5 % error).

We noticed the same behavior for all the other angular speeds and we obtained the relative curves from which we can create the fuel consumption table used in the controller.

Also these values are really similar in the range that we said before for the model and the original data, in particular we noticed that the fuel consumption of the original model is only related with the maximum torque and not with the power, instead the maximum torque curve is related with both parameters.

To use these data we created a Matlab function that with only the input of the maximum torque, related as said before with the power, can create the lookup tables for the ICE.

2.3.2 MGU Sizing

The evaluation of the parameters of the MGU and their relations to obtain the data that we need are made after reading the consideration about sizing a GMU [25] [26].

To obtain all the models we used the data obtained from the AMESIM tool using these parameters:

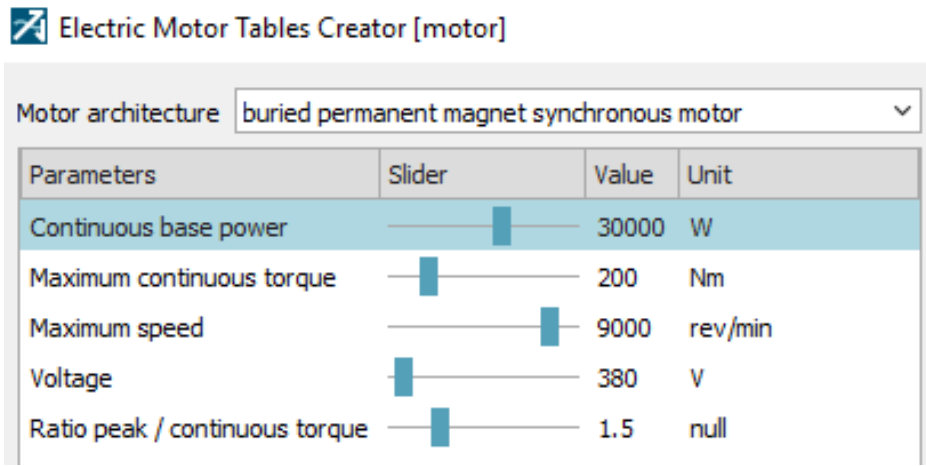


Figure 2.11: Setting of the GMU Parameters

We will keep the same continuous torque, maximum speed, voltage and ratio peak-continuous torque, varying the continuous base power.

Similarly to the ICE, the first set of data are for the maximum continuous torque of the GMU, here we will show the comparison for $P_{GMU} = 40 \text{ kW}$:

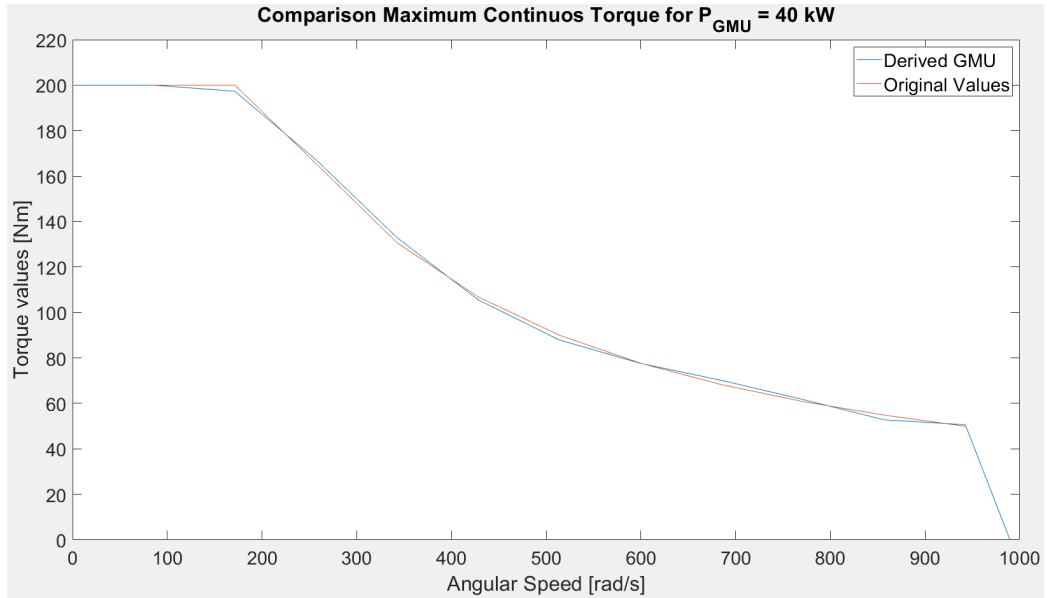


Figure 2.12: Maximum Torque GMU Model Comparison

As we can notice the two curves are really similar, we can observe that the maximum error is of 2.7 Nm around 170 rad/s (1.3% error).

We obtained this model fitting the data with a polynomial curve of the 3th order. We can obtain results with this kind of error between the original one and the modeled one in this range of values for the maximum continuous power:

$$20 \text{ kW} < P_{MAX} < 50 \text{ kW}$$

The next data needed are for the efficiency or the Power losses of the GMU, in this case we used an approach similar to the ICE one, subdividing the data on the torque and obtaining all the different curves, it's important to notice that the parameters for angular speed $n = 0 \text{ RPM}$ or $n = 700 \text{ RPM}$ are not related with the maximum power but are constant, the same happens for torque $T = 0 \text{ Nm}$, all these parameters depend on the architecture of the motor and not only on the power.

Here we will show the results of the power losses for the case of $P_{GMU} = 40kW$ and $T = 40 Nm$:

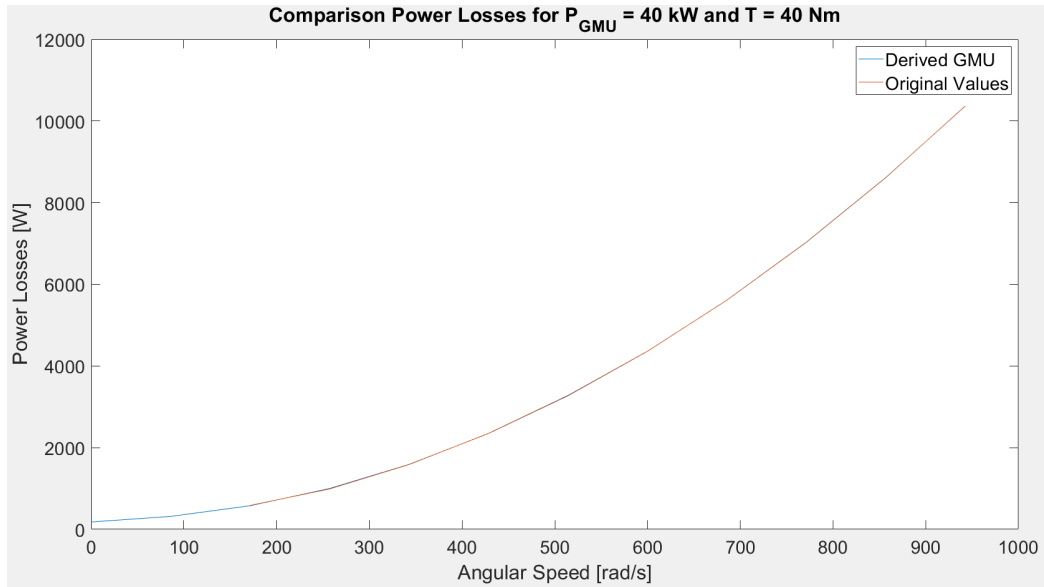


Figure 2.13: Power Losses GMU Model Comparison

We can notice that the two curves are quite overlapped, with a maximum error lower than 1%.

Merging all the curves for the different torques we can obtain the values for the table of the power losses used in the controller. As done before we created a function that needs as input only the maximum continuous power of the GMU to create all the lookup tables for the controller.

2.3.3 Battery Sizing

To developed the model of our battery we have taken in consideration other studies on the battery sizing to find a mathematical relation between the OCV and the SOC and also to see how it is related the internal resistance of the circuit with the other parameters [27] [28].

In the case of the battery we have analyzed the data of different cylindrical LiFePO₄/graphite batteries from the database of AMESIM using the following parameters in the specific tool there to create to different kind of batteries:

Parameter	Unit	Battery 1	Battery 2
Voltage Target	V	380	
Power Target	kW	50	75

Table 6: Battery Data

In both cases starting from the data we have obtained the curve for the OCV related to the SOC and we can show an example of one of the battery at $T = 40^{\circ}C$:

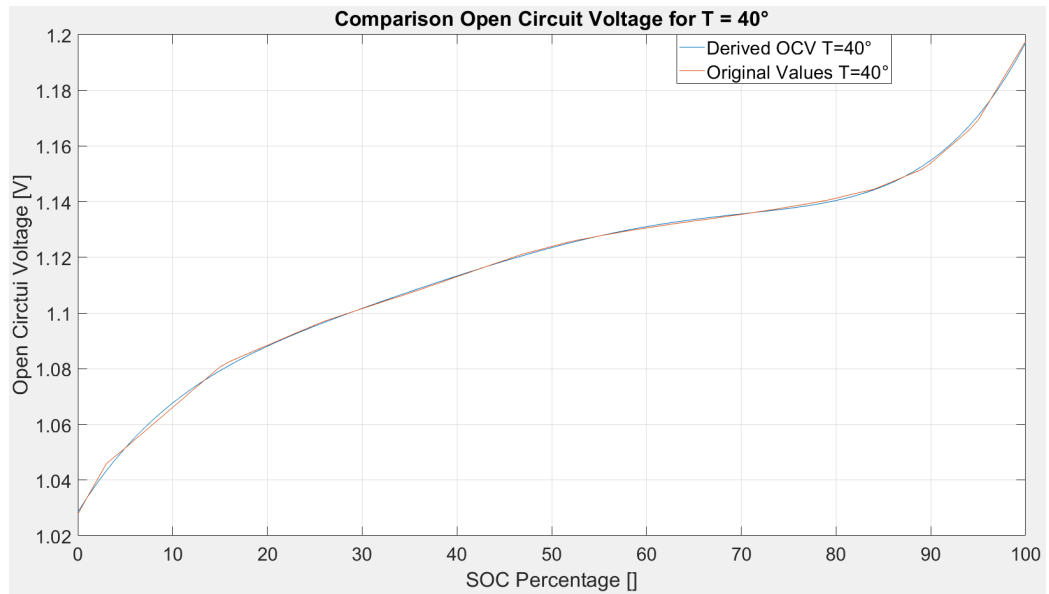


Figure 2.14: Open Circuit Voltage Trend

We can see that the two graphs can differ for no more than 0.002 V with an error lower than 1%. We obtained this model fitting the data with a polynomial curve of the 5th order.

In the two cases we can use the following ranges of Energy Target to can use this model with an error similar to the one showed:

Parameter	Unit	Battery 1	Battery 2
Energy Target	kWh	$2 < E < 10$	$5 < E < 15$
Temperature	°C	$20 < T < 40$	

Table 7: Functions Battery Range

The next step is to analyze the behavior of the internal resistance in all the range of the parameters shown before, here we have the comparison for the Battery 2 with $E_{Batt} = 15 kWh$:

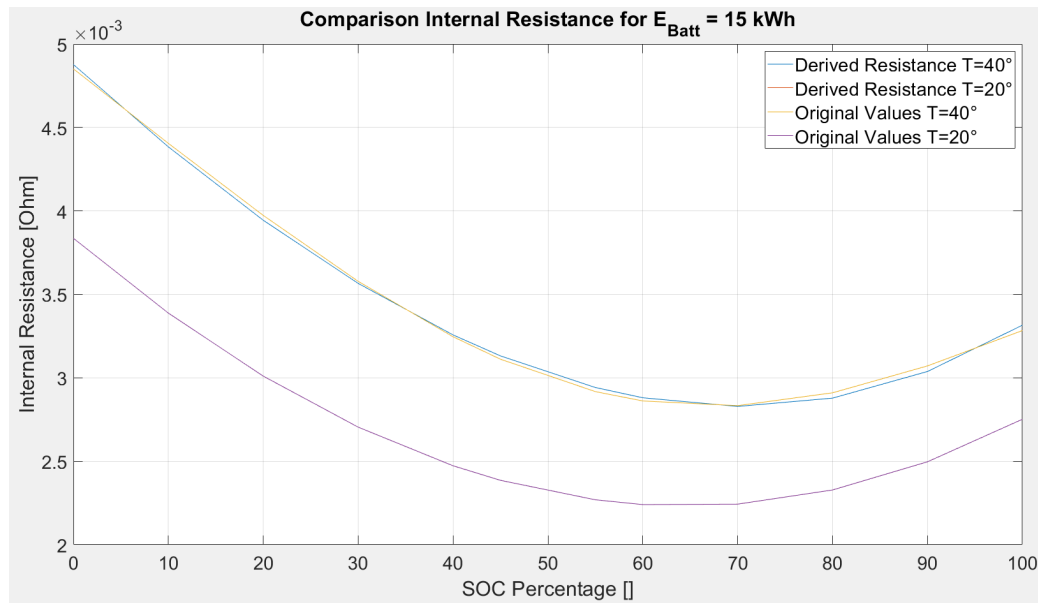


Figure 2.15: Internal Resistance Trend

We can notice from the figure that the curves for $T = 20^\circ\text{C}$ are seems overlapped, the derived curve for $T = 40^\circ\text{C}$ is really close to the original one. All the intermediate temperature would be the result of the interpolation between these two main curves. We obtained this model fitting the data with

a polynomial curve of the 5th order.

Also in this case we created a function that needs as inputs the chosen Model, the Temperature and the Energy Target of the battery, it will generate all the data about OCV and Internal Resistance needed.

3 Energy Management Strategy

In this section we will explain what is the aim of an Energy Management Strategy (EMS) and which kind of different strategies are used for the HEVs, what are usable in the real driving and why [2][29][30][31].

The EMS is a control strategy used for HEVs to decide the strategy on a mission on a precise circuit, in particular is necessary to decide for each time-step what components has work and how, respecting all the constrains due to the components architectures.

In our case we have to manage the components of a Parallel (P2) Hybrid Vehicle that has an ICE, a MGU, a Battery, the transmission and the final drive.

To develop a controller with one of these strategies are used some different driving cycles [32][33], here we will enlist the cycles used to elaborate the controller:

- Artemis Rural Driving Cycle (ARDC);
- Artemis Urban Driving Cycle (AUDC);
- Highway fuel economy test (HWFET);
- Japanese 10-15 mode cycle (J1015M);
- Japanese JC08 Cycle (JC08);
- Los Angeles Cycle (LA92);
- New European driving cycle (NEDC);
- New York City Cycle (NYCC);
- SC03 Supplemental Federal Test Procedure (SC03);
- Urban Dynamometer Driving Schedule (UDDS);
- US06 Supplemental Federal Test Procedure (US06);
- Worldwide harmonized light vehicles test procedure (WLTP).

In the initial phase we have studied all the different cycles to have more data to elaborate and from which get the information needed to develop the A-ECMS, then we have decided to select the most various driving cycles and

the most relevant ones.

All these cycles are not taking into account the grade of the street, we will show some results of the strategy with some driving cycles elaborated from some researchers of the "Politecnico di Torino" that are recorded in Turin with also the altitude of each time step from which we can obtain the grade of the street.

Here we show the velocities from the WLTP cycle to have an example of how could be one of these cycles:

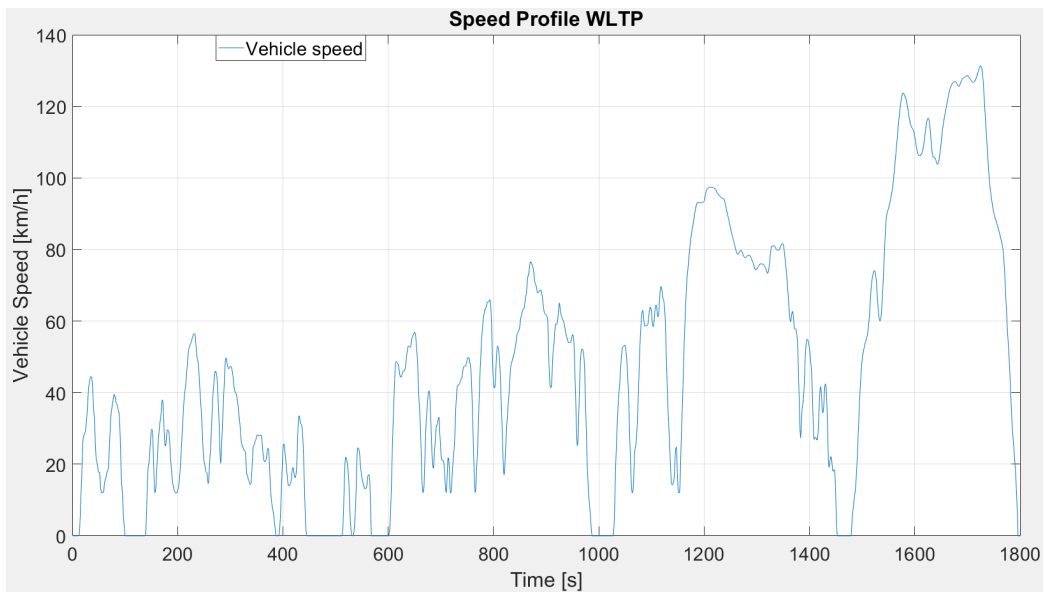


Figure 3.1: WLTP Speed Profile

Going back to talk about the EMS, theoretically optimal control of more than one energy sources at all time-steps, given that driver's power request is satisfied, will engender a non-linear constrained optimization problem [2]. For this reason there are many different control strategies to solve this non-linear problem, we can subdivide the in two different categories:

Global Optimal Controls and Local Optimal Controls.

- The first category includes the strategies that will analyze the velocities of the mission knowing both the past and the future steps, in this way is possible to find the best solution possible for that vehicle in that specific circuit with that velocities;

- The second one that will find the best solution only with the past information of the vehicle, in this case based on the research space for the controller we will obtain our maximum.

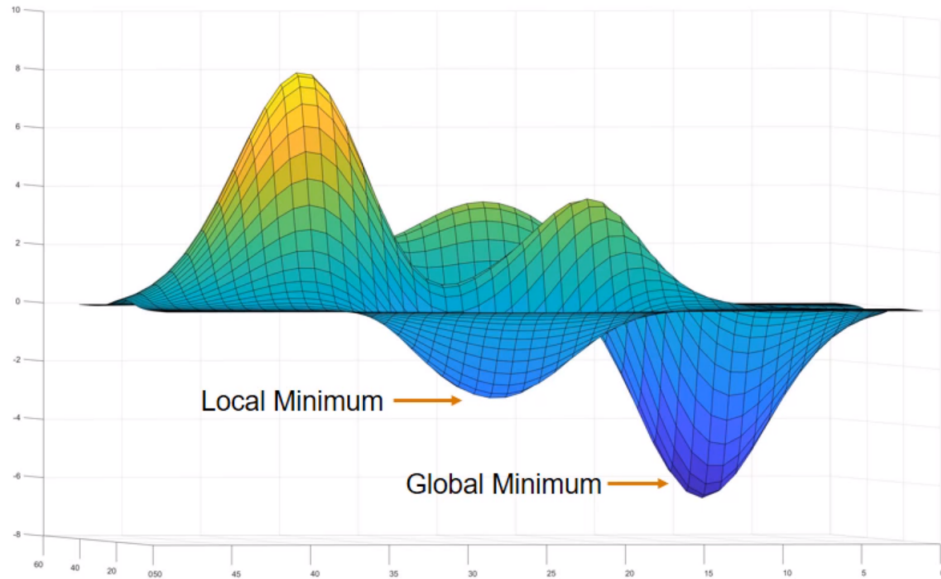


Figure 3.2: Global Minimum and Local Minimum Representation

We can call the first one also Offline Control Strategy and the second one Online Control Strategy, we will see more details in the following sections. In particular we will focus on the A-ECMS that is an online control strategy that can be used in a real-driving situation and implemented in the vehicles currently on the market.

Developed from the standard ECMS that is not suitable for this purpose, due to the parameters that need to be tuned for different driving situations, compared to the Rule Based strategy that is currently used in the HEVs shows really good result for the management of the vehicle, with less FC and the possibility to decrease the pollutant emissions.

In all the following cases we can study the dynamic system with two decoupled states, which are the vehicle longitudinal speed and the battery SOC.

$$x(t) \in R \quad x(t) = SOC \quad (3.1)$$

Since are mutually independent, the vehicle speed would be separately controlled from the battery SOC that is used as a state variable [eq. 3.1].

The problem has the following constraints:

- Initial and Final value of the state variable:

$$x(t_0) = x(t_f) = x_0 \quad (3.2)$$

- Instantaneous restriction on the variable:

$$x_{min} \leq x(t) \leq x_{MAX} \quad (3.3)$$

- Physical constrains due to the power-train limits and driving cycle requirements

$$\begin{cases} P_{GMU}(t) + P_{ICE}(t) \geq P_{OUT}(t) \\ \omega_{ICE}^{min} \leq \omega_{ICE} \leq \omega_{ICE}^{MAX}, \quad T_{ICE}^{min} \leq T_{ICE} \leq T_{ICE}^{MAX} \\ \omega_{GMU}^{min} \leq \omega_{GMU} \leq \omega_{GMU}^{MAX}, \quad T_{GMU}^{min} \leq T_{GMU} \leq T_{GMU}^{MAX} \end{cases} \quad (3.4)$$

In general according to the control theory we can define a control variable $u(t)$ [eq. 3.5] leading to the minimization of the cost function [eq. 3.6] in a continuous interval $t_0 \leq t \leq t_f$. In our case the control variable would be a general function of the battery power.

$$u(t) \in R^k \quad u(t) = \{P_{Batt}(t)\} \quad u(t) \in U(t) \quad (3.5)$$

$$J(x(t_0), u(t), x(t_f)) = \Phi(x(t_0), x(t_f)) + \int_{t_0}^{t_f} L(x(t), u(t), t) dt \quad (3.6)$$

The first term of the cost function identifies the cost linked to the final value of the state variable $x(t)$, while the second term denotes the instantaneous cost.

In the EMS the aim is to reach the CS so that the final cost is equal zero, this would be the aim of the battery strategy from which we can ensure the CS.

To define the dynamic of the system we will focus on the evolution of the state variable as follow:

$$\dot{x}(t) = f(x(t), u(t)) \quad (3.7)$$

This equation will keep trace of the battery SOC variations as function of the control variable and it depends by the battery model adopted in the strategy. According to the model showed before in chapter 2.2.3 we can use the following equation for the system evolution:

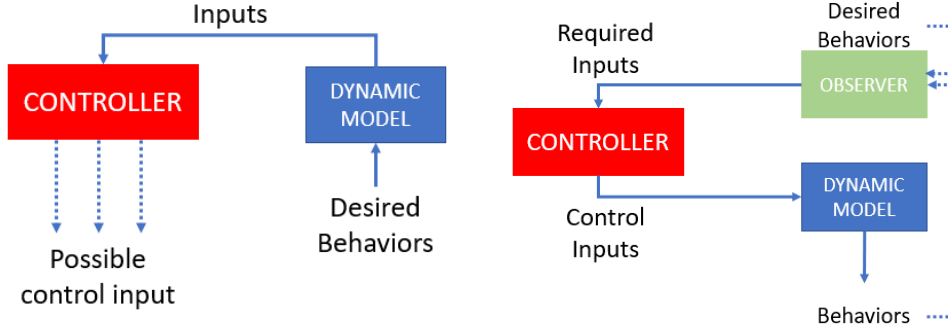
$$\dot{x}(t) = -\frac{1}{Q_{nom}} \cdot \frac{V_{OC}(x) + \sqrt{V_{OC}(x)^2 - 4R_o(x) \cdot P_{Batt}(t)}}{2R_o(x)} = f(x, P_{Batt}) \quad (3.8)$$

It is important to notice as said before that the model used in Matlab is a quasi-static model that not take into account of some minor dynamic phenomena affecting the fuel consumption in a minor extend, for that is interesting to see the comparison with the results from a dynamic model.

Before starting to illustrate the different strategies it's important to distinguish between two kind of control flows [34]:

- Backward-looking Model: the dynamic model calculates the exact input required to produce a desired behavior, in this way the controller can test different control sets that satisfy the required input. In case we have to test different combination of power split among the components this way is method is favorable
- Forward-looking Model: is allowed only one control input per time, otherwise are required parallel calculations, this model needs an observer to compare the desired behavior with the obtained one. This model can be implemented in a real-time logic comparing the data obtained with the desired ones. Can also be suitable for more sophisticated models with an higher fidelity grade due to the lower computational efforts of the model.

In the following figure there is a schematic representation of the two different flows:



(a) Backward-looking Model

(b) Forward-looking Model

Figure 3.3: Comparison Backward and Forward Looking Models

3.1 Offline Control Strategies

As told before we can call this category Global Optimum or Offline Control Strategy, because the controller can examine all the circuit and do all the calculation to find the best possible solution, without taking care about the computational time.

For the fact that is not a predictive strategy all the efforts are focused about the best combination possible of all the components and their parameters.

In this category there are many different strategies developed in the last years starting from mathematical principles and applying them to the Automotive sector and in particular to the HEVs world.

In general an optimal control problem in a continuous spatial coordinate s is:

$$\left\{ \begin{array}{l} \underset{u}{\text{minimize}} \quad \int_{s_i}^{s_f} f_0(s, \mathbf{x}(s), \mathbf{u}(s)) ds + \phi(\mathbf{x}(s_f)) \\ \text{subject to} \quad \frac{d\mathbf{x}}{ds} = f(s, \mathbf{x}(s), \mathbf{u}(s)) \\ \mathbf{x}(s_i) \text{ given} \\ \mathbf{x} \in \mathbf{X}(s) \\ \mathbf{u} \in \mathbf{U}(s) \end{array} \right. \quad (3.9)$$

Where s_i is the initial position, s_f is the final position, \mathbf{x} is the state vector, \mathbf{u} is the control vector, f_0 is the cost function, f is the vector field which gives the dynamics, $\mathbf{X}(s)$ is the set of admissible states as a function of the position s and $\mathbf{U}(s)$ is the set of admissible controls a a function of the position [35].

3.1.1 Dynamic Programming

This mathematical optimization method was developed by Richard Bellman in the 1950s [36], can be used to solve problems where occurs sequential decision making, meaning that every action lead to and evolution of the state acquiring a reward.

As said is a method that can lead to the global optimum (eq. 3.9), since is a sequential optimization problem that we can express as follow:

$$x_{k+1} = F_k(x_k, u_k), \quad t = t_k \quad \text{with } k = 0, 1, \dots, N - 1 \quad (3.10)$$

The objective is to find the optimal control strategy π minimizing the discretized cost function J:

$$J_0(\pi) = \phi(x_N) + \sum_0^{N-1} L(x_k, u_k, t_k) \quad (3.11)$$

$$\pi^* = \arg \min_{\pi} J_0(\pi) \quad (3.12)$$

Dynamic programming is based on the "Principle of Optimality", cause the algorithm minimizes the cost function from the starting point till the end of the discretization. Is analyzed every possible alternative, in this sense will lead to the global optimum within an approximation defined by the discretization step, since is a numerical method.

The optimal cost is calculated moving from the last instant of the optimization process up to its initial point [[37]]:

$$J_N^*(x) = \phi(x_N), \quad t = t_k \quad (3.13)$$

$$J_k^*(x) = J_{k+1}^*(x) + \min_{u_k \in U_k} L(x_k, u_k, t_k), \quad t = t_k \quad (3.14)$$

with $k = N - 1, N - 2, \dots, 0$

The biggest drawback of this strategy is that it cannot be used for the design analysis, due to the computational cost that increase exponentially with the number of states and the number of inputs, in this sense cannot be used to optimize a design parameter, but only with already a predefined architecture. This problem is well know in literature as "Curse of Dimensionality" [38].

Is important to underline that the DP algorithm usually is not used in real applications for HEV controls, due to the fact that needs to know the driving

cycle before, that is why is in this section of the offline control strategies.

To overcome this problem has been developed the Stochastic Dynamic Programming (SDP) that permits to account for casual system perturbations, the result quality is strongly affected by the random process model.

The more sophisticated approaches existing in literature uses a random Markov chain process to derive the future power demand as both function of both current output and vehicle velocity [39].

The main advantage of the DP is to use it as a benchmark for the other strategies to see how close to the global optimum can be, to see the behavior suggested from this strategy to extrapolate some driving rules.

3.1.2 Pontryagin's Minimum Principle

Pontryagin's Minimum Principle (PMP) is an analytic optimization algorithm that can lead to optimal performances for the HEV energy management problem if can operate in a convex area of the battery power and fuel consumption graph, that can be seen also as $S\dot{O}C$ as a concave function of the SOC [34].

The method consists in the minimization at each time step a performance measure, called Hamiltonian function:

$$H\left(x(t), P_{Batt}(t), t, \lambda(t)\right) = -\lambda(t) \cdot f\left(x(t), P_{Batt}(t)\right) + \dot{m}_f\left(P_{Batt}, P_{req}(t)\right) \quad (3.15)$$

$$\dot{\lambda}(t) = -\frac{\partial H\left(x(t), P_{Batt}(t), t, \lambda(t)\right)}{\partial x} \quad (3.16)$$

Where λ is a co-state variable, $f\left(x(t), P_{Bat}(t)\right)$ is a time-derivative function of SOC equation that represent the system dynamics, \dot{m}_f is the best fuel consumption rate according to P_{Batt} .

The optimal control can be obtained from:

$$P_{Batt}^* = \arg \min_{P_{Batt}} H\left(x(t)^*, P_{Batt}^*(t), t, \lambda^*(t)\right) \quad (3.17)$$

To apply the strategy, it is often convenient to introduce some simplifications on the state variable equation. First it can be rewritten considering that the fuel consumption does not depend on the SOC so we get that the the optimal

co-state function λ^* can be calculated as:

$$\dot{\lambda}^*(t) = -\lambda^* \frac{\partial f(x^*(t), P_{Batt}^*(t))}{\partial x} \quad (3.18)$$

The benefits of this control idea is that we can instantaneously determine the optimal control P_{Batt}^* with current information when an optimal co-state λ^* is given.

We can approximate the co-state function to a constant function if is neglected the dependency of the state variable to the system dynamic equation. This would mean that the Internal Resistance and the OCV are considered independent from the SOC and constant, this could be a good approximation only in a short range of SOC, will not work for a Plug-in HEVs or a control of HEV in which is supposed to use a larger range of SOC.

This is the main backwards of this strategy for which is necessary to tune an off-line procedure to create variations in the co-state function to respect the behavior of the values linked with the SOC, otherwise would be suitable also for the on-line control since is considerably lower computational demanding than DP.

3.1.3 Slope-weighted Energy-based Rapid Control Analysis (SERCA)

This method has been introduced recently and is described in this paper [21]. The procedure consists of 3 main phases:

- 1 - Sub-problems Exploration;
- 2 - Generalized Optimal Operating Points Definition
- 3 - Energy Balance Realization

Here we will explain more in the detail in what consists each phase:

- Step 1: after subdivide the main problem in sub-problems, the exploration of the possible solutions can be performed in three sub-stages:
 - Discretization of the control variables: all the data of the variables of the components showed in the previous chapter are discretized based on their resolution;
 - Solutions formation: the combination of the different operating points lead to different solutions that has to respect the physical constrains of the problem seen before, can be considered both pure electric or hybrid points.
 - Solutions evaluation: are evaluated the different performances to find the best suitable solution, according to the least fuel consumption and the SOC constrains.
- Step 2: all the different solutions can be represented in a graph based on the SOC variation and the FC, they will create a cloud of points with a descending trend, increasing the FC will decrease the SOC variation, forming a sort of Pareto frontier, as in the following example:

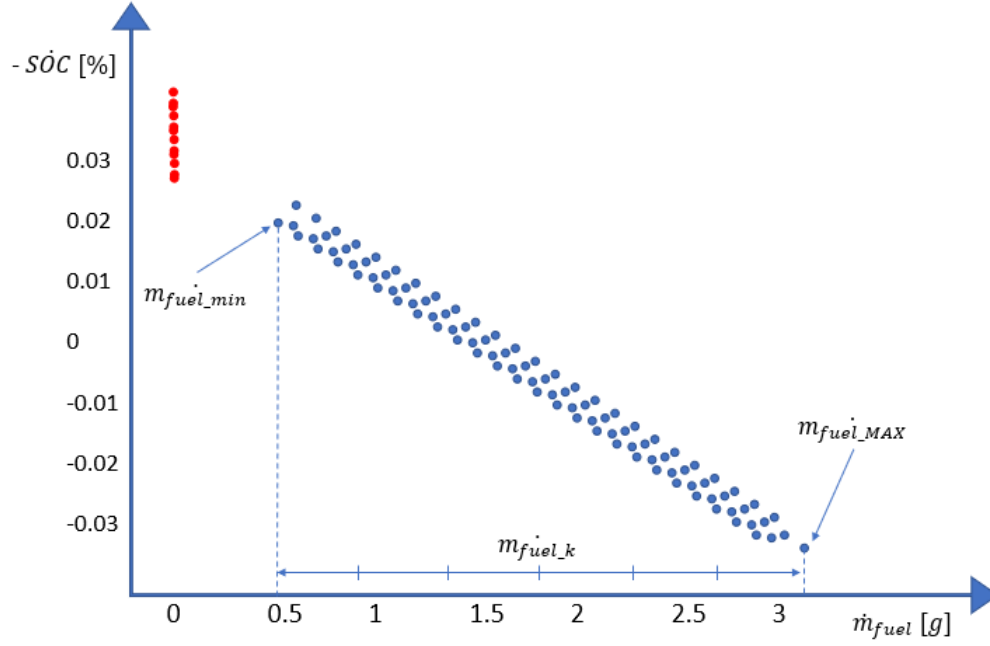


Figure 3.4: SERCA FC and SOC graph

We would choose the point that allow to reach the CS (0% variation) with the lowest FC possible.

We would store the optimal solution in a variable using the following steps:

- Discretization of the fuel consumption interval: the FC would be subdivided in the interval $[\dot{m}_{fuel_min}, \dot{m}_{fuel_MAX}]$ with k number of equidistant points (\dot{m}_{fuel_k} ;
- Optimal solutions identification: For each selected point can be found a corresponding optimal solution that respect the following:

$$\begin{aligned} & \min [S\dot{O}C(\dot{m}_{fuel})] \\ & \text{subjected to : } \dot{m}_{fuel} \in \left[\left(\dot{m}_{fuel_k} - \frac{\Delta\dot{m}_f}{2} \right); \left(\dot{m}_{fuel_k} + \frac{\Delta\dot{m}_f}{2} \right) \right] \end{aligned} \quad (3.19)$$

We will repeat the operation for each member of the discretized interval for each sub-problem, obtaining a vector representing the

discrete hull of the optimal solutions of each sub-problem.

- Slope-based relaxation: local hollows characterized by a lack of increase in the SOC despite the increasing in the fuel consumption could be present, the local concave region can affect the global optimization, for this reason is needed a filter:

$$SOC(\dot{m}_{fuel_k}) < SOC(\dot{m}_{fuel_k+1}) \quad (3.20)$$

Now it is possible to select adjacent working point to form an envelop of piece-wise linear function starting from the EV mode ($\dot{m}_{fuel_k} = 0$). The slope of the curve that connect two adjacent point is:

$$\theta(k-1, k) = \frac{\Delta SOC}{\Delta \dot{m}_{fuel}} = \frac{SOC(k) - SOC(k-1)}{\dot{m}_{fuel}(k) - \dot{m}_{fuel}(k-1)} \quad (3.21)$$

We can see this relation on the graph showed before:

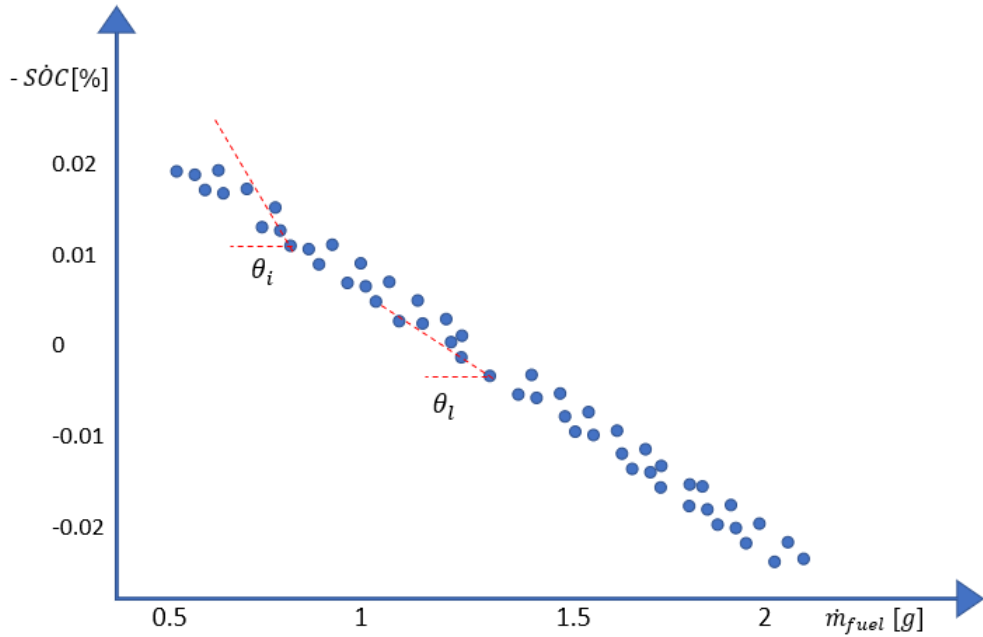


Figure 3.5: Slope Evaluation of Adjacent points

To ensure the convexity there is one more backward scanning of

the points that have to respect this relation:

$$|\theta(k-1, k)| \geq |\theta(k, k+1)| \quad (3.22)$$

Are allowed only steeper slopes for lower level of fuel consumption. Now it is time to store all the result points into a matrix, slope, SOC variation and \dot{m}_{fuel} are stored for the i driving cycle point in the k row of the matrix using the following variables:

$$\begin{aligned} u_{1|i,k} &= \theta_i(k-1, k) \\ u_{2|i,k} &= SOC_i(k) - SOC_i(k-1) \\ u_{3|i,k} &= \dot{m}_{fuel_i}(k) - \dot{m}_{fuel_i}(k-1) \end{aligned} \quad (3.23)$$

There is also a variable for the pure electric condition used as a benchmark for the optimal performance.

- Step 3: this step is inspired by the energy-balance procedure of the PEARS algorithm [40]

This step can be summarized with four sub-steps:

- Pure Electric Mode: starting to assume that when is possible we would use only the pure electric mode, $FC=0$, to see the total electrical energy E_{EV} required;
- Variable Replacement: from the matrix obtained before we will get the variables associated to the $|\theta_i| = |\theta_{MAX}|$ for that point of the cycle;
- Variables Update: once the operating point is selected the electrical energy and the FC will change and must be updated:

$$\begin{aligned} E_{EV} &= E_{EV} + u_{2|i,1} \\ \dot{m}_{fuel_TOT} &= \dot{m}_{fuel_TOT} + u_{3|i,1} \end{aligned} \quad (3.24)$$

Also the state and control variables would be updated, performing a left shift in the table of the k different operating points.

- Check: now is needed to verify if we reach the CS, in case we need to iterate the last two steps to reach that condition. Once done we can extrapolate all the optimal points and all the values needed.

We can visualize this loop in the following flowchart:

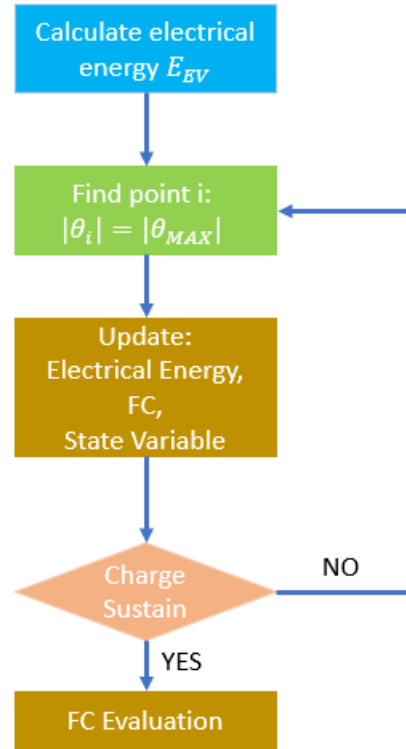


Figure 3.6: Fuel Consumption Evaluation

Has been shown [40] that is really important the mesh size of the control variables to reach a solution really closer to the DP one, instead the mesh size of the fuel consumption is less incisive for the trend of the final values after a certain point.

In our work we would elaborate some parts of the controller based on the results of the SERCA algorithm with the starting vehicles, we will also use the results as a benchmark for our work. We made this decision because has been showed that the SERCA could reach final FC values really close to the DP ones, less than 1% difference. In any case we would try to follow as much as possible the mode variation of the SERCA, but for the fact that this algorithm is an off-line one that knows a priori all the variables linked with the driving cycle, would not be fair to compare the results.

This would remain a benchmark of the performances of the controller and about the possibilities to improve that controller.

3.2 Online Control Strategies

This category can be called Local Optimum or Online Control Strategies, for the fact that as in the real life the controller can know only what happened and what is happening right now to make its decisions. Our aim is to develop a controller that could be used in a real driving situation, on the same idea of other studies done before [41], [42].

These kind of controller could be near-optimal ones, so they have a great potential if their parameters are tuned in a proper way, to improve these controllers are often used the strategies presented before as a benchmark, trying to see the deviations in the behavior of the two in the same situations.

3.2.1 Rule-Based

In this section we will present the real-time Rule-Based optimal EMS, that derives from the observation of the offline performances of other algorithm that can lead to the global optimum solution.

This technique [43] [44] [42] consist of the extrapolation of some rules on two different levels: selection of the operating mode (Pure Electric or Hybrid one) and torque split between ICE and GMU.

It's important to notice that this technique has to be set up for each kind of architecture and in particular on the components used in our case [45].

This method will lead to create some look-up tables in which we can find for example the Power Demand, the SOC level, the velocity and so on.

Then we will create if-then-else statements to cover the different possibilities and to be as close as possible to the optimal behavior observed with an off-line controller [46].

The main drawback is that the set up procedure of the rules is fundamental and can profoundly affect the performance of the controller, each driving cycle can add slightly different rule to the controller, for this we need to find a compromise to the best rules overall.

Another drawback is that the controller is linked with the components, for this we cannot use this strategy to see different designs, each time we would need to change the rules.

On the other hand is really low computationally demanding and that's why could be implemented in the real-time driving, nowadays the majority of the HEVs have a rule-based controller [2].

This kind of controller is so diffused because is a near-optimal controller, so the potential of the controller is really high, in our work we will use also this controller to compare our result with another one controller that could be

more similar for his characteristics and usage.

We can see this controller as the actual alternative used to be beaten to decrease the emissions and also to develop a more flexible and wide range controller. Here there is an example of how could be subdivide a look-up table and how can be identified the different rules:

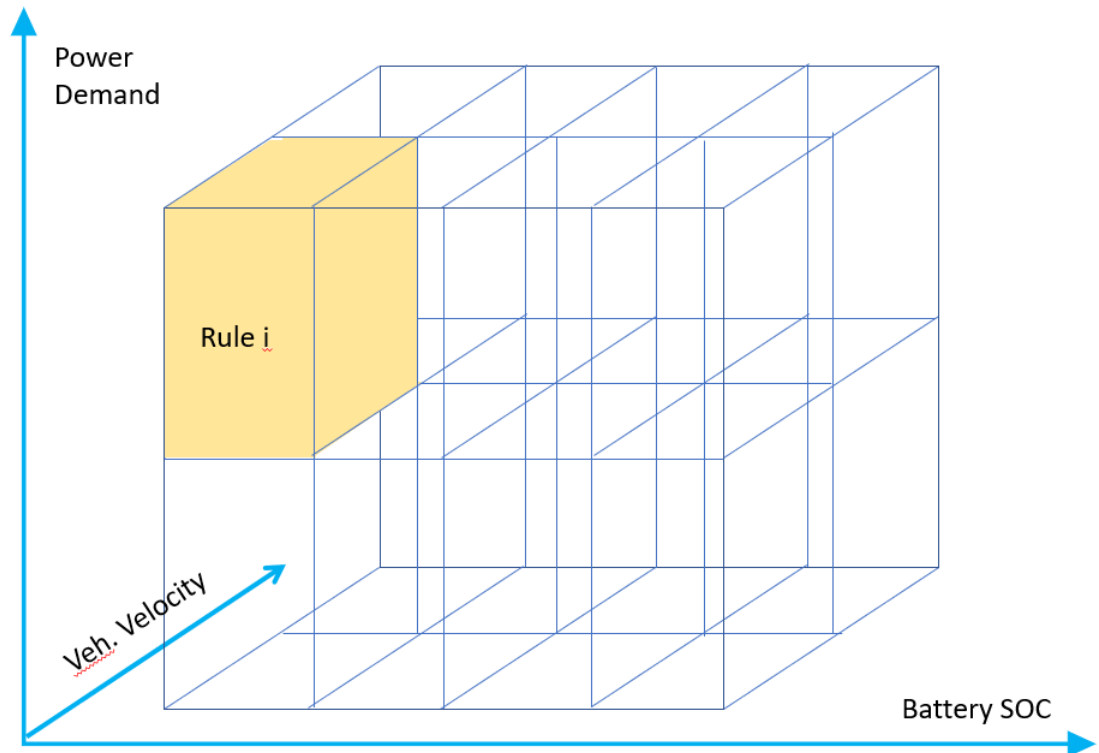


Figure 3.7: Rule-Base look-up table

We can see from the figure that the limits for each rule must be accurate and also that we need to cover all the space with rules for every kind of situation.

3.2.2 Equivalent Consumption Minimization Strategy (ECMS)

This method is an on-line approach that can be used for real-time applications in his adaptive version that we will present later, first we will focus on the original method.

The aim of the ECMS is to minimize for each time step the fuel consumption using an equivalence factor between the electrical power and the mechanical one.

The objective function of ECMS is normally defined as follow [47]:

$$J(u(t), t, s(t)) = \dot{m}_f(u(t), t) + s(t) \frac{P_m(u(t), t)}{H_{LHV}} \quad (3.25)$$

The physical constrains on the torque, speed, power and battery SOC are the same presented before. That can lead to the optimal solution:

$$u^* = \underset{u \in \Omega}{\operatorname{arg\,min}} \left[J(u(t), t, s(t)) \right] \quad (3.26)$$

In the eq. 3.23 we have presented the equivalence factor (EF) called $s(t)$, this is the core of this strategy. As we can see this parameter is function of the time and the tuning of this parameter will influence all the results.

The big challenge is to find a proper way to vary this parameter to reach the CS and also to be as close as possible to the optimal solution.

It's important to notice that every driving cycle, every design, every architecture would lead to different equivalence factor. The main problem is to find a path, some rules, to be able to use an appropriate equivalence factor over the time before starting the trip.

Normally this method can be used only knowing before the cycle, starting an iterative procedure we can run the driving cycle till when we find that particular EF that can lead to the CS, that value will be used for all the cycle, as a constant.

Here we present an example of how could vary the EF for the same vehicle in different driving cycles:

Driving Cycle	EF	Average Speed [km/h]	Length [m]
AUDC	1.62	17.6	4870
HWFET	2.29	77.7	16507
J1015M	2.21	22.7	4166
JC08	2.23	27.0	10318
LA092	2.27	39.6	15798
NEDC	2.25	33.3	10932
NYCC	1.45	11.4	1899
SC03	2.24	34.5	5761
UDDS	2.24	31.4	11984
UNECE	2.28	47.9	7950
US06	2.30	77.3	12888
WLTP	2.28	46.5	23263

Table 8: Equivalence Factors Comparison

We can notice that the EF values are in a wide range [1.45, 2.30], this range depend on the vehicle design and architecture, but in every case we have seen that for passenger cars the $EF \in [1.4, 3.5]$.

The main problem is that there is no particular correlation between the average speed or the length on the circuit, we can see that the lowest values are associated with low values of average speed, but the highest values of EF are associated with really different values of average speed.

For this reason this procedure is difficult to be used in a predictive way, not knowing the future velocities, because also a small change in the EF will bring to a final SOC far from the CS.

For this reason on this base we developed a controller that can be more flexible and adjust the EF values to be as close as possible to the charge sustain not knowing the future velocities of the driving cycle, as in a real driving situation.

Here we present the core structure of the code:

ICE Torque	GMU Torque	ICE Speed	GMU Losses	Battery Power Required	Battery Voltage	Battery Resistance	Battery Current	Battery Power	Fuel Consumption	Fuel Power Consumption	Equivalent Fuel Consumption
------------	------------	-----------	------------	------------------------	-----------------	--------------------	-----------------	---------------	------------------	------------------------	-----------------------------

Table 9: ECMS Table

- The first column will contain all the different torques that the ICE can develop
- In the second column there is the difference $T_{GMU} = T_{ICE} - T_{Req}$, where T_{Req} is calculated as in eq. 2.6 once we have selected the proper gear.
- The ICE speed depends on the gear selected.
- We can calculate the GMU losses based on the GMU torque and its speed from the data we have presented in the previous chapter.
- The Battery Power required depends on the torques of the ICE and GMU and their speeds.
- The Battery voltage can be calculated starting from the SOC level with OCV curve presented in the last chapter.
- The Battery Resistance can be calculated in a similar way using the internal resistance data of the battery.
- The Battery current would be calculated as said in eq. 2.12
- Once that we have the current and the voltage of the Battery we can calculate the output Battery Power.
- To calculate the FC we will use the data presented in the last chapter about the ICE using its torque and speed.

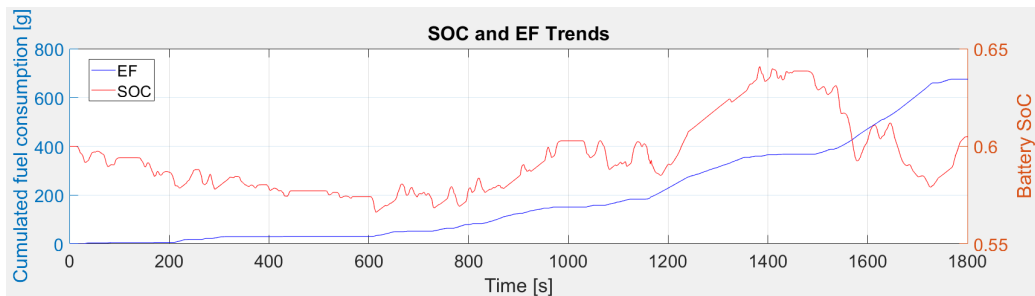
- The last column will give us the most important value of the Equivalent Fuel Consumption, calculate as follow:

$$Eq_{FC} = ICE_{FC} \cdot H_{LHV} + EF \cdot BatteryPower \quad (3.27)$$

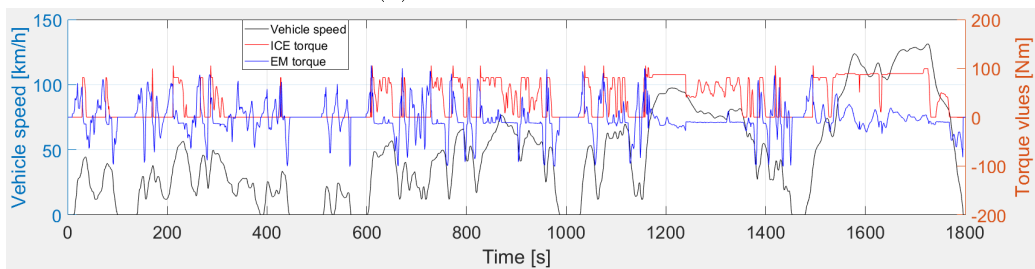
Based on the EF value the controller will choose the lowest value in the column to use the minimum energy possible, for this reason the EF can vary the behavior of the controller in such a significant way.

We will use this procedure for every time step of the simulation, updating all the values of the components. At the end of the cycle we would have all the values of the instant fuel consumption that we can sum to see the total FC on the driving cycle, we will also get the final value of the SOC of the battery to see if we reached the CS.

In the following figures we will show an example of the results of a driving cycle (WLTP), with the values of the ICE and GMU torque and also the SOC and the FC trends:



(a) SOC and FC trends



(b) ICE and GMU torques with the vehicle speed

Figure 3.8: ECMS Results

3.2.3 Adaptive Equivalent Consumption Minimization Strategy (A-ECMS)

The core of this strategy is the same of the standard ECMS, the main upgrade is the possibility to change the EF over the time using a controller, in this way would be possible to use this strategy in a real-time driving situation in which the controller will calculate the best EF for each different time step [48] [49] [50].

To develop this strategy is important to use an off-line strategy to estimate the EF over the time on a driving cycle, extrapolate some laws and use them to control the EF in the A-ECMS.

For this reason the calibration is really important and would determine how close the result would be to the optimal one and also if we would reach the CS or not.

In the following chapter we will explain all the different step elaborated to define the controller and how the EF is adjusted over the time.

We have to remember that the aim of the controller is to be used out from the driving cycles in a real situation, having the possibility to know only the current situation or the past ones.

In particular the challenging part is to adapt the controller to different vehicles and be able to perform well in all the cases.

4 A-ECMS Controller

In this chapter we will show the procedure used to develop the A-ECMS controller starting from the standard version presented before, we will cover all the steps to improve its performance and to be adaptable to different component sizes and different vehicles.

As already said before we would use the SERCA as benchmark for the performance of the controller and also to extract some patterns or rules to use in our controller.

The controller has been developed initially on the mid-size vehicle with some components from the library of AMESIM and a 5 gear transmission, then we have changed the size of the components and also tried to adapt to a 3 gear and a 8 gear transmissions.

After this step we have also changed vehicle starting to use the mini SUV data about the vehicle and of its ICE.

Once that the controller can handle this different situations we started to see if the controller can handle also all the different combinations generated by the functions showed in the section 2.3.

In the following sections we will follow as much as possible the order in which the procedures were carried out.

Here we show the work-flow to have an overview of the process:

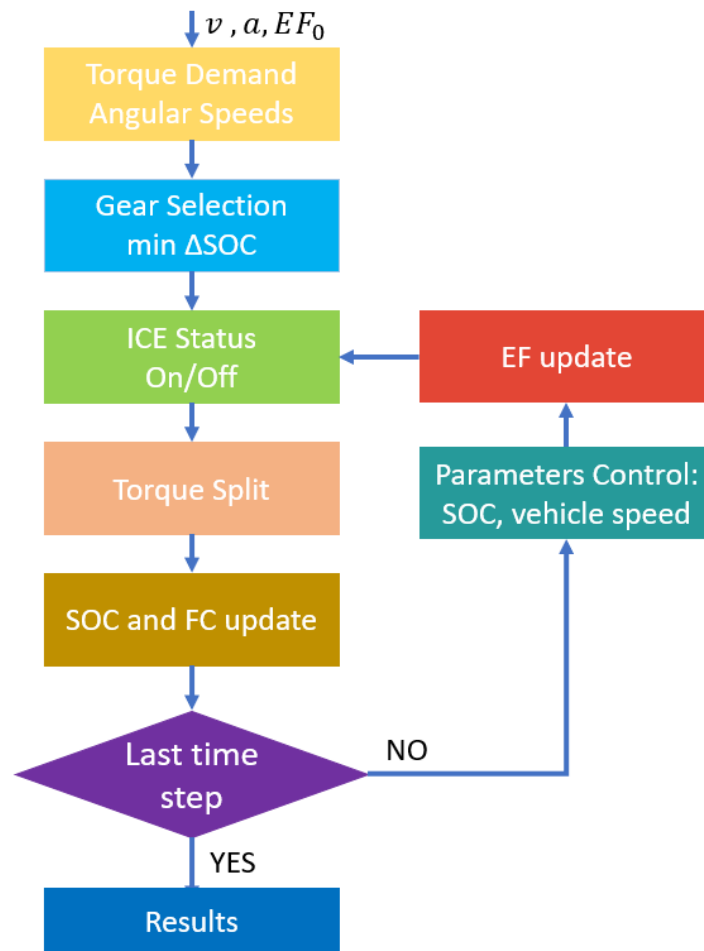


Figure 4.1: A-ECMS workflow

4.1 Gear Selection

The first step before calculate the ECMS table 3.2.2 is to select the gear, also in other works are shown different strategies to complete this goal [51].

We have noticed that the SERCA is trying to be in the Electric Mode as much as possible, in particular using all the different cycles presented before, about the 86 % of the time the vehicle is in the Electric Mode.

We have also seen that there are a great preponderance of situations in which the 5th gear is inserted:

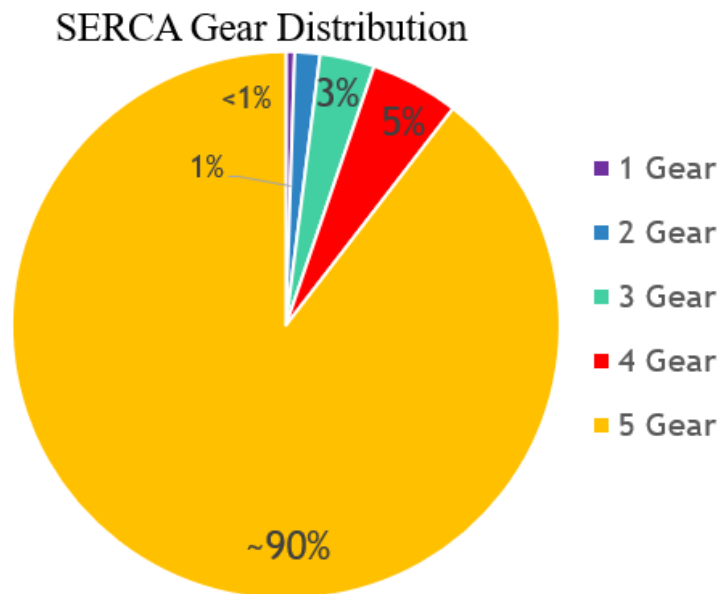


Figure 4.2: SERCA Gear Distribution

The SERCA is using for the 90% of the time the 5th gear to reduce the FC, has to use the other gears only for the transitions during the strongest accelerations or decelerations.

Based on these facts we have to check deeply if there is a relation during the E.M. with the gear selected.

Firstly we analyzed the relation between the Torque developed by the Motor, the Vehicle Speed and the different gears:

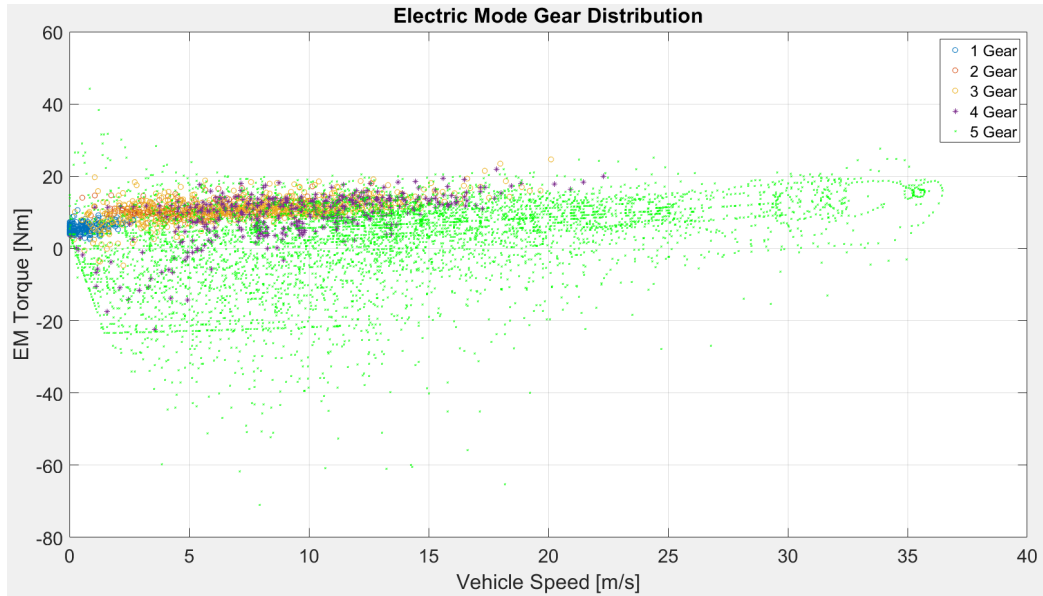


Figure 4.3: EM Torque for the Different Gear at different Speed

We can see from the figure that for negative torques we are using only the 4th and 5th gears, we can also see a triangular shape for the points of the 5th gear that are reaching the highest torque at low speed.

This graph is useful also to have an idea about which range of torques we are dealing with using the mid-size vehicle.

Analyzing the other data we noticed that there is a pattern for the Battery Power, the Vehicle Speed and the different gears:

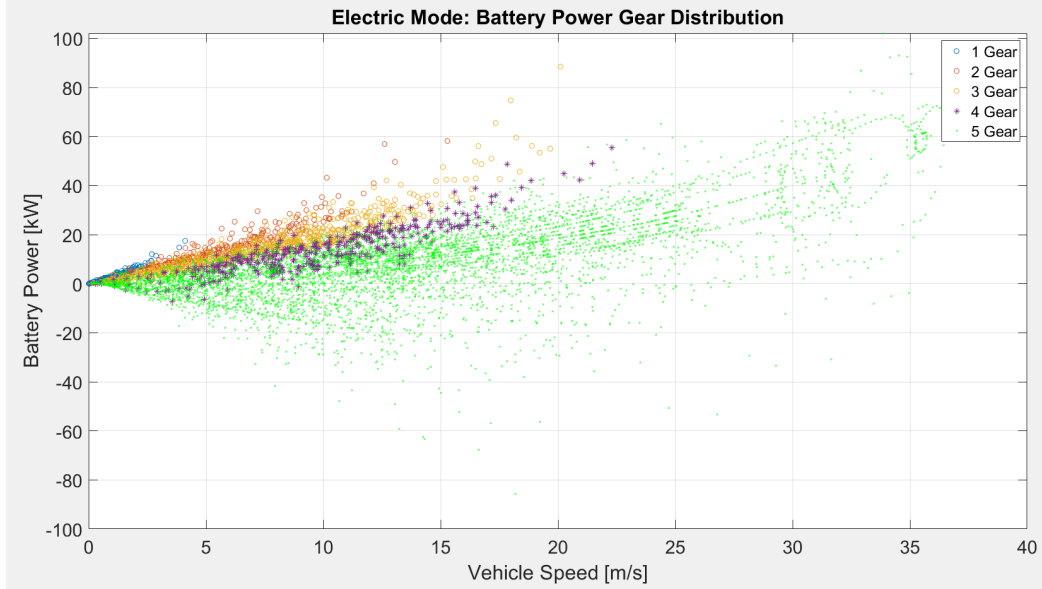


Figure 4.4: Battery Power for the Different Gear at different Speed

From this figure we can notice that there are 5 different curve, one for each gear, with the battery power involved.

From this fact we introduced in the controller a loop in which it will check all the feasible gear and find out the gear for which we will obtain the minimum ΔSOC that is related with the minimum Battery Power requested.

This because we can see in the graph that as the same speed with an higher gear the battery power is decreasing.

So now our controller would first select the gear according to the minimum ΔSOC in the Electric Mode, ICE Torque = 0 Nm, and then will compare the consumption with the different ICE torques and the E.M.

The controller is not using anymore the standard automatic shifting logic as in a standard vehicle and in the standard ECMS.

We have noticed that the more is free to shift gear the more is decreasing the FC, but we want to make a fair comparison and also we want to deal with a reasonable number of shifts during a driving cycle.

For this reason we have analyzed the number of shifts with the standard automatic transmission during the different driving cycles and also with the SERCA controller to set a parameter to penalize the shifts in way in which

we would reach a number closer to the AT benchmark, here the data:

Driving Cycle	Gear Shifts AT	Gear Shifts SERCA	Gear Shifts A-ECMS
AUDC	97	106	121
HWFET	9	5	7
J1015M	32	33	25
JC08	80	87	90
LA092	112	110	105
NEDC	53	48	45
NYCC	51	56	85
SC03	31	37	39
UDDS	83	80	98
UNECE	17	18	15
US06	32	33	43
WLTP	93	86	83

Table 10: Gear Shifts Comparison

It is important to underline that these results are a sample from the mid-size vehicle with the 5 gears transmission, the SERCA ones in particular are obtained tuning a parameter for each different driving cycle, are shown only because is important also for the following comparison that the gear shifts are close to the AT ones or lower.

On the other hand we can observe that the A-ECMS values are in most of the case close to the AT ones, only in a couple of cycles is not really close to that value but is still an acceptable increase of shifts to not compromise our driving experience.

All the A-ECMS values are obtained with the same settings of the controller, unlike the SERCA, because our aim is to automate as much as possible the controller to deal with all the different situations.

4.2 ICE Status Determination

Now that we have selected the correct gear we have to determine if it is necessary to turn on the ICE or not, as said the SERCA controller to reduce the FC is trying to reduce as much as possible the number of ignitions for the ICE and to reduce as much as possible the time in which the ICE is working. To reach our aim we have analyzed the data comparing the Electric Mode with the Hybrid Mode, to see if there is a discrimination between the two situations.

We found a pattern in the Power Demand and Battery Power data that we show in the following figure:

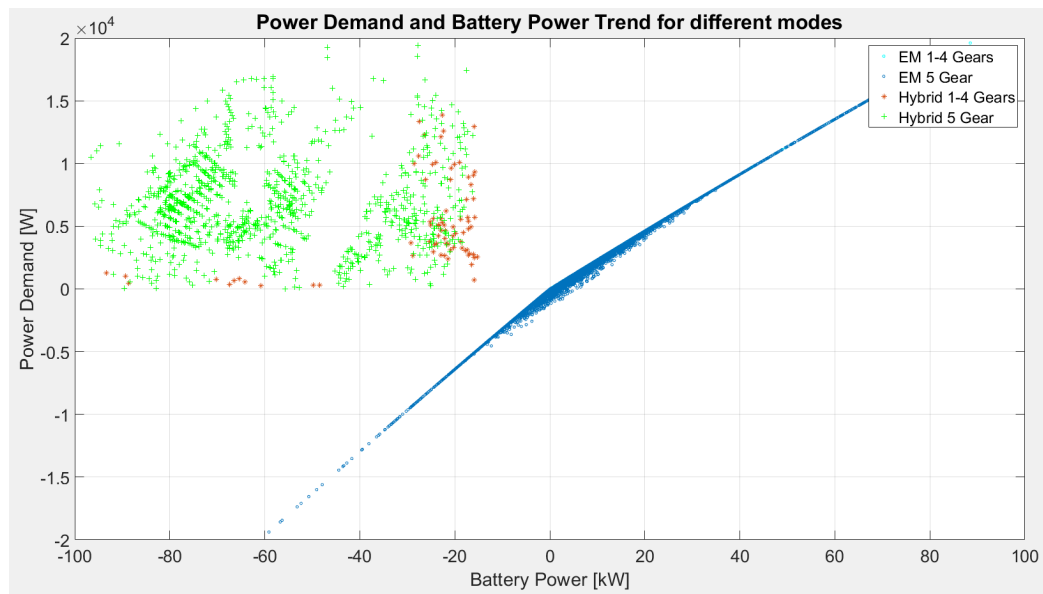


Figure 4.5: Battery Power and Power Demand graph

We can observe that there is a specific region in which the SERCA is activating the ICE:

$$\begin{aligned} BatteryPower &< 0 \\ PowerDemand &> 0 \\ \frac{BatteryPower}{PowerDemand} &< 1 \end{aligned}$$

We would use these rules to select in which situation is necessary to turn on the ICE.

We noticed that the standard ECMS is turning on the ICE several times

during the trip, in this way is increasing the consumption because the ignition has a relatively high value of fuel consumption.

We can see the comparison between the number of ignitions here:

Driving Cycle	ICE Ignitions SERCA	ICE Ignitions ECMS	ICE Ignitions A-ECMS
AUDC	5	32	7
HWFET	1	1	2
J1015M	1	7	1
JC08	3	14	5
LA092	2	23	4
NEDC	1	13	1
NYCC	1	14	1
SC03	1	9	2
UDDS	1	18	5
UNECE	2	4	1
US06	3	8	2
WLTP	2	13	3

Table 11: ICE ignitions Comparison

As we can observe from the table the SERCA is turning on the ICE only one time in most of the cycles, anyway the highest is 5 ignitions in the AUDC one, on the other hand the standard ECMS is floating between 4 and 32, not considering the HWFET.

We can notice that using this kind of rules the A-ECMS is working properly and in a similar way to the SERCA that is our benchmark.

The number of ignitions can influence up to the 10% the final FC of the vehicle in a driving cycle, for this reason our goal is to limit the number of ignitions and select the best situation in which start the ICE and then keep it on to charge the battery to reach the CS at the end of the circuit same as what is doing the SERCA.

4.3 Torque Split Determination

In this section we will show, once we determine that is better to turn on the ICE, how to split the torque between the Electric Motor and the ICE.

We observed how the SERCA is deciding to split the torque in the different driving cycles, here is a figure that shows the behavior:

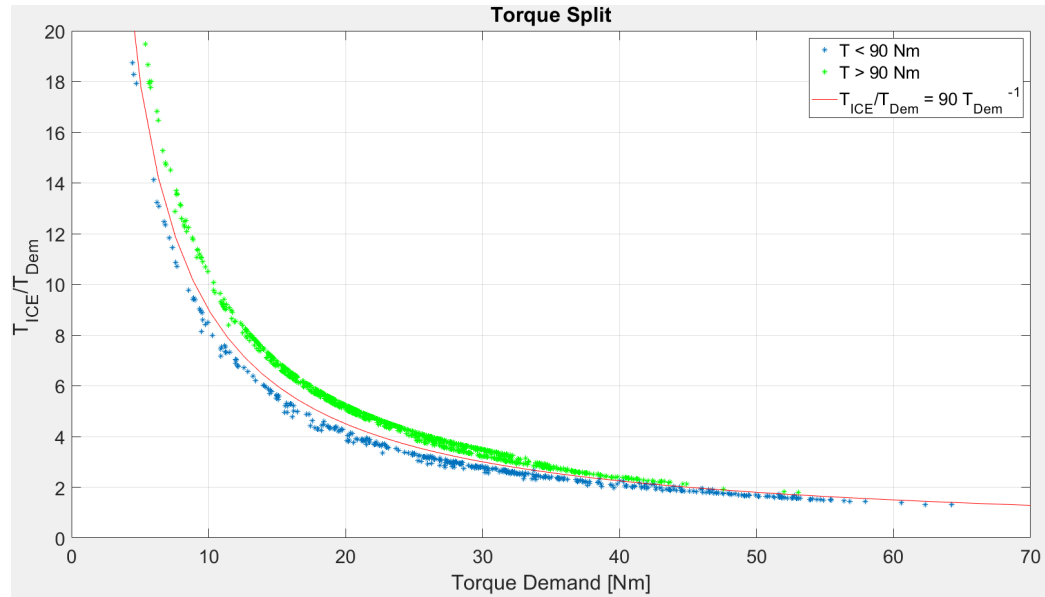


Figure 4.6: Torque Split

We can notice that the points fit two curves, distinguished by the value showed in the figure of 90 Nm for this particular vehicle, it is important to notice that we can plot the curve:

$$\frac{T_{ICE}}{T_{DEM}} = 90 \cdot \frac{1}{T_{DEM}} \quad so \quad T_{ICE} = 90$$

the SERCA is using the ICE with an output torque in the following interval [77 Nm, 104 Nm], where the maximum output torque is 114 Nm, from this fact we can set a minimum output torque from the ICE based on the size of the vehicle.

We would use a value smaller in percentage to the one used from the SERCA to be more conservative.

4.4 Equivalence Factor Control

In this section we will show the procedure that we used to set the Adaptive Equivalence Factor in the controller.

We will first show the preliminary study about the EF in different situations and then we will explain step by step the behavior of the controller of the Equivalence Factor.

4.4.1 Preliminary Studies on EF

Before starting to explain how we can manage the EF in the different situations we have to see the behavior of the SERCA controller and how is changing the EF during the time, for this purpose we want to see the correlations between the EF and other parameters.

To calculate the EF from the SERCA data we are using a formula from eq 3.25:

$$EF(t) = -\frac{FC(t) \cdot H_{LHV}}{P_{Batt}(t) \cdot P_{Dem}(t)} \quad (4.1)$$

We are normalizing for the P_{Dem} to compare the other parameters.

Is important to notice that in the following graphs will be showed EFs from the SERCA data obtained with the final results of the cycles, these values are not the same that we can use in the ECMS controller, we would only compare the behavior of the EF in the different situation to extrapolate some rules.

Using that formula the first relation that we want to show is the following:

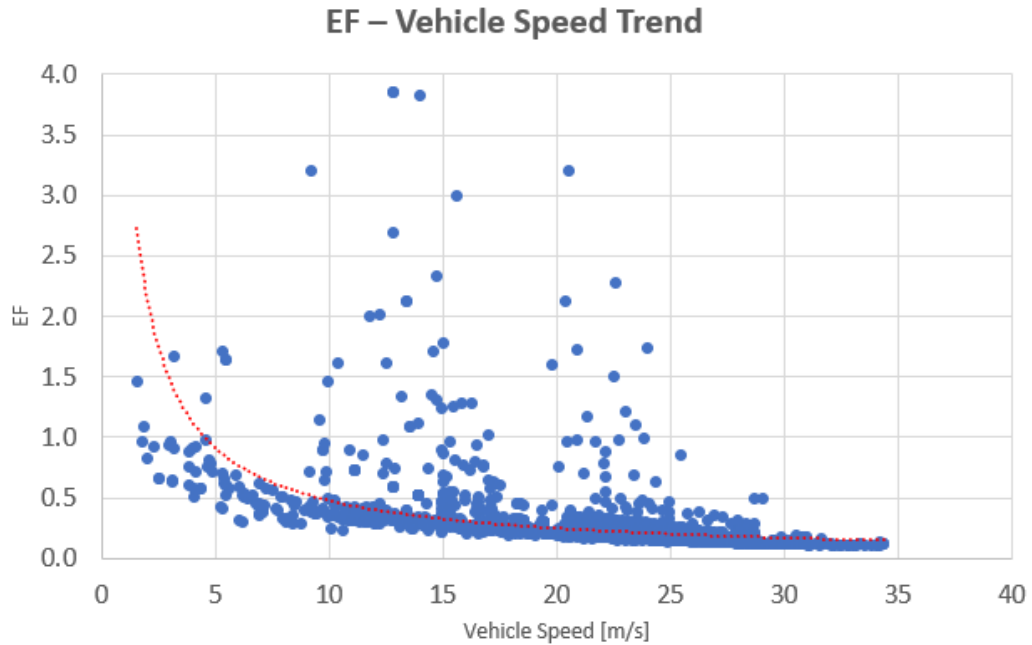


Figure 4.7: EF related to the Vehicle Speed

We can notice that there is a trend with the speed of the vehicle for the EF that is decreasing, there are also some points that are out of the trend for this reason we have to give the right weight to this relationship.

The next study that we want to show is the one with the acceleration, we have subdivided the cases in which we are accelerating, decelerating or cruising, we have noticed that while cruising the EF is almost constant, on the other hand the situations in which the ICE is working while we are decelerating are really a few (20%) compared to the ones in which we are accelerating, and do not show an interesting trend for our purpose.

For this reason we will show only the case in which we are accelerating:

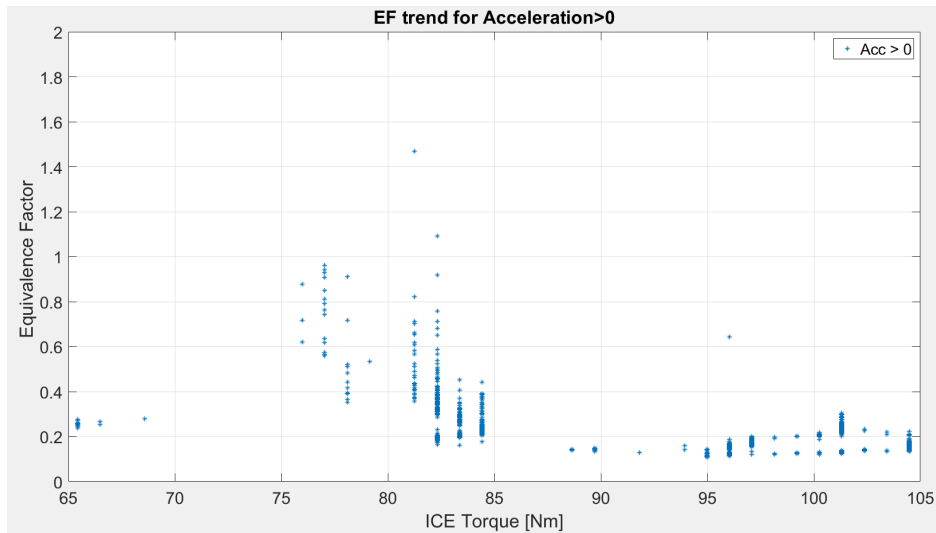


Figure 4.8: EF related to the Vehicle Acceleration

We can see that all the EFs are in a short range of values, the mean is lower than the other situation because we want to use high torques only, and in particular the cases in which we are using a torque higher than 90 Nm the EF is around 0.20, accentuating this way of acting.

Here we want to show some 3D graphs that will show the dependency of the EF from the SOC and the parameters showed before in this section, the first one is the following:

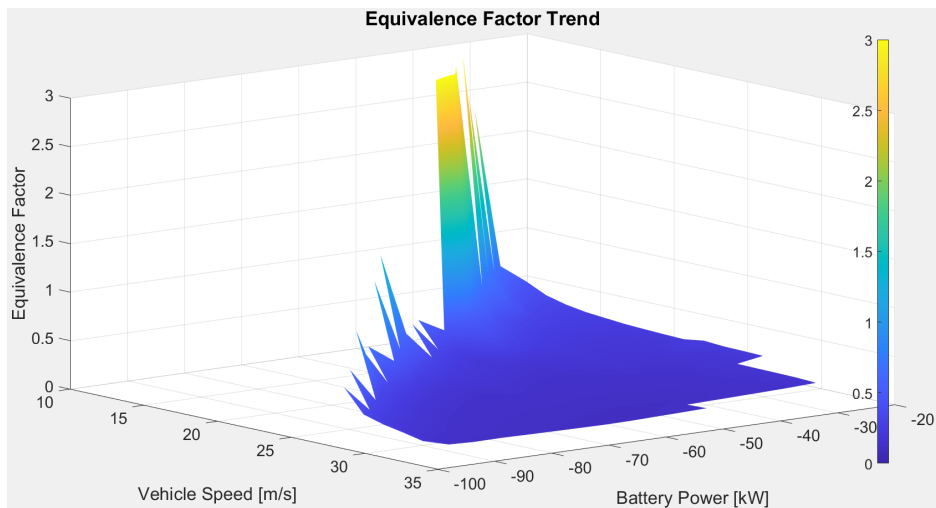


Figure 4.9: 3D trend of EF, Vehicle Sp. and Battery Power

We can see here how both the speed and the Battery power, related with the ΔSOC , how are leading the EF, in particular we can observe that for a low battery power, low ΔSOC , and a low vehicle speed corresponds an higher EF.

We can also observe that there are some areas that are not covered, high absolute battery power and low vehicle speed. This graph is useful to have an overview of how is important to manage the EF in the different situations. We will show it in the next section. The second plot that we want to show is this one:

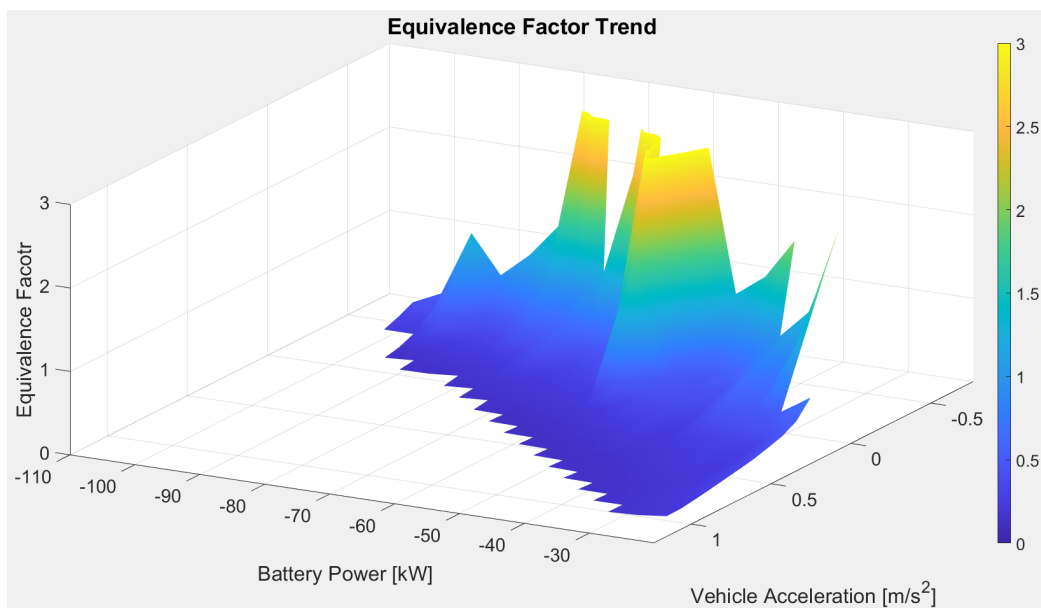


Figure 4.10: 3D trend of EF, Vehicle Acc. and Battery Power

In this case we are representing the acceleration instead of the speed of the vehicle, we can observe the EF is increasing for a lower acceleration and a lower absolute value of the Battery Power.

The acceleration is related with the output torque of the vehicle and we would use these information to correlate ICE torque with the SOC and the EF.

4.4.2 EF Controller Overview

Here we will show step by step how the controller will work in the different situations.

Before that, we want to show the different steps explained before how can influence the FC values in the different cycles, all the values would be for the ECMS controller with different setting:

Driving Cycle	Automatic Transmission [g]	Free Shifting [g]	ΔSOC [g]	ΔSOC ICE on/off [g]
AUDC	232.97	131.61	156.20	108.50
HWFET	603.56	516.86	585.28	536.81
J1015M	177.90	109.98	142.38	97.34
JC08	413.60	289.92	354.40	252.48
LA092	592.50	479.55	533.49	371.61
NEDC	425.49	319.99	412.29	284.63
NYCC	101.06	51.11	65.66	40.24
SC03	215.49	164.18	203.59	129.55
UDDS	476.43	340.56	418.98	297.15
UNECE	289.37	236.08	266.72	219.18
US06	465.14	449.43	480.75	416.57
WLTP	874.42	733.75	860.56	621.54

Table 12: ECMS Versions FC comparison

From the table we can observe that the improvement in the controller are leading to a reduction of the Fuel Consumption, as said before the possibility to not follow the automatic transmission rules can decrease sensibly the FC but is not possible to admit this case.

Then for the other two steps, one introducing the gear selection by the minimum ΔSOC and introducing a rule to turn on the ICE, we can notice that the FC is decreasing from the standard version. This could be a good proof that we are going in the right direction to tune the controller. Now we want to show the last step before the tuning of the EF, we will show the FC of the standard vehicle only with the ICE, the performance of the standard ECMS

and then of the version with all the three upgrades showed before, is important to notice that with a fixed EF is not possible to set an high minimum torque as a threshold value.

For this reason we would use a lower value of 75 Nm to reach the charge sustain in all the cycles:

Driving Cycle	Standard Vehicle [g]	Standard ECMS [g]	Tuned ECMS [g]	Ratio Tun. ECMS Standard V.	Ratio Tun. ECMS St. ECMS
AUDC	246.99	232.97	107.20	43.4 %	46.0 %
HWFET	563.37	603.56	529.65	94.0 %	87.8 %
J1015M	182.84	177.90	95.40	52.2 %	53.6 %
JC08	359.89	413.60	199.72	55.5 %	48.3 %
LA092	539.06	592.50	377.77	70.1 %	63.8 %
NEDC	373.04	425.49	241.36	64.7 %	56.7 %
NYCC	97.82	101.06	35.75	36.5 %	35.4 %
SC03	243.10	215.49	124.54	51.2 %	57.8 %
UDDS	413.35	476.43	273.68	66.2 %	57.4 %
UNECE	283.29	289.37	163.58	57.7 %	56.5 %
US06	438.33	465.14	356.05	81.2 %	76.5 %
WLTP	800.67	874.42	584.47	73.0 %	66.8 %

Table 13: Tuned ECMS FC comparison

The table shows how the tuned ECMS is performing better than the standard version in all the situations and also that we are saving fuel from the non hybrid version of the vehicle, we are saving around 57% of fuel as a mean of the different cycles.

The problem with this version of the controller is that is really sensitive of the EF that we set, as we showed in the table 8 , the values of the EF is fluctuating for every driving cycle around values between 2 and 3.

For this reason we need to set some rules to manage this factor [52], that can allow the controller to reach the charge sustain without tuning every time the initial equivalent factor.

We would control the EF using both the SOC state value and the vehicle speed of that time step, due to the relationship showed in the section 3.2.2

and section 4.4.1, we would use a PI controller, as suggested in other studies [47], to tune the EF.

The EF would be tuned in this way:

$$EF(t) = EF(t-1) + k_p \cdot (\Delta SOC(t)) + k_I \cdot \int_{t_0}^t (\Delta SOC(t)) - \\ + k_v \cdot (v(t) - v(t-1)) \quad (4.2)$$

where $\Delta SOC(t) = SOC_{start} - SOC(t)$

In the eq 4.2 the k_p is the proportional gain from the SOC, the k_I is the integral gain from the SOC in the interval t_0 , that is the last time in which the SOC was the same of the starting moment, till the actual instant, k_v is the proportional gain from the velocity.

The main influence is from the SOC but also the velocity is giving a small contribute.

Here we can schematize the behavior of the EF:

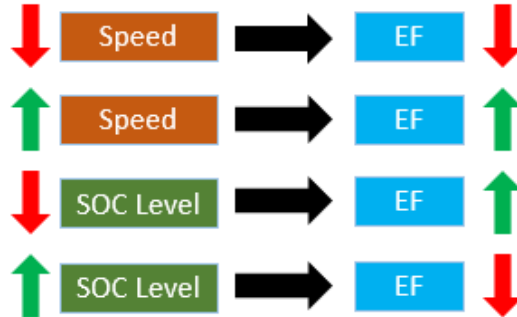


Figure 4.11: ECMS Rules: SOC and EF

As we can observe from the scheme, the Speed will lead the EF to change in the same way, on the other side the SOC is having an opposite behavior, this means that when the speed is increasing we need to raise the EF so that we would use more the ICE cause of the cost of the electric energy.

This point is related with one of the main drawbacks of the electric vehicles, at high speed they consume more energy related to the conventional ICE.

On the other hand if the SOC is decreasing too much we need to activate more the ICE to charge the battery, so for this aim is necessary to increase the cost of the electrical energy raising the EF.

These are the main rules that will work during all the trip, then is necessary

to put some limitations on the minimum and maximum SOC levels, and from what we noticed about the EF during different cycles and also on different vehicles we can say that there is a best interval in which the controller should work, that is mainly between 2 and 3.

For this goal we can present the next scheme:

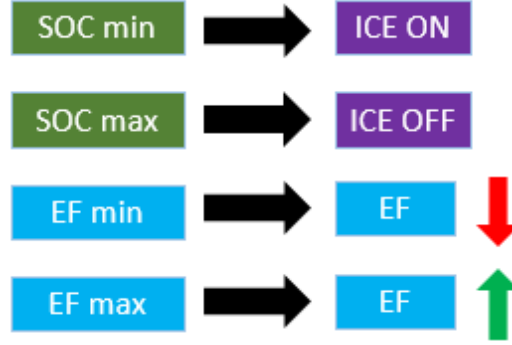


Figure 4.12: ECMS Rules: Speed and SOC

From the figure we can notice that to control the levels of the SOC we need to control the ICE ignition, forcing to turn off if it is still charging or turning it on if it is not, to avoid to discharge completely the battery that will also deteriorate its state of health.

We set these limits as follow:

$$30\% \leq SOC(t) \leq 95\% \quad (4.3)$$

For the EF we set this rule to keep it in the right interval:

$$EF(t) = EF(t) + s_{PEN} \cdot k_p \cdot \left(EF_{min/max} - EF(t) \right) \quad (4.4)$$

Where the s_{PEN} is just a factor that multiplies the proportional gain.

A similar procedure is applied on the EF for the overcome of two soft threshold on the SOC [52], in particular we want to penalize when the SOC is not in the interval [50%, 70%] with the following:

$$EF(t) = EF(t) + s_{PEN} \cdot k_p \cdot \left(SOC_{start} - SOC(t) \right) \quad (4.5)$$

The next step is to control the torque split with the SOC level, in case the SOC is decreasing too much we have to help the controller to turn on the

ICE, in this case we are admitting lower values of minimum torque with an equivalent consumption that is lower.

In case we are charging too much we can increase the threshold to make more difficult to turn on the ICE.

We can see with a figure this procedure:

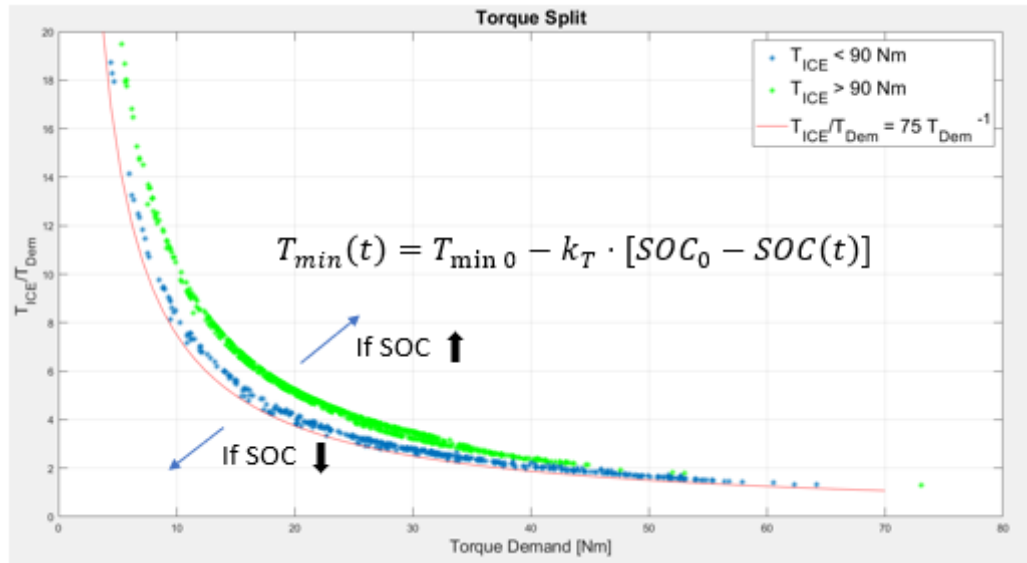


Figure 4.13: ECMS Rules: Torque Split

As you can see in the figure the minimum torque is regulated with a parameter k_T and the instant value of the SOC.

With this configuration we were able to reach the charge sustain in all the driving cycles for the starting setup of the first vehicle, but then changing the size of the components or the entire vehicle was not possible anymore to reach the CS in every situation.

For this reason we have introduced some more rules that will take place only after a certain percentage of the trip.

The percentage of the trip is calculated by the covered distance on the total distance, so is not based on the time of the trip but on the length.

We wanted to try to not introduce nothing that needs some information about the future time steps, in this case we would need only to know how far is the destination from the current point.

This feature can be easily implemented by the use of a navigator system in the car for every trip of the user. It is important to underline that without this rules the controller was able to reach a final SOC in the interval [45%,

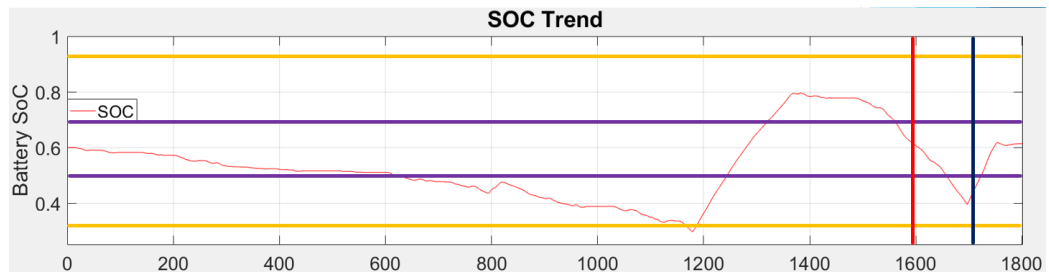
70%] that is not too wide and is still close to the CS.
We introduced two rules on the trip percentage:



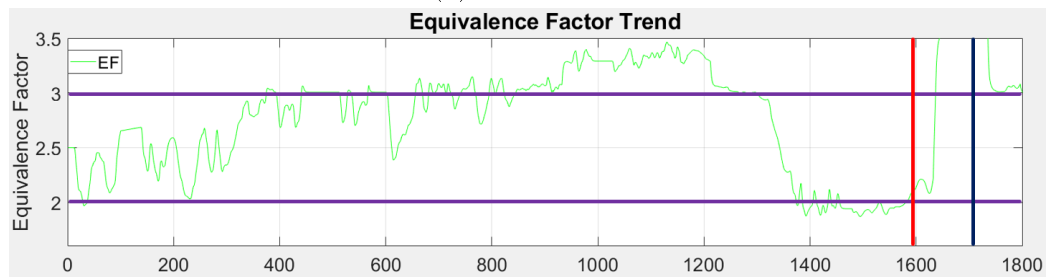
Figure 4.14: ECMS Rules: Trip %

The first will start after the 75% and will control the torque split and the EF, the minimum torque would be raise for the cases in which the SOC is lower than the starting one to be able to charge the battery, in case we are overcharging the vehicle the minimum torque would be reduced. For the EF there would be only an increase of the penalty factor showed in the eq. 4.4 The second one is used at the end of the trip to reach the CS and will replace the other rules showed before, as said before we have seen that without the control we would be in the range $45\% < \text{SOC}(t) < 70\%$, for this situation is enough to force the ICE to turn on or off depending on the SOC for the last part of the cycle.

Here we will show the trend of the EF and the SOC in a WLTP cycle:



(a) SOC Trend



(b) EF Trend

Figure 4.15: SOC and EF Trends

In the figures are shown the two hard limits for the SOC in orange after which we would act directly on the ICE and the other controls, in purple, for which we would only penalize the EF, are shown also the two trip controls at 75% and 90% of the trip with which we can see that we are able to reach the CS.

We have noticed that this strategy will increase a little bit the FC because we are not charging the best possible situation but can allow us to use the controller for a wide range of components always reaching the CS.

As said before we can avoid this control once we choose the component size and the gear ratios, tuning the other parameter shown before on that particular architecture and also decreasing the FC.

So we can say that is possible to improve the FC that we will show later in the final results deleting that rule.

It is important to notice that this kind of A-ECMS is able to perform in the same way with any starting value of the EF, in the literature presented before we underlined how the starting value is really important to be able to reach the CS, in our case the EF would be adjusted by all the other parameters and will be in the right range in few time steps.

4.5 FC Comparisons

In this section we will exhibit the results obtained from the controller with all the features presented in the past sections.

We will compare it with the standard ECMS, the SERCA and also with the conventional vehicle performances.

We will show the performance of the controller in three different situations changing the number of speeds of the transmission: we would show the 3, 5 and 8 speed transmissions using the same power-train components, as saying same ICE, GMU and Battery. In particular the size of the components would be the following:

- ICE: Max. Torque 120 Nm, Max Power 66 kW;
- GMU: Max Torque 250 Nm, Max Power 40 kW;
- Battery: Power 75 kW, Energy 10 kWh.

4.5.1 3 Speed Transmission

For the 3 speed transmission we would use the following gear ratios:

$$[3.5 \ 1.4 \ 0.6]$$

With these data we will obtain the following results:

Driving Cycle	Final SOC	ICE starts	Equivalent Fuel Consumption [g]	Fuel Consumption [km \dagger]
HWFET	58.2 %	2	258.29	47.53
UDDS	56.3 %	11	150.95	59.05
US06	62.3 %	2	217.77	44.02
WLTP	61.3 %	8	360.53	48.00
HUUW	60.8 %	21	974.39	49.34

Table 14: 3 Speed Transmission A-ECMS Results

We selected only 4 driving cycle to test the performance of the controller, based on the most relevant ones, the last one is the union of the 4 cycles to test the performance in a longer situation.

We can see that the ICE starts are reasonable out of the UDDS that have an high value based on the length of the cycle.

We obtained the Equivalent Fuel Consumption imposing the charge sustain utilizing the following equation:

$$\frac{(SOC_0 - SOC_f) \cdot Q_{MAX} \cdot V_{60\%} \cdot EF}{H_{LHV}} \quad (4.6)$$

Then using the fuel density of the gasoline (743.8 g/l) and the cycle length we calculated the consumption in term of km/l of gasoline.

Here we will show the comparison between the different controllers:

Driving Cycle	FC Conv. Veh. [g]	FC SERCA [g]	FC A-ECMS [g]	FC ECMS [g]
HWFET	364.30	250.27	258.29	368.74
UDDS	405.06	121.20	150.95	224.66
US06	330.49	212.47	217.77	360.82
WLTP	671.00	353.68	360.53	572.85
HUUW	1770.85	937.62	974.39	1411.82

Table 15: 3 Speed Transmission Comparison

From these value we can see that the performance of the A-ECMS controller is always better than the standard one.

To be able to analyze better the data we will calculate the ratio between the different FC of the controllers to compare in an easier way the values:

Driving Cycle	Ratio SERCA Conv. Veh.	Ratio A-ECMS Conv. Veh.	Difference A-ECMS SERCA	Difference A-ECMS - SERCA [g]
HWFET	68.70 %	70.90 %	2.20 %	8.02
UDDS	29.92 %	37.27 %	7.34 %	29.75
US06	64.29 %	65.89 %	1.60 %	5.30
WLTP	52.71 %	53.73 %	1.02 %	6.85
HUW	52.95 %	55.02 %	2.08 %	36.77

Table 16: 3 Speed Transmission Ratios

We can observe that out of the UDDS cycle all the other are in a really close range of FC values from the SERCA, around 1% o 2%. In particular on longer driving cycle is performing in a close way to the benchmark.

In the UDDS we noticed already from the number of ICE starts that were high that was not performing well, the fact that is turning on and off the ICE is leading to an increase of the FC.

Is also interesting to notice the difference in grams of fuel that is not such important, we have always to remember that we are saving a large amount of fuel from the conventional vehicle without the hybrid mode.

We will analyze in a similar way the results for the other two conditions in the following sections.

4.5.2 5 Speed Transmission

For the 5 speed transmission we would use the following gear ratios:

$$[3.5 \ 2 \ 1.4 \ 1 \ 0.85]$$

As done before we would start to show the performance of the A-ECMS controller in the following table:

Driving Cycle	Final SOC	ICE starts	Equivalent Fuel Consumption [g]	Fuel Consumption [km \ddagger]
HWFET	62.6 %	2	351.93	34.89
UDDS	57.2 %	6	206.74	43.11
US06	60.9 %	3	332.40	28.83
WLTP	61.4 %	3	513.68	33.68
HUUW	61.2 %	15	1397.95	34.39

Table 17: 5 Speed Transmission A-ECMS Results

We can notice that the performance in terms of ignitions and average of the final SOC is better than before.

Now we present the comparison between the different controllers:

Driving Cycle	FC Conv. Veh. [g]	FC SERCA [g]	FC A-ECMS [g]	FC ECMS [g]
HWFET	563.37	350.55	351.93	536.81
UDDS	413.35	187.02	206.74	297.17
US06	438.33	326.54	332.40	416.57
WLTP	800.67	498.52	513.68	621.54
HUUW	2156.9	1365.63	1397.95	2364.48

Table 18: 5 Speed Transmission Comparison

As seen before we can see that the A-ECMS is performing always better than the standard version, we introduce also the ratios between the different controllers:

Driving Cycle	Ratio	Ratio	Difference	Difference
	SERCA Conv. Veh.	A-ECMS Conv. Veh.	A-ECMS SERCA	A-ECMS - SERCA [g]
HWFET	62.22 %	62.47 %	0.24 %	1.38
UDDS	45.25 %	50.01 %	4.77 %	19.71
US06	74.50 %	75.83 %	1.34 %	5.87
WLTP	62.26 %	64.16 %	1.89 %	15.16
HUUV	63.61 %	65.11 %	1.51 %	32.32

Table 19: 5 Speed Transmission Ratios

As aspected from the data of the A-ECMS we can see that the difference between A-ECMS and SERCA is near the 1% with the maximum lower than 5%.

We can see that in this condition the controller is performing even better than before.

This is due to the fact that the gear ratios of the 5 speed transmission are more reliable than the 3 speed one.

Another fact is that the controller was developed at the beginning use the 5 speed transmission due to the large use of this kind of transmission in the vehicles on the market nowadays.

4.5.3 8 Speed Transmission

For the 8 speed transmission we would use the following gear ratios:

$$[4.60 \ 2.72 \ 1.86 \ 1.46 \ 1.23 \ 1.0 \ 0.8 \ 0.68]$$

Also in this last case we will show first the results of the A-ECMS controller:

Driving Cycle	Final SOC	ICE starts	Equivalent Fuel Consumption [g]	Fuel Consumption [km \dagger]
HWFET	60.1 %	7	287.43	42.72
UDDS	52.6 %	6	172.79	51.59
US06	63.9 %	2	254.37	37.69
WLTP	61.9 %	2	417.39	41.45
HUUV	61.3 %	10	1676.89	43.49

Table 20: 8 Speed Transmission A-ECMS Results

We can notice that the cycles are performing well out of the UDDS that is far from the CS, we are under the 55% of the final SOC so the data are not so reliable.

Here there is the comparison with the other controllers:

Driving Cycle	FC Conv. Veh. [g]	FC SERCA [g]	FC A-ECMS [g]	FC ECMS [g]
HWFET	396.57	287.43	287.78	414.44
UDDS	322.47	142.89	172.79	267.89
US06	359.44	250.83	254.37	359.32
WLTP	598.41	416.04	417.39	572.85
HUUV	1676.89	1097.50	1105.51	1608.58

Table 21: 8 Speed Transmission Comparison

We can observe that the UDDS is performing worse than the other cases, but also in this case better than the standard ECMS.

To compare in a easier way the controllers we show the ratios as done for the other situations:

Driving Cycle	Ratio SERCA Conv. Veh.	Ratio A-ECMS Conv. Veh.	Difference A-ECMS SERCA	Difference A-ECMS - SERCA [g]
HWFET	72.56 %	72.48 %	0.08 %	0.31
UDDS	44.31 %	53.58 %	9.27 %	29.90
US06	69.78 %	70.77 %	0.98 %	3.54
WLTP	69.52 %	69.75 %	0.22 %	1.35
HUUW	65.45 %	65.93 %	0.48 %	8.01

Table 22: 8 Speed Transmission Ratios

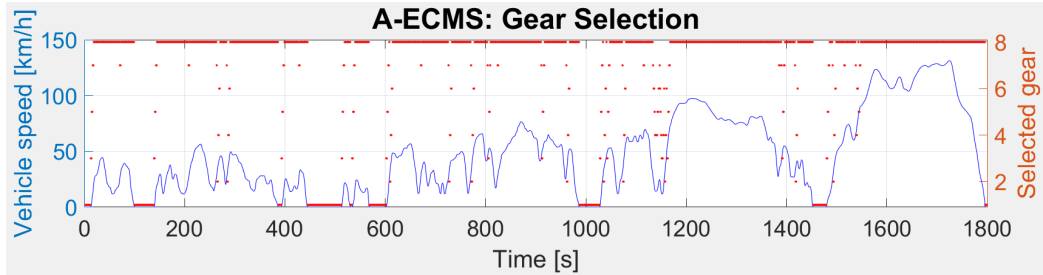
In this case we can see that the performance are really close to the SERCA controller, all the driving cycles are under 1% difference out of the UDDS that is not performing well.

It is important to notice that in this case for the fact that the final SOC of the UDDS cycle is far from the CS the formula in eq. (4.6) is not so reliable for the final value of FC.

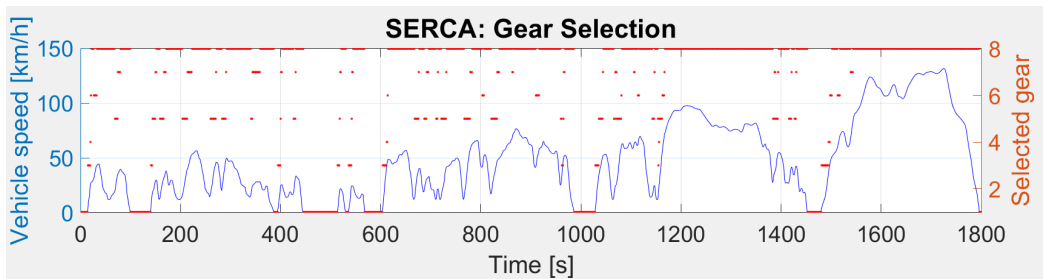
We want to show also for this case the trend of the parameters of the vehicle during the cycle.

We selected the WLTP for the variety of situations present in the cycle.

The first comparison is about the Gear Selection, as shown before the A-ECMS is selecting the gear in the Electric Mode to reduce the Battery Power needed, here the comparison between the two controllers:



(a) A-ECMS Trends



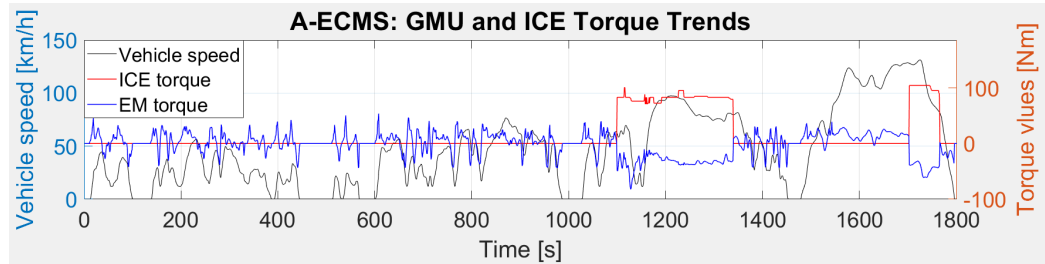
(b) SERCA Trends

Figure 4.16: Comparison A-ECMS & SERCA Gears Selection

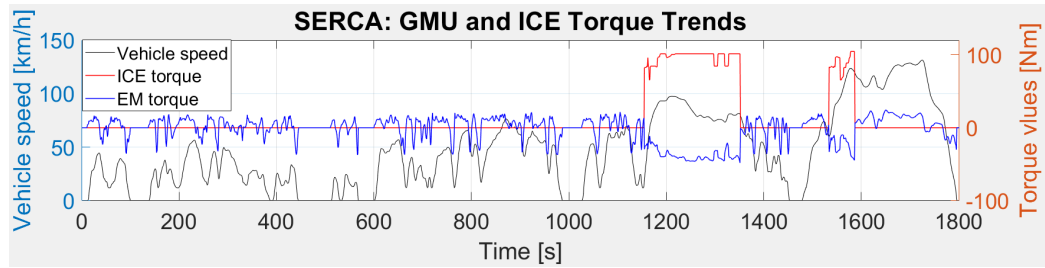
We can see from the graphs that for the most of the time the two controllers are performing in a similar way, as said over 90% of the time steps there is the highest gear selected.

We can notice that in the transition between the still position and the cruising the A-ECMS is shifting a little bit more to decrease the battery usage. As seen in the previous chapter the total number of shifting is pretty similar for the two cases for the fact that while cruising the SERCA changes some times the gear where the A-ECMS is keeping the same gear.

The second comparison is about the torques requested by the ICE and the Motor during the cycle, in this way we can also see if we are in the electric mode or the hybrid one, first we will show you the A-ECMS trends and then the SERCA ones:



(a) A-ECMS Trends



(b) SERCA Trends

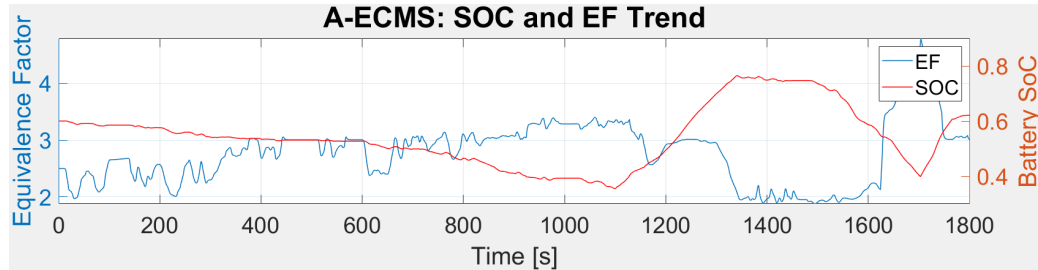
Figure 4.17: Comparison A-ECMS & SERCA Torques Trends

We can notice that the main part of the cycle is done in the Electric Mode in both cases, than we can see that there are two ignitions of the ICE, the first one is happening in the same part of the cycle and also the duration of the hybrid mode is quite similar, the SERCA is starting and finishing a little bit later this mode.

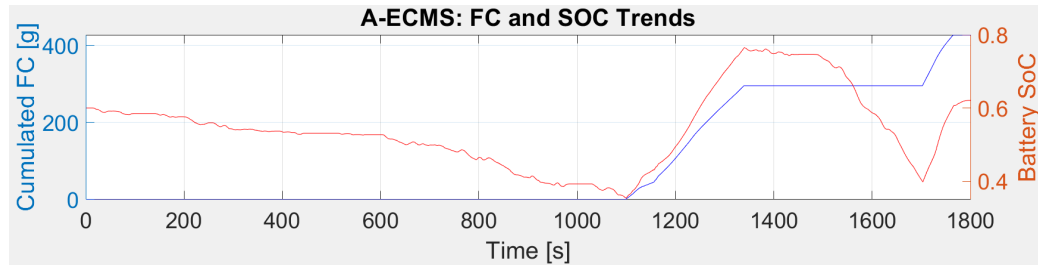
We can notice on the other hand that the second ignition is different for the two controllers, the SERCA is choosing this mode at the beginning of the next acceleration around the time step 1550, the A-ECMS is waiting till the time step 1700 in which we are closer to the end of the cycle and we need to charge the vehicle using the ICE.

Also using two different parts of the cycle to recharge the battery we have seen that the FC is really similar, this because the characteristics of the velocities and accelerations of the two part are really similar and will lead to two situations that have many parameters in common.

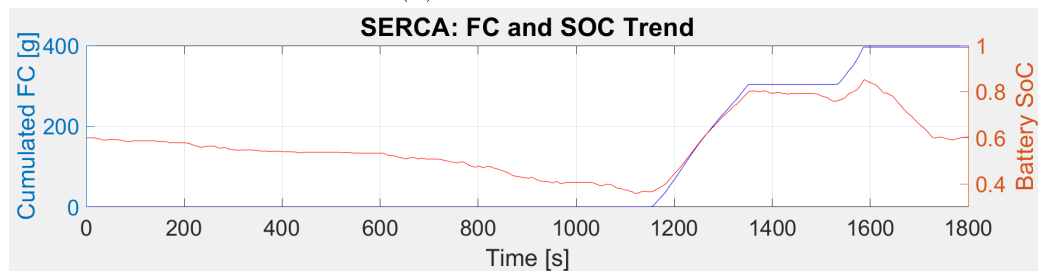
Now we can also appreciate the SOC and FC trend for both the controllers and also the EF trend for the A-ECMS one:



(a) A-ECMS Trends



(b) A-ECMS Trends



(c) SERCA Trends

Figure 4.18: Comparison A-ECMS & SERCA FC, SOC and EF Trends

We can see that two graphs of the SOC are really similar in the first part and also the FC can be overlapped, then for the fact that the SERCA decides to switch on the ICE before the other controller we see that the SOC is overcoming the initial value and is decreasing in the last part in which we are cruising at an high velocity.

On the other hand the A-ECMS one want to charge the battery, that arrives around the 40% of the SOC and then is charging till the initial value.

This behavior is due to the fact that the SERCA knows that charging at that moment would be enough to reach the end of the cycle, on the other hand the A-ECMS is avoiding to charge till the end of the cycle because doesn't

know how far it is from the arrival point.

About the EF we can notice his trend, it is slowly increasing till when the ICE will start to work and then will decrease rapidly.

We can see that for the most of the time the EF is in the range [2 3] and when is outside the boundaries is easier to start the hybrid mode as we can see around the time step 1700 in which the EF is around 4.5 and will start the hybrid mode.

We have seen how having the same FC the two controller are behaving in two different ways for some decisions, but in both case the parameters that are leading the decisions are the same and for this they will lead to similar situations.

The A-ECMS in interpreting the situations with less data of the SERCA but applying a set of rules that make it able to adapt to the different situations.

4.6 Graphical User Interface

In this section we will show the final result of the work on the controller with the development of a Graphical User Interface (GUI) in which is possible to appreciate the performance of the controller exhibited before, compared with other controllers and the standard vehicle. Here we show the results of one simulation with this application:

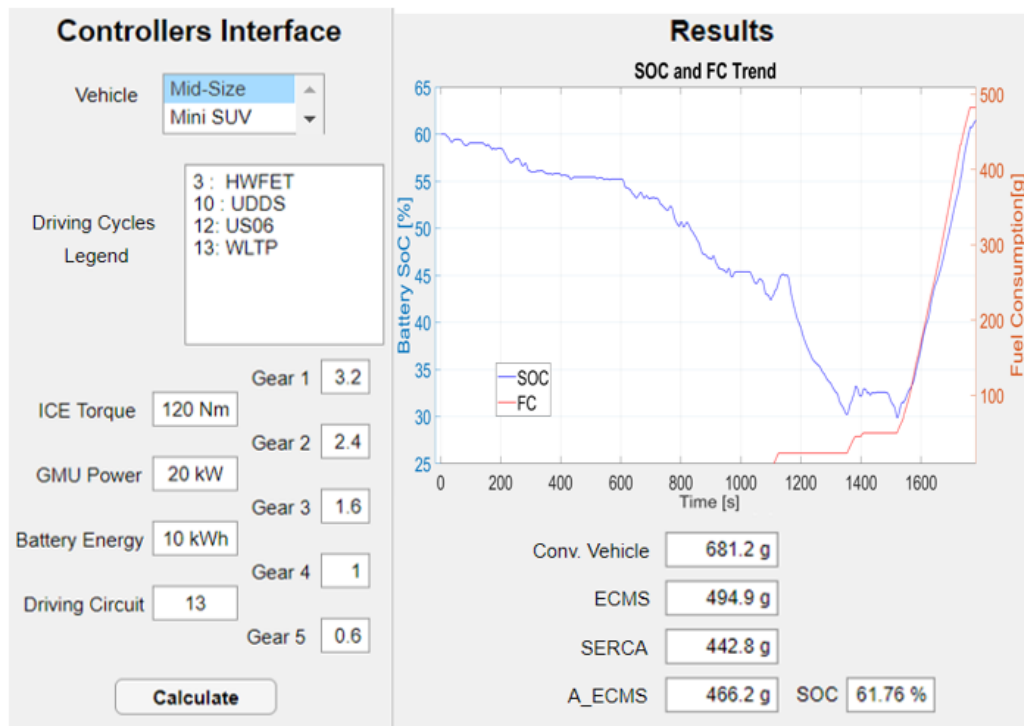


Figure 4.19: Controller Interface

We can appreciate that on the left there are all the inputs to insert for the simulation:

- Vehicle Selection: choosing between the Mid-size or the Mini SUV;
- Driving Cycle: we can choose from a list of 13 different driving cycles, in the legend are reported the 4 most important;
- ICE Torque: we can insert a torque in the range [120 360] Nm;
- GMU Power: we can insert a power in the range [20 50] kW;

- Battery Energy: we can insert a Energy Target in the range [5 15] kWh;
- Gear Ratios: insertion of the 5 gear ratios;
- Calculate Bottom: will start the simulation.

This version is the one for the 5 speed transmission, but the same interface can work also with the 3 speed and 5 speed transmissions.

The output of the simulation are on the right and are the following:

- FC of the Conventional Vehicle;
- FC of the Standard ECMS;
- FC of the SERCA;
- FC of the A-ECMS and the final SOC;
- Graph with the cumulated FC and the SOC trend.

5 Optimization Algorithms

In this chapter we will explain some different optimization algorithms applied to the HEVs.

The aim of this part is to evaluate the different possible combinations of the parameters linked with the design of the vehicle to see with ones can lead to a decrease of FC respecting all the constrains of the physical model, being as close as possible to the CS and also respecting some performance indices [13] [53].

We will use the functions present in the previous sections (2.3.1, 2.3.2, 2.3.3), with the limits said before about the range of reliable values, to generate the data for the controller that will evaluate the FC, evolution of SOC and some performance indices.

In particular we are taking in consideration two main parameters:

- Acceleration Time from 0 km/h to 100 km/h: This parameter is one of the most diffused characteristic for a vehicle, is important to take into account also the performances of the vehicle and not only the minimum FC, this parameter has to be under a certain threshold depending on the kind of vehicle and will influence the final parameter based on his value.

For both the Mid Passenger car and the Mini SUV we would use as reference other vehicles on the market of the same size:

Parameter	Mid-size	Mini SUV
Minimum Time [s]	10	8

Table 23: Minimum Acceleration Times

- Maximum grade of climb affordable from the rest position: This second value would be important for all the real-driving situations in which the vehicle is starting from the rest position to climb a slope, it's important that the vehicle can exceed a minimum value depending on the kind of vehicle and then based on the final value would reach an higher score. We will set as a minimum value the 15% slope for a public road, that would cover the main restrictions of different countries all over the world.

This two parameters would be both considered to evaluate the final performance index (PI), with the final SOC that must be in the following range:

$$55\% \leq SOC_f \leq 65\% \quad (5.1)$$

With all this constrain we would run the driving cycle to see which components will lead to the best FC result.

Now we will present three different algorithms that are often used for HEVs to optimize some parameters.

5.1 Genetic Algorithm

The Genetic Algorithm is a meta-heuristic method based on the genetic scheme in living creatures, introduced by J. Holland in the 1970's [54] [55].

The algorithm abstract the problem space as a population of individuals, and try to find out the fittest individual by producing iterative generations.

The GA will develop the population to an higher quality individuals one, in which each one of them represents a solution for the problem proposed.

The rules are evaluated by a fitness function to see their quality, observing the quantitative adaptation of each rule to a certain environment.

The algorithm can optimize multi modal functions because of the multi-point search methods, is also applicable to discrete search space problems.

The procedure will start from a randomly generated population, a fitness function would be evaluated for each individual, during each generation three basic genetic operator are sequentially applied to each individual to create the new population:

- Selection: select two parent individuals from a population according their fitness function (higher fitness value would increase the chance to be selected), there are many different way to select them according some methods, such as Boltzmann selection, tournament selection or elitism selection.
- Crossover: there is the probability to have a cross over of the parents to form a new offspring(children), without it would be an exact copy of parents. There are three different kind of crossover: single-point, two-point and uniform one.

- Mutation : there is a mutation probability for each individual, the operator produces a small random changes to the bit string by choosing a single bit at random.

After this procedure to create the new population it will replace the old one, now the algorithm will run using the new individuals.

It's important to underline the importance of the fitness function that will rank all the potentials results according to the criteria chosen in the code,

Here we will show the flowchart of the operations done by the GA:

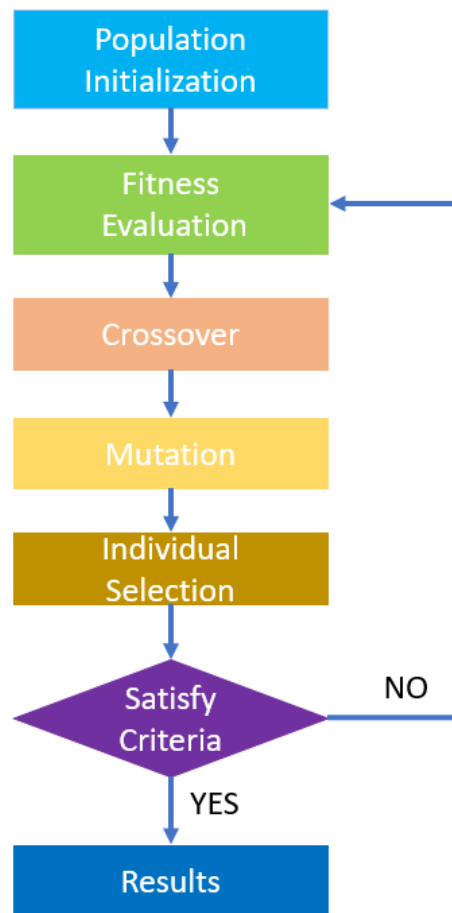


Figure 5.1: Flowchart of Genetic Algorithm

5.2 Machine Learning

The Machine Learning as an area of Artificial Intelligence (AI) aimed at detecting and predicting patterns [56] coined in 1959 by A. Samuel, the area is divided into various sub-topics with different models employed based on the field in which we want to use the method.

In particular we will show the Reinforcement Learning (RL) method, used for similar problems on hybrid vehicles [57].

The RL is concerned with how software agents ought to take actions in an environment so as to maximize some notion of cumulative reward, focused on the balance between exploration, of uncharted territory, and exploitation, of the current knowledge.

In this method there is a decision maker, called Agent, and everything outside that is called Environment. For each time step there is the following interaction between the two:



Figure 5.2: Interactions representation of Reinforcement Learning

As we can see at each time step the agent control the environment state $s_t \in S$ and on that base takes an action $a_t \in A$, where S and A are the set of possible states and actions respectively.

In the next step the Agent will receive the Reward r_{t+1} that will lead to a new environment state s_{t+1} .

There is a policy π of the Agent that link each state $s \in S$ with an action $a \in A$ respecting $a = \pi(s)$. The aim of the method is to find the optimal policy in which the following equation is maximized for each state $s \in S$:

$$V^\pi(s) = E\left(\sum_{k=0}^{\infty} \gamma^k \cdot r_{t+k+1} | s_t = s\right) \quad (5.2)$$

The value of this function is the expected return at the time step t following the policy π starting from the environment state s , γ is a parameter called

Discount Rate, $0 < \gamma < 1$ ensure that the infinite sum converges to a finite value, this parameter reflects also the uncertainty in the future.

r_{t+k+1} is the reward received at time step $t + k + 1$.

Now is needed to define the State Space, using the variables that characterize the system and finding a proper way to subdivide them into useful ranges for the optimization, as seen before for our case we could use the Battery SOC, the vehicle speed or the Power Demand.

Then we need to define the Action Space, with a finite number of actions, for example about the current I to discharge the battery pack, the gear to select or the switching off of the ICE, also in this case are defined ranges for each variable.

As seen for the GA is really important to define the reward, cost function for GA, to be able to reach the best situation possible, in case there are many factors in our function is also important to give the right weight to each of them.

Lastly we have to define the learning algorithm, as for example the Temporal Difference (TD) one [57].

This would derive the optimal policy, using $Q(s,a)$ value associated with a pair of state-action. Are initialized arbitrarily values at the beginning, is picked a pair and then is calculated the reward function.

To choose the pair there is an eligibility function $e(s,a)$ that could vary between 0 and 1 based on how many times is used that pair in the algorithm as the best option.

The eligibility function takes into account only the last M pairs of states-actions.

5.3 Particle Swarm Optimization

The Particle Swarm Optimization is a computational method that optimizes a problem by iteratively trying to improve a candidate solution with regard to a given measure of quality. The algorithm is inspired by the behavior of the birds in a swarm.

The individuals are called particles and the population is called swarm, each particle have his own velocity in the search space, its value is affected by information of the neighbors [58] [59].

For each iteration the best position is saved in a variable, then this value is compared with the best overall position till that moment and in case updated. In this way we can see the evolution of different optimal during the iterations and also the best particle position at the end of the optimization.

Here we present a figure of the particle evolution during an iteration:

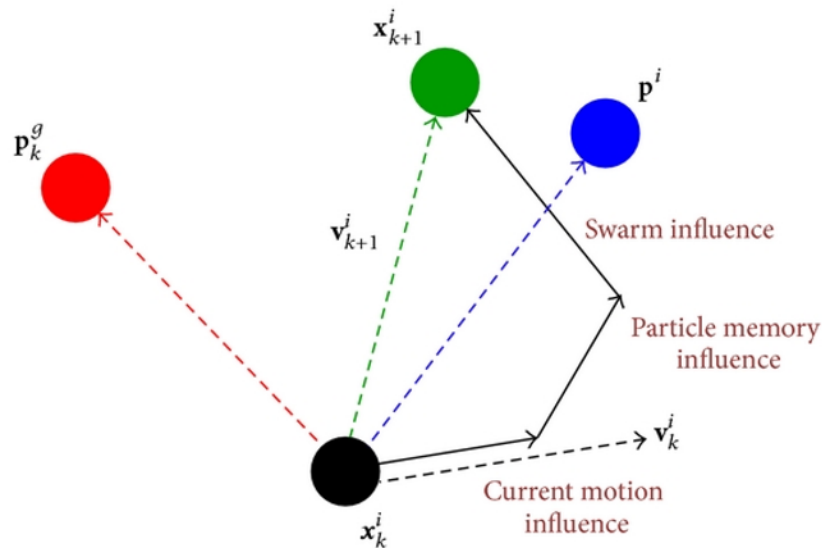


Figure 5.3: Particle Swarm Optimization scheme

We can notice that every particles is characterized by a position x_k^i and a velocity v_k^i and is also represented the best position p_k^g , to update the particle's velocity there is the following equation:

$$v_{k+1}^i = \omega v_k^i + c_1 r_1 (p_k^i - x_k^i) + c_2 r_2 (p_k^g - x_k^i) \quad (5.3)$$

Where ω is the inertia weight, c_1 is the personal confidence factor, c_2 is the swarm confidence factor, r_1 and r_2 are the random coefficients $\in [0, 1]$.

Then will be updated the position of the particle:

$$x_{k+1}^i = x_k^i + v_{k+1}^i \quad (5.4)$$

All the positions of the particle must be in the search space, here we will show a flowchart of the algorithm:

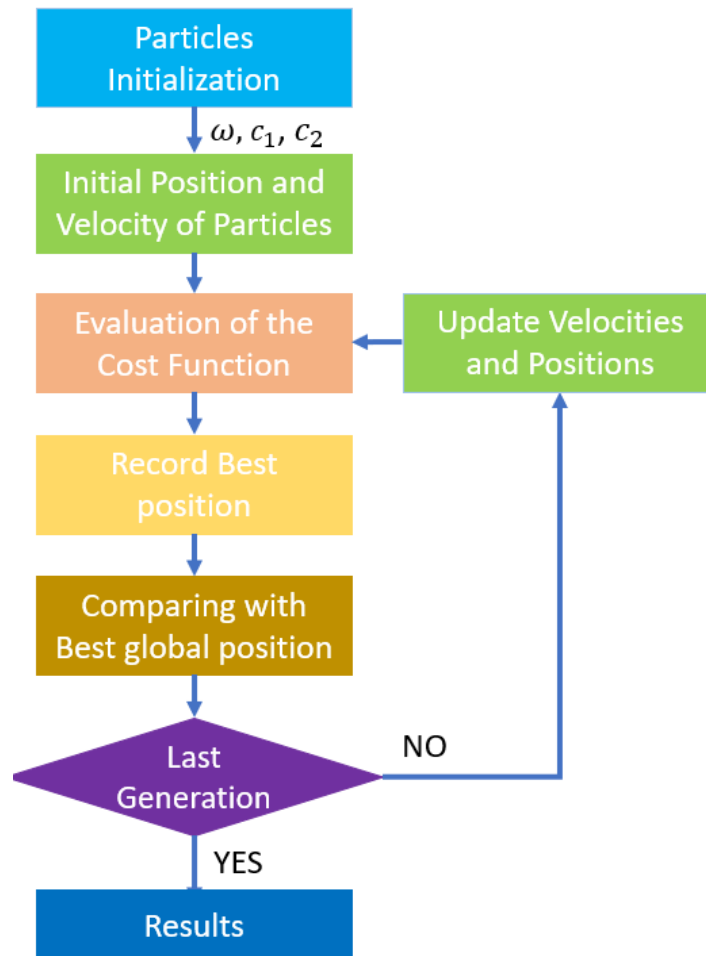


Figure 5.4: Particle Swarm Optimization workflow

As said we will fix a maximum number of generations and the algorithm will calculate the cost function for each particle of each generation saving all the best positions, at the end will show the best results with their relative state parameters.

We have seen that the logic of these algorithm is really similar, in each case the cost function is the core of the method that can lead to good results or not.

In our case we have decided to proceed with the PSO algorithm for our component sizing optimization, that is used also in other projects related with HEV [22], we have seen that could lead to very good results once identified a region in the search space, instead of the two others algorithms that are more influenced by random parameters.

We will start from the algorithm presented in this section and we will modify it for our case, in particular we would need to optimize two different parameters, one related to the FC and the CS of the vehicle and another one linked with the performance index.

6 Multi-Objective Particle Swarm Optimization

In this chapter we will show the main features of the algorithm that is taken from Victor Martinez-Cagigal [60].

Here we show the Input Parameters:

```

% Input parameters:
% - params: Struct that contains the customized parameters.
% * params.Np: Number of particles.
% * params.Nr: Repository size (in particles).
% * params.maxgen: Maximum number of generations.
% * params.W: Inertia coefficient.
% * params.C1: Personal confidence factor.
% * params.C2: Swarm confidence factor.
% * params.ngrid: Number of hypercubes in each dimension.
% * params.maxvel: Maximum velocity (search space percentage)
% * params.u_mut: Uniform mutation percentage.
% - MultiObj: Struct that contains the parameters relative to the
% optimization functions.
% * MultiObj.fun: Anonymous multi-obj function to minimize.
% * MultiObj.nVar: Number of variables.
% * MultiObj.var_min: Vector that indicates the minimum values
% of the search space in each dimension.
% * MultiObj.var_max: Same than 'var_min' with the maxima.
% -----
%

```

Figure 6.1: Particle Swarm Optimization Parameters

As shown in the last chapters is important to choose the number of generations and all the coefficients.

This algorithm is checking for each generation the Dominants parameters, this means:

$$f_i(x_1) \leq f_i(x_2) \quad \forall i \quad \text{and} \quad f_i(x_1) < f_i(x_2) \quad \text{for at least one } i \quad (6.1)$$

The algorithm is looking for the lowest parameter of the generation and is putting them in a repository array to save them for the next generation.

In each generation is peeking some parameters and is doing some mutation to the values to see if there are also other possible combinations that could lead to lower values instead of proceeding only around the best parameters found.

The main feature of this algorithm is the possibility to optimize more than one function per time, we need to take in consideration the FC and also the performance, so we need to select the best parameters for both of them.

Here we will show the optimization for the 5 speed transmission with all the power-train components for the Mid-size vehicle:



Figure 6.2: Optimization of FC and PI: Powertrain 5 Speed Transmission

In this optimization we are taking into account two driving cycles: WLTP and HWFET, to have a larger number of situations in which we are using the controller.

Here we will show the optimization for the 3 speed transmission with all the power-train components for the Mid-size vehicle:

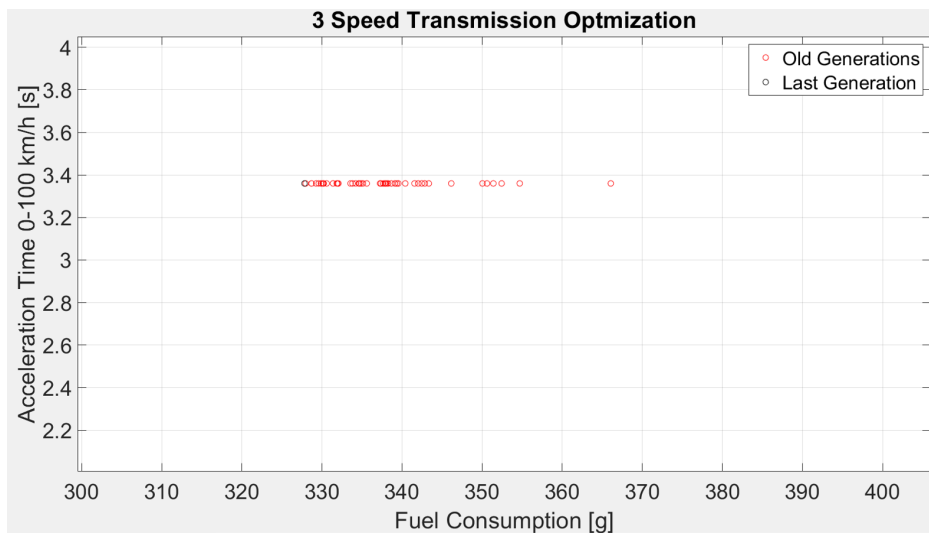


Figure 6.3: Optimization of FC and PI: Powertrain 3 Speed Transmission

Now we can collect the data in a table to see which set of components in the two situations is leading to the least FC maintaining a good performance:

Transmission	ICE T [Nm]	GMU P [kW]	Batt En [kWh]	Gear ratios
3 Speed	187.38	49.9	14.6	[5.00 0.80 0.30]
5 Speed	185.50	50.0	15.0	[3 2.20 1.33 0.74 0.30]

Table 24: Optimized Components by FC and PI

From the table we can see that the size of the two ICEs is quite similar and is around the 185 Nm with 100 kW of maximum Power, for the motor both are trying to use the biggest motor present around the 50 kW, to be able to perform better in the Electric Mode, that as seen before is used most of the time in each cycle.

The same idea can explain the size of the battery that is close to the higher edge of the range, in this way we need to use less the ICE and activate the hybrid mode a lower number of times.

About the gears we can see that last gear is the same for both, as seen before the 90% of the time the vehicle is using the highest gear and to save FC we need to use the lowest possible gear ratio.

For the other gears the values are determined more by the acceleration test that needs a good performance in the first speeds, but for the fact that the target velocity is 100 km/h is not needed an high gear to reach that goal.

Now we can also show the data about the FC and the Acceleration time:

Transmission	FC WLTP [g]	FC HWFET [g]	Avg FC [km/l]	Acc. Time [s]
3 Speed	187.59	140.23	89.86	3.36
5 Speed	189.44	135.51	90.97	3.79

Table 25: Optimized FC and PI

We can see that the final values of FC are really close, one is performing better in the HWFET and the other in the WLTP, due to the characteristics of the cycle and the number of gear shifts and ignitions.

For both the cases we are around the 90 km per liter of gasoline burnt, that is really higher than the starting condition analyzed in 14, in which we were analyzing a general condition without any particular optimization.

Also talking about the acceleration time we can see that the values are really close each other, in both case the values are low for the fact that we are using an high maximum torque for the GMU that is providing an high torque since the rest position of the vehicle.

It is important to notice that in this case we are not taking in consideration of various losses and so the final values could be far from these presented but the magnitude would be similar.

We can observe that with similar components of the power-train the performances are quite the same, the transmission is not having such a great influence in the final behavior of the vehicle.

We want also to show the improvement from the starting situation observed in the section 4.5 in the following table:

Transmission	FC Opt.	FC Non-Opt.	FC Opt.	FC Non-Opt.
	WLTP	WLTP	HWFET	HWFET
	[g]	[g]	[g]	[g]
3 Speed	187.59	360.53	140.23	258.29
5 Speed	189.44	513.68	135.51	351.93

Table 26: Comparison Optimized and Non Optimized FC

We can notice that the FC is strongly reduced in both the situation, in particular the 5 speed transmission one, in which is reduced by more the 60%. In this way we can see how important could be the optimization of the power-train and all the energy that we can say with this procedure.

As said before the values could be an underestimation of the real ones but can give us an idea about the potential of this method.

Now we want to compare these results with the optimization only of the two driving cycles just checking if the performance is respecting the condition in the tab 23, here the results for the 5 Speed Transmission:

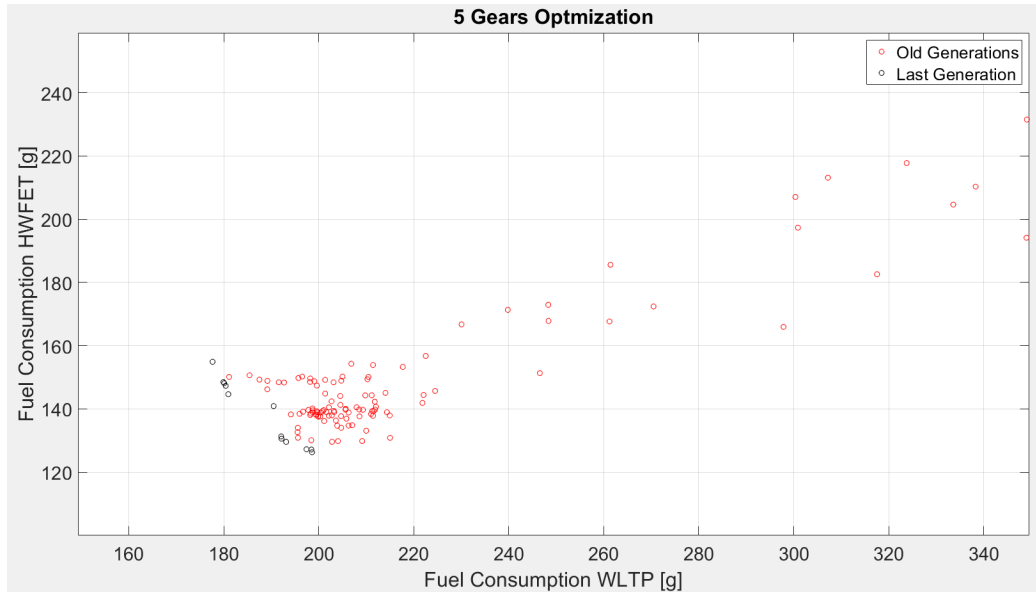


Figure 6.4: Optimization of FC: Powertrain 5 Speed Transmission

We have done the same optimization also for the 3 speed transmission, on the same vehicle, checking the performance of the results.

Here the final graph:

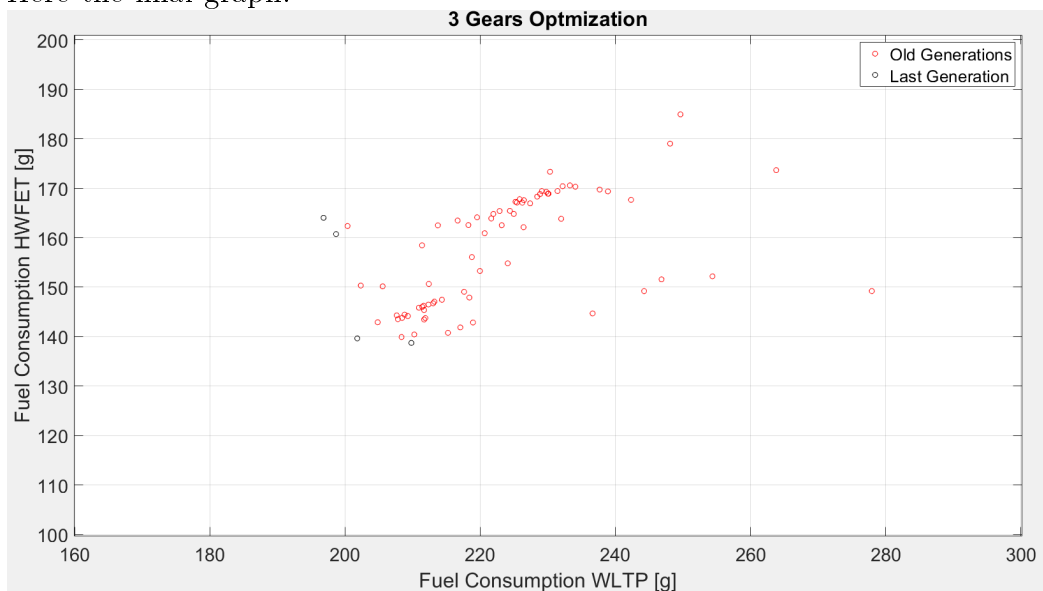


Figure 6.5: Optimization of FC: Powertrain 3 Speed Transmission

In the following table we report the best sets of components selected from the optimization in both cases:

Transmission	ICE T [Nm]	GMU P [kW]	Batt En [kWh]	Gear ratios
3 Speed	134.5	50.0	15.0	[3.31 0.80 0.308]
5 Speed	135.4	48.6	13.5	[4.86 2.60 1.97 0.64 0.30]

Table 27: Optimized Components by FC

As before the components selected are really similar for the two kind of transmission, the GMU and Battery components are the same of the previous optimization, the ICE size is smaller than before due to the fact that we are not looking for the best performance but only checking that the vehicle is respecting the threshold imposed.

This optimization is more focusing about the FC in the cycle and for this reason is needed a smaller ICE that could reduce the FC.

About the gear ratios we can see that the values of the highest gears are similar to previous ones, because as said before are not so important for the acceleration performances, the first gears are slightly different from before to save more fuel during the acceleration from the still position.

Here we present also the table with the FC performances:

Transmission	FC WLTP [g]	FC HWFET [g]	Avg FC [km/l]
3 Speed	186.42	138.79	90.83
5 Speed	189.14	131.33	91.55

Table 28: Optimized FC

As expected the FC is lower than the previous case for the size of the ICE, lower than 1 km/l, but still lower.

This shows how the size of the ICE is not so important for the FC saving, for the fact that reducing the size of the 25% we are reducing the FC only about 1-2%, and the different ICEs at the same torques will lead to a similar FC. In a certain condition we can save fuel selecting the best torque output from the

ICE, in both the situation the controller is performing this, the possibility to have an higher torque would be useful only in particular situations in which we need more power for a limited amount of time.

This is a consequence of the graph about the FC of the ICE showed in fig. 2.10.

7 Considerations

In this thesis we have presented a methodology to calibrate the A-ECMS controller to be able to reach the CS in different situations mimicking the behavior of the SERCA one.

We have seen that we can reach really good performances close to the SERCA FC result in many different cases.

We want to highlight that once we select a particular vehicle and a set of components for the power-train we are able to tune the parameters to improve the performance of the controller and reduce the FC.

Another important point is that, contrary to what is reported in the literature consulted, is not important the first guess of the EF if the PI controller is able to bring this back within a reasonable range in the first part of the cycle.

Another fact is that for a specific we can be able to exclude the control over the percentage of the trip and not using any information about the future path of the cycle, as we would like from a true real-time controller.

We have seen that we can be around 1% error from the SERCA FC and even to reduce it, without change no one of the parameters for the gear shifts or for the ICE ignition, as saying that the controller is totally automatic in his performance.

Another strength of the control is that the computational time is very low and would be able to perform in real-time.

We have shown the application of the controller in the Graphic Interface in the section 4.6, how is possible to an user to set the parameters of a vehicle of interest and see the behavior of different controllers and compare them in an easy and rapid way.

The aim is to be implemented in the design of a vehicle adding a more sophisticated model to be more reliable and precise in the final values presented.

At this point of the development is already really useful to have a rapid comparison and an idea of the magnitude of the final values.

Still talking about the design aim, the optimization would be an useful tool to select some set of components and see their performance in detail.

For the fact that the controller does not require an heavy computational effort would be possible to study different designs in a limited amount of time and select the best candidates to be investigate more in detail.

7.1 Future work

For the future work would be interesting to move from the quasi-static model of Matlab to a Dynamic one such as Simulink or Amesim.

We have already planned a possible co-simulation between the two software in the following way:

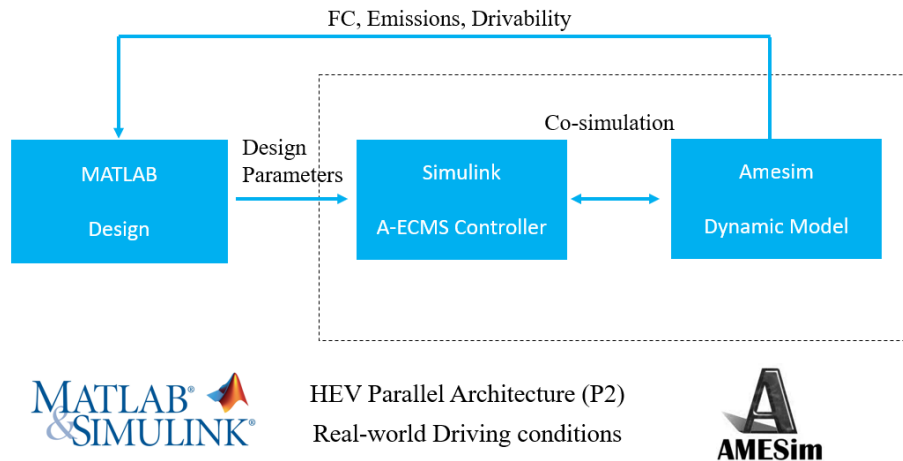


Figure 7.1: Co-Simulation Workflow

This workflow would be able improve the actual control and validate it for a real application, due to the higher level of reliability of the model.

Another point could be the refinement of the calibration of the controller to be able to adapt more to different vehicles and in particular a validation of the transmission and the other components with real data to see if the controller is performing well.

From this point, once we select a vehicle, as said before, we would need to calibrate the parameters on that particular vehicle and reach the best performance possible.

References

- [1] Motorised Images LTD. Toyota prius 1997.
- [2] A. Biswas. Energy management systems for electrified powertrains: State-of-the-art review and future trends. *IEEE Transactions on Vehicular Technology*, VT-2019-00173.R1, 2019.
- [3] G. Buccoliero, G. Belingardi, A. Emadi, P. Anselma. Design selection of multimode power split hybrid electric vehicle powertrains. *Master Thesis, Politecnico di Torino*, 2018.
- [4] Union of Concerned Scientists. Standards, a brief history of u.s. fuel efficiency.
- [5] H. Nils, M. Maarten, V. M. Joeri, C. Thierry. A review of the european passenger car regulations – real driving emissions vs local air quality. *Renewable and Sustainable Energy Reviews*, vol. 89, pp. 1-21, 2018.
- [6] European Environment Agency. Average co2 emissions from new cars and new vans increased in 2018.
- [7] A. Emadi. Transportation 2.0. *EEE Power and Energy Magazine* , vol. 9, pp. 18-29, 2011.
- [8] Sarwant Singh. Top automotive trends in 2019: A year of wows and woes.
- [9] A. Emadi, K. Rajashekara, S. Williamson, S. Lukic. Topological overview of hybrid electric and fuel cell vehicular power system architectures and configurations. *Vehicular Technology, IEEE Transactions*, vol. 54, pp. 763-770, 2005.
- [10] K. V. Singh, H. O. Bansal, D. Singh. A comprehensive review on hybrid electric vehicles: architectures and components. *DOI:10.1007/s40534-019-0184-3*, 2019.
- [11] Y. Guezennec, G. Rizzoni. Optimal energy management in series hybrid electric vehicles. *American Control Conference (ACC), Chicago, IL*, 2000.
- [12] Y. Yang, K. Aeshad-Ali, J. Roeleveld, A. Emadi. State-of-the-art electrified powertrains - hybrid, plug-in, and electric vehicle. *Int. J. Powertrains*, Vol. 5, No. 1, 2016.

- [13] R. Finesso, D. Misul, E. Spessa, M. Venditti. Optimal design of power-split hevs based on total cost of ownership and co2 emission minimization. *Energies* 11, 1705, 2018.
- [14] G. Buccoliero, P. Anselma, S. Amirfarhangi Bonab, G. Belingardi, A. Emadi. A new energy management strategy for multimode power split hybrid electric vehicles. *IEEE Transactions on Vehicular Technology*, 2019.
- [15] P. Anselma, Y. Huo, J. Roeleveld, G. Belingardi, A. Emadi. Integration of on-line control in optimal design of multimode power-split hybrid electric vehicle powertrains. *IEEE Transactions on Vehicular Technology*, 2019.
- [16] J. M. Miller. Hybrid electric vehicle propulsion system architectures of the e-cvt type. *IEEE Transactions on Power Electronics*, vol. 21, n. 3, pp. 756-767, 2006.
- [17] J. W. Xiaohua Zeng. *Analysis and Design of the Power-Split Device for Hybrid Systems*. Springer, 2017.
- [18] T. Burrell, S. Campbell, C. Coomer, C. W. Ayers, A. Wereszczak, J. Cunningham, L. Marlino, L. Seiber, H. Linr. Evaluation of the 2010 toyota prius hybrid synergy drive system. *Oak Ridge National Lab. (ORNL), Oak Ridge, TN (United States). Power Electronics and Electric Machinery Research Facility*, 2011.
- [19] Y. Yang, A. Emadi. Integrated electro-mechanical transmission systems in hybrid electric vehicles. *IEEE Vehicle Power and Propulsion Conference, Chicago, IL*, 2011.
- [20] H. Karlsson, E. Sörensen. Road surface influence on rolling resistance: coastdown measurements for a car and an hgv. *Swedish Road Administration, VTI*, 2011.
- [21] P. G. Anselma, Y. Huo, J. Roeleveld, G. Belingardi, A. Emadi. Slope-weighted energy-based rapid control analysis for hybrid electric vehicles. *Submitted to: IEEE Transactions on Vehicular Technology*, 2018.
- [22] S. Ebbesen, C. Dönitz, L. Guzzella. Particle swarm optimization for hybrid electric drive-train sizing. *Int. J. Vehicle Design, Vol. 58, Nos. 2/3/4*, 2012.

- [23] D. Chrenk, S. Gan, Z.H. Che Daud, Z. Asus, E. Aglzim, L. Le Moyne. Sizing of ice and lithium-ion battery for series hybrid vehicle over life cycle with battery aging. *Submitted to: IEEE Transportation Electrification Conference and Expo (ITEC)*, 2013.
- [24] H. Hofmann, M. Ouyang Z. Song, X. Zhang, J. Li. Component sizing optimization of plug-in hybrid electric vehicles with the hybrid energy storage system. *Energy Volume 144, 1 February 2018, Pages 393-403*, 2018.
- [25] F. Le Berr, A. Abdelli, D.M. Postariu, R. Benlamine. Design and optimization of future hybrid and electric propulsion systems: An advanced tool integrated in a complete workflow to study electric devices. *Oil and Gas Science and Technology – Rev. IFP Energies nouvelles, Vol. 67 (2012), No. 4, pp. 547-562*, 2012.
- [26] E. A. Grunditz, T. Thiringer. Modelling and scaling procedure of a vehicle electric drive system. *Chalmers Publication Library (CPL)*, 2017.
- [27] C. Zhang, J. Jiang, L. Zhang, S. Liu, L. Wang, P. C. Loh. Generalized soc-ocv model for lithium-ion batteries and the soc estimation for Inmco battery. *Energies 2016, 9(11), 900; <https://doi.org/10.3390/en9110900>*, 2016.
- [28] M. Petit, N. Marc, F. Badin, R. Mingant, V. Sauvart-Moynot. A tool for vehicle electrical storage system sizing and modelling for system simulation. *Submitted to: IEEE Vehicle Power and Propulsion Conference (VPPC)*, 2013.
- [29] Y. Hu, W. Li, K. Xu, T. Zahid, F. Qin, C. Li. Energy management strategy for a hybrid electric vehicle based on deep reinforcement learning. *Applied Sciences 8(2):187*, 2018.
- [30] J.Y. Liang, J.L. Zhang, X. Zhang, S.F. Yuan, K. V. Singh, H. O. Bansal, D. Singh. Energy management strategy for a parallel hybrid electric vehicle equipped with a battery/ultra-capacitor hybrid energy storage system. *Journal of Zhejiang University - Science A: Applied Physics and Engineering*, 2013.
- [31] A. Ali, D. Söffker. Towards optimal power management of hybrid electric vehicles in real-time: A review on methods, challenges, and state-of-the-art solutions. *Energies 11, 476*, 2018.

- [32] CAR Engineer. The different driving cycles, <http://www.car-engineer.com/the-different-driving-cycles>.
- [33] R. Barnitt, J. Gonder. Drive cycle analysis, measurement of emissions and fuel consumption of a phev school bus. *SAE 2011 World Congress Detroit, Michigan*, 2011.
- [34] K. Namwook, R. Aymeric. Sufficient conditions of optimal control based on pontryagin's minimum principle for use in hybrid electric vehicles. *Proceedings of the Institution of Mechanical Engineers, Part D: Journal of Automobile Engineering*, vol. 226, n. 9, pp. 1160-1170, 2012.
- [35] U. Jonsson. Optimal control. *Royal Technical Institute of Technology*, 2010.
- [36] R. Bellman. Dynamic programming. *Princeton University Press*, 1953.
- [37] S. Lorenzo, O. Simona, R. Giorgio. A comparative analysis of energy management strategies for hybrid electric vehicles. *Journal of Dynamic Systems, Measurement, and Control*, vol. 133, n. 3, 2011.
- [38] N. Kim, S. Cha, H. Peng. Optimal control of hybrid electric vehicles based on pontryagin's minimum principle. *IEEE Transactions on Control Systems Technology*, vol. 19, n. 5, pp. 1279-1287, 2011.
- [39] C.-C. Lin, P. Huei, G. J. W. Grizzle. A stochastic control strategy for hybrid electric vehicles. *Proceedings of the 2004 American Control Conference, Boston, MA*, 2004.
- [40] P. G. Anselma, Y. Huo, E. Amin, J. Roeleveld, G. Belingardi, A. Emadi. Mode-shifting minimization in a power management strategy for rapid component sizing of multimode power split hybrid vehicles. *SAE Technical Paper 2018-01-1018*, 2018.
- [41] P. Anselma, Y. Huo, J. Roeleveld, G. Belingardi, A. Emadi. From offline to on-line control of a multimode power split hybrid electric vehicle powertrain. *IEEE Transactions on Vehicular Technology*, 2019.
- [42] P. Anselma, A. Biswas, J. Roeleveld, G. Belingardi, A. Emadi. Multi-fidelity near-optimal on-line control of a parallel hybrid electric vehicle powertrain. *IEEE Transportation Electrification Conference (ITEC)*, 2019.

-
- [43] P. G. Anselma, Y. Huo, J. Roeleveld, G. Belingardi, A. Emadi. Real-time rule-based near-optimal control strategy for a single-motor multi-mode hybrid electric vehicle powertrain. *FISITA 2018 World Automotive Congress, At Chennai, India*, 2018.
- [44] R. Finesso, E. Spessa, M. Venditti. An unsupervised machine-learning technique for the definition of a rule-based control strategy in a complex hev. *SAE Int. J. Alt. Power, Vol. 5, Issue 2*, 2016.
- [45] R. R. Gugale, S. K. Chada, E. A. Dsouza. Rule based energy management strategy for a parallel mild hybrid electric vehicle. *Seminar Eelectromobility SS*, 2017.
- [46] V. Gupta. Ecms based hybrid algorithm for energy management in parallel hybrid electric vehicles. *Int. J. Technology Innovations and Research, Vol. 14*, 2015.
- [47] F. Zhang, K. Xu, L. Li, R. Langari. Comparative study of equivalent factor adjustment algorithm for equivalent consumption minimization strategy for hevs. *IEEE Vehicle Power and Propulsion Conference, VPPC.2018.8604986*, 2018.
- [48] S. Onori, L. Serrao, G. Rizzoni. Adaptive equivalent consumption minimization strategy for hybrid electric vehicles. *ASME 2010 Dynamic Systems and Control Conference, DSCC2010-4211, September 12-15*, 2010.
- [49] C. Musardo, G. Rizzoni, Y. Guezennec, B. Staccia. A-ecms: An adaptive algorithm for hybrid electric vehicle energy management. *European Journal of Control, Vol. 11:509-524*, 2015.
- [50] M. HauBmann, D. Barroso, C. Vidal, L. Bruck, A. Emadi. A novel multi-mode adaptive energy consumption minimization strategy for p1-p2 hybrid electric vehicle architectures. *IEEE Transportation Electrification Conference and Expo (ITEC)*, 2019.
- [51] A. Motin, S. Liu, B. Nault. Mathematical optimization of gear shift schedules for hybrid electric vehicle's fuel economy improvement. *IEEE Transportation Electrification Conference and Expo (ITEC)*, 2019.
- [52] A. Rezaei, J. Burl, B. Zhou, M. Rezaei. A new real-time optimal energy management strategy for parallel hybrid electric vehicles. *IEEE Transactions on Control Systems Technology, Vol. 27, no. 2*, 2019.

- [53] C. Xia, C. Zhang. Power management strategy of hybrid electric vehicles based on quadratic performance index. *Energies* 8(11):12458-12473 . November, 2015.
- [54] L.Haldurai, T. Madhubala, R. Rajalakshmi. A study on genetic algorithm and its applications. *International Journal of Computer Sciences and Engineering*, 2016.
- [55] T. Iswari, A. Asih. Comparing genetic algorithm and particle swarm optimization for solving capacitated vehicle routing problem. *IOP Conference Series: Materials Science and Engineering*, 2018.
- [56] Z. Whang, M. O'Boyle. Machine learning in compiler optimization. *Proceedings of the IEEE* , Volume: 106 , Issue: 11, Nov. 2018.
- [57] X. Lin, P. Bogdan, N. Chang, M. Pedram. Machine learning-based energy management in a hybrid electric vehicle to minimize total operating cost. *IEEE/ACM International Conference on Computer-Aided Design (ICCAD)*, 2015.
- [58] A. Alin, M. Tawhid. A hybrid particle swarm optimization and genetic algorithm with population partitioning for large scale optimization problems. *Ain Shams Engineering Journal Volume 8, Issue 2*, June 2017.
- [59] C. Desai, S. Williamson. Particle swarm optimization for efficient selection of hybrid electric vehicle design parameters. *IEEE Energy Conversion Congress and Exposition (ECCE)*, 2010.
- [60] Víctor Martínez-Cagigal. Multi-objective particle swarm optimization (MOPSO). <https://www.mathworks.com/matlabcentral/fileexchange/62074-multi-objective-particle-swarm-optimization-mopso>, 2019.